

MONTHLY NOTICES
OF THE
ROYAL ASTRONOMICAL SOCIETY

Vol. III No. 6 1951

Published and Sold by the
ROYAL ASTRONOMICAL SOCIETY
BURLINGTON HOUSE
LONDON, W. 1

Price Nine Shillings

NOTICE TO AUTHORS

1. *Communications*.—Papers must be communicated to the Society by a Fellow. They should be accompanied by a summary at the *beginning* of the paper conveying briefly the content of the paper, and drawing attention to important new information and to the main conclusions. The summary should be intelligible in itself, without reference to the paper, to a reader with some knowledge of the subject; it should not normally exceed 200 words in length. **Authors are requested to submit MSS. in duplicate. These should be typed using double spacing and leaving a margin of not less than one inch on the left-hand side. Corrections to the MSS. should be made in the text and not in the margin.** Unless a paper reaches the Secretaries more than seven days before a Council meeting it will not normally be considered at that meeting. By Council decision, MSS. of accepted papers are retained by the Society for one year after publication; unless their return is then requested by the author, they are destroyed.

2. *Presentation*.—Authors are allowed considerable latitude, but they are requested to follow the general style and arrangement of *Monthly Notices*. References to literature should be given in the standard form, including a date, for printing either as footnotes or in a numbered list at the end of the paper. Each reference should give the **name and initials** of the author cited, irrespective of the occurrence of the name in the text (some latitude being permissible, however, in the case of an author referring to his own work). The following examples indicate the style of reference appropriate for a paper and a book, respectively :—

A. Corlin, *Zs. f. Astrophys.*, **15**, 239, 1938.

H. Jeffreys, *Theory of Probability*, 2nd edn., section 5.45, p. 258, Oxford, 1948.

3. *Notation*.—For technical astronomical terms, authors should conform closely to the recommendations of Commission 3 of the International Astronomical Union (*Trans. I.A.U.*, Vol. VI, p. 345, 1938). Council has decided to adopt the I.A.U. 4-letter abbreviations for constellations where contraction is desirable (Vol. IV, p. 221, 1932). In general matters, authors should follow the recommendations in *Symbols, Signs and Abbreviations* (London: Royal Society, 1951) except where these conflict with I.A.U. practice.

4. *Diagrams*.—These should be designed to appear upright on the page, drawn about twice the size required in print and prepared for direct photographic reproduction except for the lettering, which should be inserted in pencil. **Legends should be given in the manuscript indicating where in the text the figure should appear.** Blocks are retained by the Society for 10 years; unless the author requires them before the end of this period they are then destroyed.

5. *Tables*.—These should be arranged so that they can be printed upright on the page.

6. *Proofs*.—Costs of alterations exceeding 5 per cent of composition must be borne by the author. Fellows are warned that such costs have risen sharply in recent years, and it is in their own and the Society's interests to seek the maximum conciseness and simplification of symbols and equations consistent with clarity.

7. *Revised Manuscripts*.—When papers are submitted in revised form it is especially requested that they be accompanied by the original MS.

Reading of Papers at Meetings

8. When submitting papers authors are requested to indicate whether they will be willing and able to read the paper at the next or some subsequent meeting, and approximately how long they would like to be allotted for speaking.

9. Postcards giving the programme of each meeting are issued some days before the meeting concerned. Fellows wishing to receive such cards whether for Ordinary Meetings or for the Geophysical Discussions or both should notify the Assistant Secretary.

MONTHLY NOTICES
OF THE
ROYAL ASTRONOMICAL SOCIETY

Vol. III

No. 6

MEETING OF 1951 NOVEMBER 9

Professor H. Dingle, President, in the Chair

The election of the Council of the following Fellows was duly confirmed:—

M. C. Chaki, M.A., Savoy Hotel, 27 Sashi bhusan De Street, Calcutta, India (proposed by F. J. M. Stratton);

Richard Davies, M.Sc., 71 Mount Park Road, Ealing, W. 5 (proposed by B. C. Browne);

Captain Henry Luxmoore Hitchins, C.B.E., 33A The Crescent, Maidenhead (proposed by H. Spencer Jones);

Peter Ballantyne McFarlane, B.Sc., Gonville and Caius College, Cambridge (proposed by R. H. Garstang); and

Charles Plumptre, M.A., 53 Leathwaite Road, London, S.W. 11 (proposed by Harold Jeffreys).

The election by the Council of the following Junior Member was duly confirmed:—

Gordon Ingram Thompson, 73 Rodenhurst Road, Clapham Park, London, S.W. 4 (proposed by R. W. B. Pearse).

Sixty-one presents were announced as having been received since the last meeting, including:—

Proceedings of the London Conference on Optical Instruments (presented by the Organizing Council of the Conference).

MEETING OF 1951 DECEMBER 14

Professor H. Dingle, President, in the Chair

The election by the Council of the following Fellows was duly confirmed:—

M. H. Vainu Bappu, Mount Wilson Observatory, Pasadena 4, California, U.S.A. (proposed by Harlow Shapley);

- Hugh Findlay Campbell, 56 Clincart Road, Mount Florida, Glasgow, S. 2 (proposed by T. R. Tannahill);
- Joseph Churms, B.Sc., Royal Observatory, Cape of Good Hope, South Africa (proposed by J. Jackson);
- Major George D. Colchagoff, U.S.A.F., HQ Third Air Force, South Ruislip, Middlesex (proposed by G. C. McVittie);
- Margaret G. Davies-Scourfield, Annington House, Steyning, Sussex (proposed by H. Wildey);
- C. Hewitt Dix, California Institute of Technology, Pasadena 4, California, U.S.A. (proposed by Perry Byerly);
- Karl Dyk, Stanolind Oil and Gas Company, Box 591, Tulsa, Oklahoma, U.S.A. (proposed by Perry Byerly);
- Frank N. Edmonds, Jr., University of Missouri, Columbia, Missouri, U.S.A. (proposed by S. Chandrasekhar);
- Mohamed Fahim Mahmoud Fahim, B.Sc., Imperial College of Science, London, S.W. 7 (proposed by M. R. Madwar);
- Peter Berners Felgett, M.A., The Observatories, Madingley Road, Cambridge (proposed by A. Beer);
- Henry G. Horak, University of Kansas, Lawrence, Kansas, U.S.A. (proposed by S. Chandrasekhar);
- Harold L. Johnson, Yerkes Observatory, Williams Bay, Wisconsin, U.S.A. (proposed by S. Chandrasekhar);
- Philip C. Keenan, Ohio State University, Perkins Observatory, Delaware, Ohio, U.S.A. (proposed by S. Chandrasekhar);
- Thomas Arthur Dean Lawton, A.M.I.E.E., Watercroft, Combs, Chapel-en-le-Frith, Stockport, Cheshire (proposed by H. L. Dilks);
- Brian Richard Leaton, Royal Greenwich Observatory, Herstmonceux Castle, Hailsham, Sussex (proposed by H. Spencer Jones);
- Neil McCorkindale, M.A., B.Sc., 58 Jeanfield Road, Perth, Scotland (proposed by W. M. Smart);
- Aden B. Meinel, University of Chicago, Yerkes Observatory, Williams Bay, Wisconsin, U.S.A. (proposed by S. Chandrasekhar);
- Charles Sharp Middleton, 317 Flinders Lane, Melbourne, C.1, Victoria, Australia (proposed by E. B. Walton);
- Walter H. Munk, Scripps Institution of Oceanography, La Jolla, California, U.S.A. (proposed by Perry Byerly);
- Robert Methven Petrie, Dominion Astrophysical Observatory, Victoria, British Columbia, Canada (proposed by A. McKellar);
- Howard J. Pincus, Ohio State University, Columbus 10, Ohio, U.S.A. (proposed by Perry Byerly);
- A. S. Reid, 5 Annat Terrace, Corpach, Fort William, Inverness, Scotland (proposed by G. R. Burbidge);
- John Tucker, Southlea, Church Lane, Bognor Regis, Sussex (proposed by M. Davidson);
- Cyril Walmesley, A.M.I.C.E., M.I.W.E., 4 Albert Place, Perth, Scotland (proposed by T. R. Tannahill); and
- Allan Jay Way, D.Sc., LL.D., Ph.D., Adelphi House, 24-28 Tyrrell Street, Newcastle, New South Wales, Australia (proposed by Harley Wood).

The election by the Council of the following Junior Member was duly confirmed:—

Paul Harry Roberts, Gonville and Caius College, Cambridge (proposed by H. Bondi).

One hundred and two presents were announced as having been received since the last meeting, including:—

H. Spencer Jones, *General Astronomy* (presented by the author);

L. G. H. Horton-Smith, *The Baily Family* (presented by the author);

Paul Couderc, *L'Astrologie* (presented by the author); and

Ernst Zinner, *Astronomie, Geschichte ihrer Probleme* (presented by the author).

Dr J. C. P. Miller and Mr K. C. Blackwell were appointed honorary auditors of the Treasurer's accounts for the year 1951.

SURFACE PHOTOMETRY OF SOUTHERN ELLIPTICAL NEBULAE

David S. Evans

(Received 1951 May 16)*

Summary

Photometric measures of the surface brightness of a number of elliptical nebulae have been made. The isophotes determined are compared with the distribution of surface intensity found by Hubble in studies of elliptical nebulae. The same law is found to give a good general description of the brightness variation in the present case, but there are differences of detail which appear to be real, some of which suggest incipient development of spiral structures and the presence of differential rotation. Detailed discussion is deferred until material for the remaining bright southern elliptical nebulae is available.

Two previous studies in the field of surface photometry of nebulae by the present author have already appeared (1, 2). The experience gained in this field emphasizes a number of points, one of which is the question of the particular class of astronomical object which can most fruitfully be studied by these methods. It seems of doubtful value merely to trace complex topographical detail, especially since, in a very real sense, a system of isophotes is less instructive than a series of photographs. Structures which are obvious in a photograph have a trick of disappearing from immediate view on an isophote map and, although more precise evidence of their form can be obtained by careful reading of the map, some skill is necessary to reconstruct the original picture from the latter. There is, however, the important advantage that photometric methods enable one to trace, with surprisingly little uncertainty, the forms of faint structures far beyond the limits detectable by visual inspection of plates, and farther still beyond the limits capable of reproduction on prints; but it is altogether a different matter to measure the surface brightness of such faint structures and to plot accurate isophotes.

A class of object which seems particularly likely to yield fruitful results is provided by the elliptical nebulae. The mode of variation of surface brightness is rather smooth, and seems to possess a certain generality which makes it particularly suitable for study by theoretical workers. There is now a fairly extensive literature dealing with surface photometry of elliptical nebulae in the northern sky (3, 4, 5, 6, 7, 8).

The observations.—There are about 15 elliptical nebulae brighter than magnitude 12 and south of declination -30° . These fall into two groups on either side of the Milky Way. The present study deals with a group of seven objects in the region R.A. $3^h-4^h 30^m$. The tables give data for these objects and of the plates used in this study. It will be seen that four of the objects are in pairs and that each pair can be photographed on one plate. One of these objects is NGC 1553 which is listed by Shapley and Ames (9) as type S (authority, plates

* Received in original form 1950 October 23.

from Bruce 24-inch refractor, exposure over 170 minutes), but it seems doubtful whether this can be correct. As we shall see, this particular object seems atypical, but, on photographic appearance, one would be strongly tempted to classify it as elliptical.

TABLE I
Nebulae Observed

Number	Position 1950			Magnitude (Shapley-Ames)	Type	Dimensions (Shapley-Ames)
	h	m	s			
NGC 1291	3	15.5	-41 17	10.2	E	5.0 × 2.0
NGC 1344	3	26.7	-31 14	11.6	E	2.0 × 1.0
NGC 1380	3	34.6	-35 09	11.4	E	3.0 × 1.0
NGC 1399	3	36.6	-35 37	10.9	E	1.4 × 1.4
NGC 1404	3	37.0	-35 45	11.5	E	1.0 × 1.0
NGC 1549	4	14.7	-55 42	11.0	E	3.0 × 2.7
NGC 1553	4	15.2	-55 54	10.2	S	3.0 × 2.5

TABLE II
Selected Plates Reduced

Number	Emulsion	Exposure	Date	Object
			1950 Feb.	
A 660	I.A.Z.	m 15	14	NGC 1399, NGC 1404
A 661	I.A.Z.	15	14	NGC 1549
A 673	103a-O	9	17	NGC 1291
A 674	103a-O	9	17	NGC 1344
A 679	103a-O	15	18	NGC 1291
A 681	103a-O	15	18	NGC 1380
A 682	103a-O	15	18	NGC 1399, NGC 1404
A 683	103a-O	15	18	NGC 1549, NGC 1553

I.A.Z. = Ilford Astronomical Zenith.
103a-O = Kodak 103a-O.

The plates were all calibrated on a new tube sensitometer specially designed for the work. This gave 28 calibration spots imprinted on clear glass. The range covered was more than five magnitudes and an additional adjustment allowed the intensities to be moved up or down as a group to secure the best results for different emulsions.

The measurement and reduction were carried out in the usual way. The nebular images were run through every 0.25 mm. and runs on to clear glass were made every millimetre. Several "extinction" readings were secured on each run. Several checks, such as are afforded by running different plates in perpendicular directions through the microphotometer were made (*cf.* Evans (1)).

The sky background.—The results were then corrected for the background light of the sky. The mathematics of this situation are very simple.

We denote by L the total incident intensity at any point and partition this between L_0 , the background luminosity, and L_v , the true intensity arising from the nebula. In terms of magnitudes these values are denoted by m , with corresponding suffixes.

Then

$$L = L_v + L_0,$$

leading to

$$m_0 - m = 2.5 \log_{10}(1 + 10^{0.4(m_0 - m)}).$$

This can be graphed (Fig. 1) and the resulting curve is used for applying background corrections.

It is also of interest to determine by how much a determined value of m_t derived from a given m will be affected by uncertainty in m_0 . This we find from

$$\frac{dm_t}{dm_0} = -(10^{0.4(m_0-m)} - 1)^{-1},$$

which is also graphed. The error in determining m is usually of the order of ± 0.02 magnitude, but since m_0 usually lies on the toe of the curve, the error in

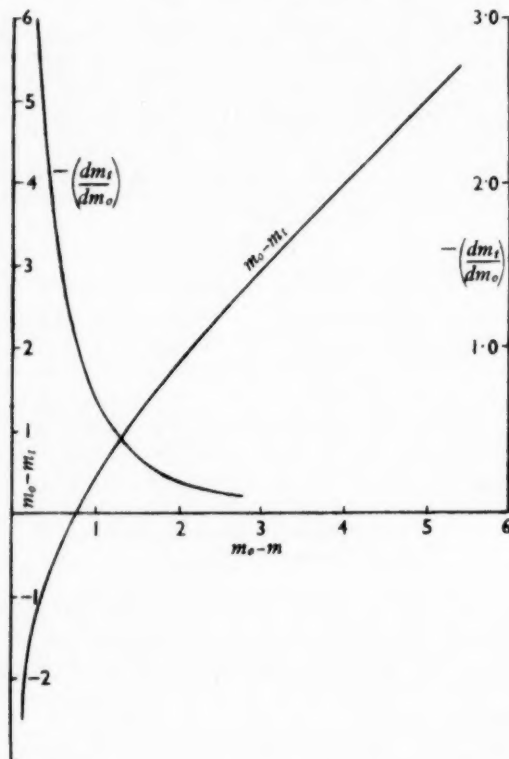


FIG. 1.—The mathematics of background light.

determining the latter may rise to the order of ± 0.15 magnitude. The error in fixing m_t due to uncertainty in m_0 will have the value

$$|\Delta m_t| = \frac{dm_t}{dm_0} |\Delta m_0|.$$

Suppose $|\Delta m_0| = 0.10$ magnitude, then Δm_t will have the value 0.02 if $m_0 - m = 2.0$, i.e. the error in finding m_t , due to uncertainty in fixing the background, will be no greater than the error of measurement of m itself if the total intensity is two magnitudes above background intensity. For differences of one magnitude and 0.5 magnitude the corresponding values of Δm_t are 0.07 and 0.17 magnitude respectively.

If the background is more intense, so that the point corresponding to m_0 falls on the straight line part of the characteristic curve, Δm_0 will fall to the ordinary error of measurement of a magnitude, which, doing rather less than justice to the measures, we have taken as ± 0.02 magnitude. If the background intensity is low, the point corresponding to m_0 falls to the toe of the characteristic curve where measures become unreliable, so that Δm_0 increases.

In practice, of course, measures will not be taken too close to the background, but it should be clear from the foregoing remarks that the presence of a weak and, hence, rather indeterminate background intensity can seriously affect the accuracy of determination of the true intensity, m , even when the measured brightness is well above the background.

In the course of the work a need was felt for a rough numerical measure of the reliability of each isophote as determined. This is especially necessary when isophotes derived from two plates are to be combined. This need was met by assigning to each isophote on a single plate a figure of merit, this figure being the product of two factors. The first factor is based on the value of Δm_i as given by the equation above. This depends first on the value of dm_i/dm_0 read off from the curve of Fig. 1, and secondly on the value of Δm_0 , which is derived from the scatter of the values of the various runs on to parts of the plate remote from the nebular image. A maximum value of unity was assigned to this factor when Δm_i was 0.02 magnitude or less. For larger errors the value is proportionately reduced.

The second factor in the figure of merit is given the value unity when the observed value of m corresponds to a point on the straight line part of a characteristic curve, and is reduced proportionately to the slope of the part of the curve actually used. The product of the two factors gives the final figure of merit for each isophote determined from a given plate. In combining plates the figures are added. This system is entirely empirical. Its usefulness lies chiefly in the fact that when isophotes from different plates are being combined and a discrepancy arises, one can at once estimate the relative reliability of the individual determinations.

The curves of Fig. 1 have proved of great utility in a variety of connections. Consider, for example, the question of the circumstances in which it is permissible to ignore the sky background altogether. This will be the case when $m_0 - m$ and $m_0 - m_i$ are indistinguishable. This is not even the case when $m_0 - m$ is as great as three magnitudes, for then $m_i - m = 0.07$. When $m_0 - m$ has the values 2.0 and 1.5, the corresponding errors are 0.19 and 0.31 magnitude respectively.

It may be thought that liability to error in a case where there is no detectable sky background will easily be avoided by confining the measures to dense parts of the nebular image. However, consider a case in which there is no detectable background, this being due to the fact that the skylight lies 0.5 magnitude below the limit of detectability. From what has been said it will be clear that measures of even the dense parts of the image will be subject to serious error. For example, a part of the nebula which is two magnitudes above the limit of the plate, and which, therefore, shows as a region of quite considerable density, will, in this case, give a value for the true intensity which is in error by a tenth of a magnitude.

Combining these remarks with those on the subject of the influence of errors of determination of the sky background, we arrive at the conclusion that, for the determination of most of the isophotes, the exact determination of the sky

background is a very important requirement. If the background is sufficiently dense to reduce the error of determination of m_0 to the level which applies to points on the straight line part of a characteristic curve, our discussion shows that the figures of merit for isophotes corresponding to quite small values of $m_0 - m$ will not be unduly low.

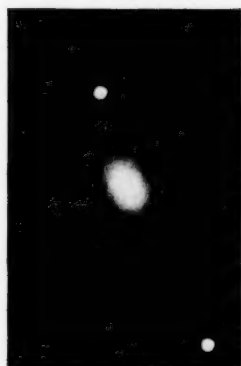
Hubble's rule.—In his studies of elliptical nebulae, Hubble (3) found that the surface brightness followed a law which, in terms of magnitudes, may be expressed as

$$m = m_0 + 5 \log (r/a + 1),$$

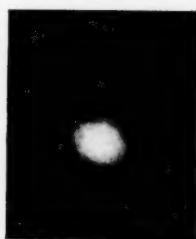
r being the distance measured along a radius and a being a constant. A curious property of this rule which does not seem to have been noted is the following: If the curve representing this function is smudged by means of a Gaussian kernel so as to represent the effects of seeing, the resulting curve can also be represented to a high degree of accuracy by the same function with new values of the constants. It is not thought that this affects the present results. What significance, if any, is to be attached to this fact, it is hard to say, but it is curious that the brightness variation law should be one which is, practically, formally invariant under the seeing transformation.

The results.—After taking the foregoing factors into account, we arrive at seven isophote maps illustrated in Figs. 2–8. The isophotes are drawn with an interval of 0.5 magnitude. The numerals indicate the figures of merit of the individual isophotes according to the system described above. The nebulae may be traced out still farther than they have been, but no great significance could be attached to these extensions. We shall probably not err on the side of over-confidence if we ascribe a probable error of 0.02 magnitude to a curve of merit unity, with errors inversely proportional to the merit for other isophotes. The error of location of an isophote of given merit on a map will, of course, vary with the determined brightness gradient at each point.

In the case of NGC 1553 the adopted background varied linearly across the plot by a total range of 0.2 magnitude between top and bottom of the figure (Fig. 8). Otherwise all backgrounds were taken as constant. The dotted lines represent "Hubble distributions" following the law cited above, which have been fitted to the observations. It will be seen that, in general, this law represents the observed distributions quite closely, except in the case of NGC 1553 which is anomalous. It is believed, following Hubble, that this law is, to a first approximation, a characteristic of elliptical nebulae, and it seems possible that it might be used as a criterion of classification. However, the fit is good only to a first approximation and, as Hubble found, there are points of deviation. For example, in the elongated nebula NGC 1380 changes of the ellipticity of successive isophotes are observable. Again, it has sometimes been stated that elliptical nebulae rarely show absorbing structures, but it will be seen from Plate 10 that a number of the objects discussed here (for example, NGC 1291) does show such structures. It will be further noted that the isophotal maps often show marked irregularities in the outer parts of the nebulae. Examples are the rift and tongue in the north following quadrant of NGC 1549, the southern patch of NGC 1380 and so on. It was thought at first that these merely represented errors of measurement at the limit of faintness which could be reached, but an examination of the material does suggest that these structures are represented



NGC 1553



NGC 1549



NGC 1344



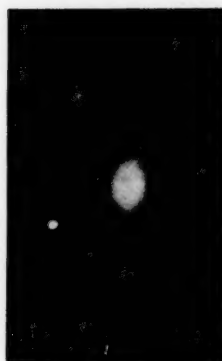
NGC 1404



NGC 1291



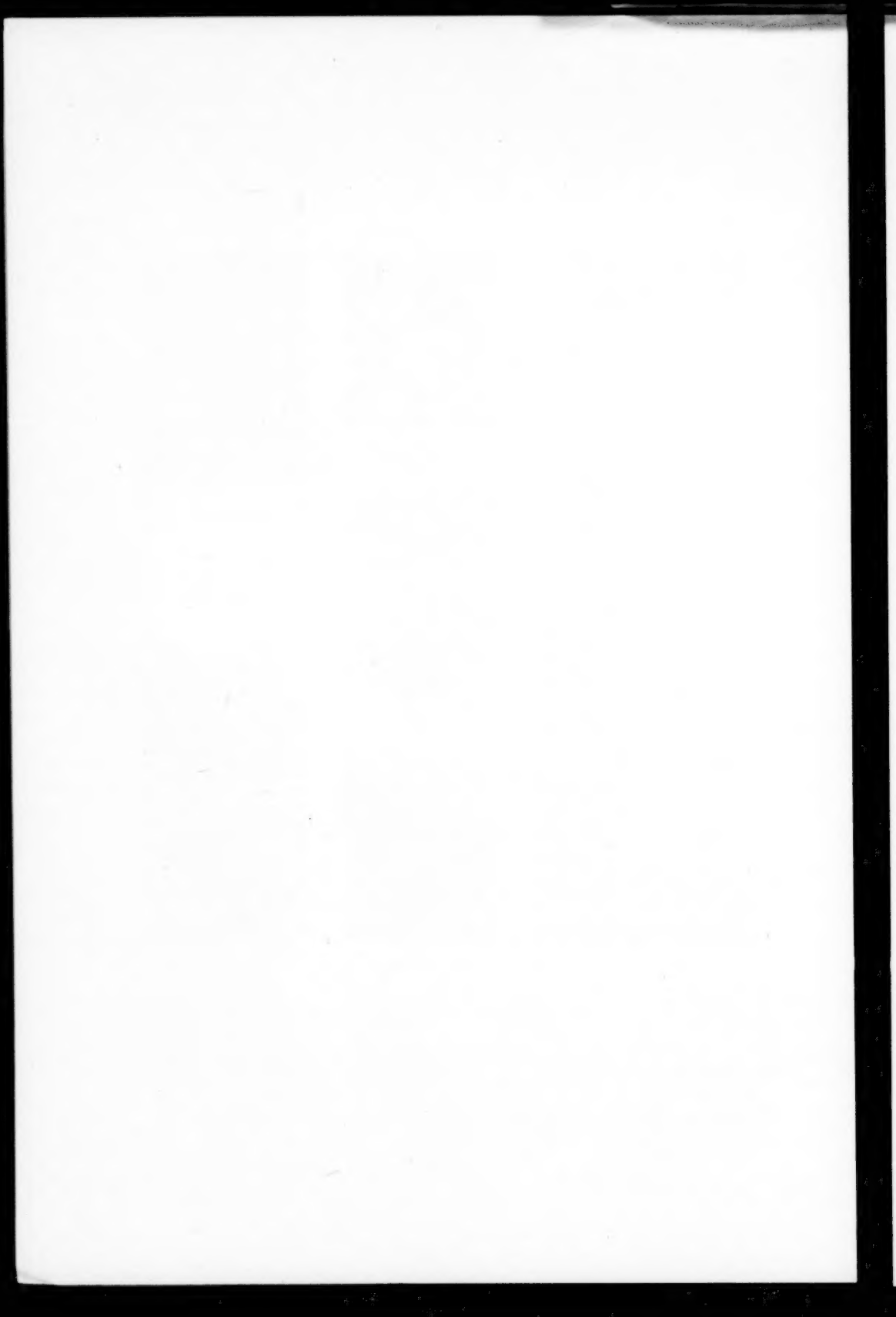
NGC 1399



NGC 1380



Scale : 1 mm. = 3".7.



on the plates and may have some basis in reality. Since they mainly occur on elongated nebulae it may be the case that these structures represent some sort of incipient spiral arms.

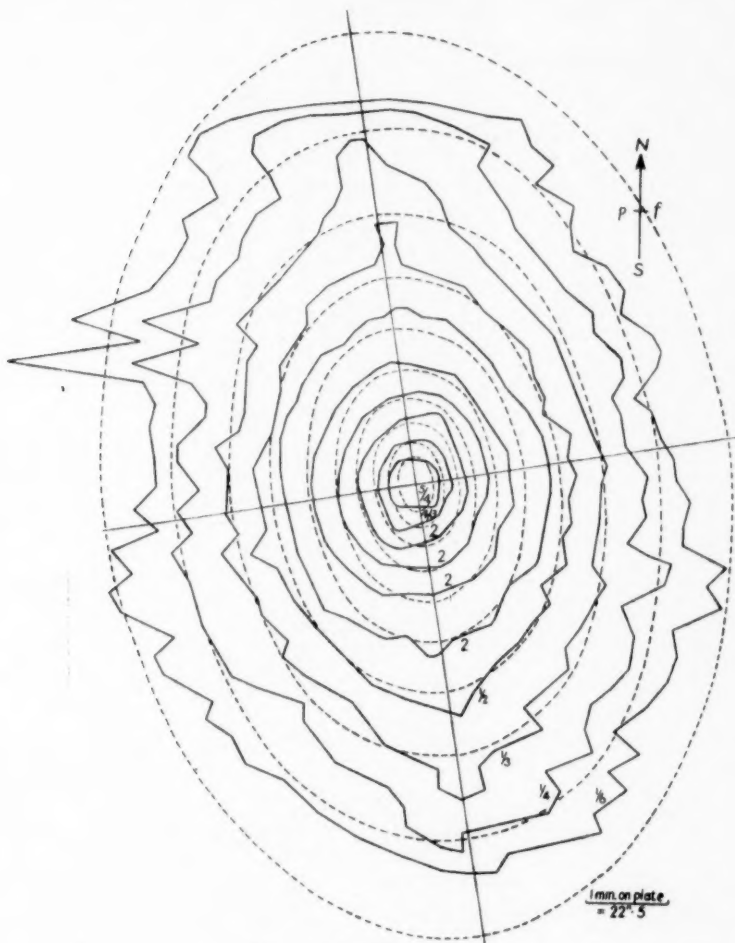


FIG. 2.—NGC 1291.

So far we have been on well-trodden ground and have done little more than provide some confirmation of Hubble's results. There is, however, a further point of interest which seems to be novel and which is best shown in the plot of NGC 1291. This is an elongated nebula of lenticular form showing axial extensions of many of the isophotes. If the central ones are re-drawn (Fig. 2(a)) it will be seen that there is a steady rotation of the line of the major axes of successive isophotes, which one would be inclined to interpret as evidence of shear due to rotation. In the case of NGC 1291 there seems little doubt that this phenomenon is real. It shows up independently on two plates microphotometered at right angles to one another: it applies to the best determined isophotes; it is

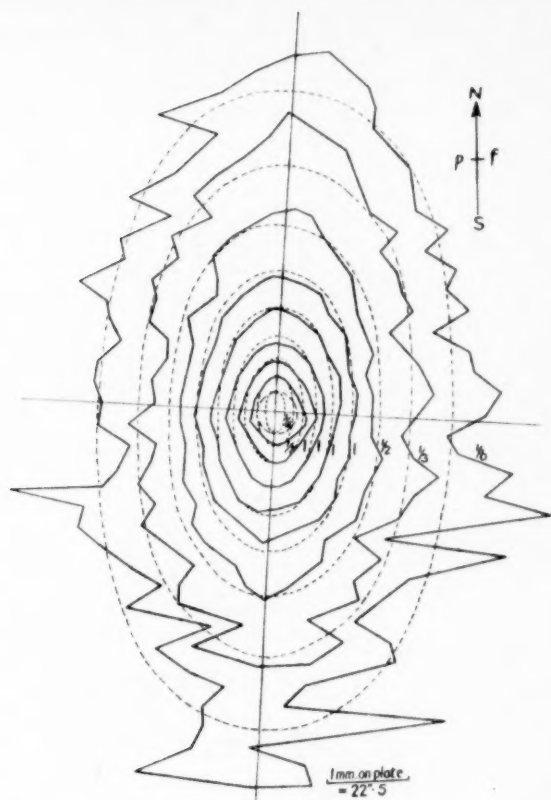


FIG. 4.—NGC 1380.

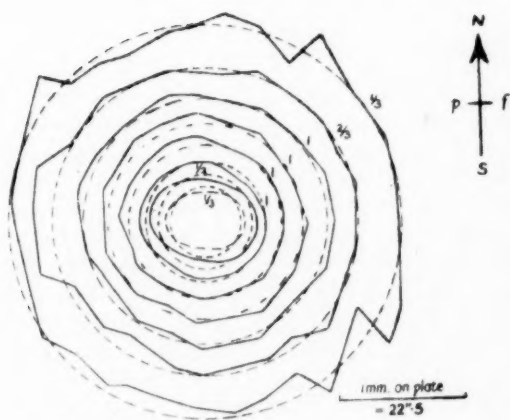


FIG. 5.—NGC 1399.

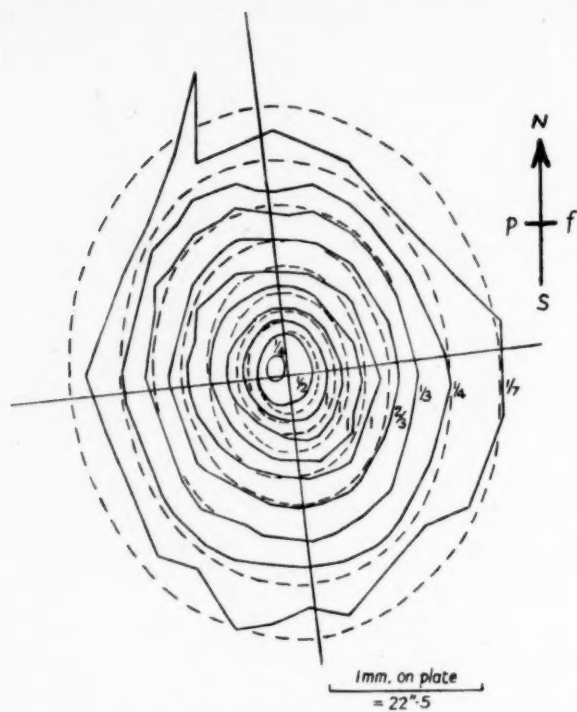


FIG. 6.—NGC 1404.



FIG. 7.—NGC 1549.

observed outside the range for which seeing, guiding and coma errors might be expected to be significant. I am inclined to believe that the similar phenomenon shown near the centre of NGC 1549 is also real, but here the effect is less well marked, and is only discernible with certainty for isophotes so small that they might be affected significantly by the errors mentioned above.

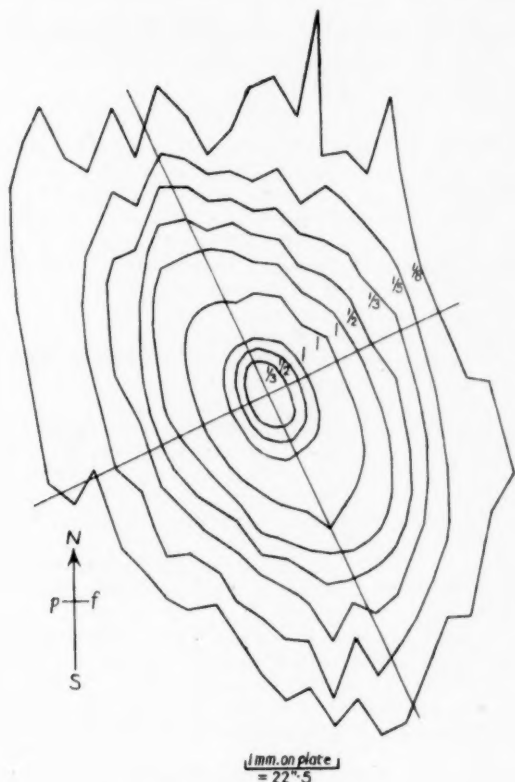


FIG. 8.—NGC 1553.

The case of NGC 1553 is anomalous. If one imagines a descent from the centre of an elliptical nebula, the brightness slope is, at first, steep, switching over to a gentler descent at an almost constant gradient. The curvature of the brightness-distance graph is always in the same sense. This is not true of NGC 1553 where, in the course of the descent, one reaches an almost level ledge. NGC 1553 resembles two elliptical nebulae seen one behind the other (it is not suggested that this is actually the case). The asymmetry about the central region of the faint "ledge", which is well shown on the isophote map, is real. While NGC 1553 seems hardly correctly classified as a spiral, as an elliptical nebula it is atypical.

The discussion of the observational results has been deliberately kept brief: the material available so far seems too limited to form the basis for generalizations about the structure of elliptical nebulae. The isophote maps are presented as

they were determined, to provide theoretical workers with material for discussion. In the meantime observational material on the remaining bright southern elliptical nebulae is being accumulated as opportunity offers, and it is hoped to present this in due course. It may then become possible to discuss general questions, such as, for example, the applicability to all elliptical nebulae of the one-parameter law of surface brightness variation found by de Vaucouleurs (7).

I am much in the debt of Dr A. D. Thackeray for his criticism and comments on the present work throughout its progress. This paper has been much shortened at the suggestion of a referee.

Radcliffe Observatory,
Pretoria :
1950 September 28.

References

- (1) David S. Evans, *M.N.*, **109**, 94, 1949.
- (2) David S. Evans, *M.N.*, **110**, 37, 1950.
- (3) E. P. Hubble, *Ap. J.*, **71**, 231, 1930.
- (4) R. O. Redman, *M.N.*, **96**, 588, 1936.
- (5) R. O. Redman and E. G. Shirley, *M.N.*, **98**, 613, 1938.
- (6) J. H. Oort, *Ap. J.*, **91**, 273, 1940.
- (7) G. de Vaucouleurs, *Ann. d'Ap.*, **11**, 247, 1948.
- (8) E. Holmberg, *Lund Medd.*, Series II, No. 128, 1950.
- (9) H. Shapley and A. Ames, *Harvard Annals*, **98**, No. 2, 1932.

AN EXPLORATION OF INFRA-RED STELLAR MAGNITUDES USING THE PHOTO-CONDUCTIVITY OF LEAD SULPHIDE

P. B. Fellgett

(Communicated by the Director of the Cambridge Observatories)

(Received 1951 May 8)

Summary

A photometer using the photo-conductivity of lead sulphide has been developed and used for stellar measurements in the $1-3\ \mu$ region. The complete circuit is given, and in the description special attention is paid to information that would be of use to anyone building a similar apparatus. Emphasis is laid more on the principles involved in the design than on the technical details. The starlight is interrupted by a chopping disk before reaching the lead sulphide cell, the amplified output of which is rectified synchronously. The advantages of this arrangement are discussed particularly with regard to signal-to-noise relations. A non-linear integrator following the rectifier increases the rate of working by responding more rapidly to signals while the deflection is taking place, than to noise when the final deflection is approached.

The sensitivity of the apparatus is compared with the fundamental limits to sensitivity in the infra-red, and an outline is given of the precautions that would be necessary in order to approach closely the limiting sensitivity. It is shown that it is fundamentally more difficult to detect infra-red radiation than visible light, unless the spectrum of the source corresponds to a temperature as low as that of planets. Thus there is little chance of detecting, in the infra-red, stars that are too cool to be visible.

On the 36-inch Common reflector, the present limit of detectability is about 6th magnitude for a star of type G₀, and the errors due to changes in atmospheric extinction exceed those arising in the apparatus for stars of this type brighter than 4th magnitude. It is shown that at Cambridge the variation of extinction is on the average consistent with proportionality to the secant of the zenith distance, but that irregular changes predominate. Correction for zenith distance is therefore seldom practicable, and stars have been measured at equal altitudes.

A catalogue of 51 lead sulphide magnitudes and colour indices is presented. The list is fairly complete within the limits of sensitivity of the present apparatus and of accessibility to the telescope. The colour indices correlate well with the heat indices of Pettit and Nicholson and with the V-I index of Stebbins and Whitford. The scatter against spectral type is larger than would be expected from the uncertainties of estimation. The M-type stars β And and β Pegs appear to be variable. Some peculiar stars deviate from the normal correlations; space-reddened stars are apparently fainter in the infra-red than would be normal for their visual colour index, and there is some evidence of infra-red emission from stars of type Be. The observations on ϵ Auri are inconsistent with the absolute magnitude that has been ascribed to the infra-red companion.

Recent improvements in photo-conductive detectors of infra-red radiation have made it possible to obtain new information concerning the infra-red radiation from stars. The purpose of the investigation described here was to explore these possibilities using a lead sulphide detector. Infra-red detectors

are fundamentally less sensitive than detectors of visible radiation, and it will be shown in Section 3.2 that they are at a disadvantage even for cool stars which radiate most of their energy in the infra-red. It was essential therefore to concentrate in the first place on obtaining the highest practicable sensitivity from the lead sulphide cells available, rather than to attempt precision measurements. The results suffice, however, to give the dependence on spectral type of the lead sulphide colour index, and of the limiting magnitude which is accessible, with an error apparently less than the natural scatter of these relations, and to indicate the correlation with other colour indices.

I. Optics

The telescope used was the 36-inch Common reflector. Fig. 1 shows the optical arrangement. Radiation from the Newtonian flat is interrupted by a chopper disk just inside the focal plane. A metal mirror intersects the focal plane at an angle of 45° and reflects light into a guiding eyepiece. The mirror is perforated by an elliptical hole which projects on to the focal plane as a circle about $\frac{1}{2}$ mm. in diameter. The starlight to be measured passes through this hole and is refocused on to the detector by a spherical concave mirror. To minimize off-axis working, the beam is twice reflected at an aluminized right-angled prism, as shown in the diagram, and finally emerges along a continuation of its original direction. The whole system is mounted in a duralumin box, attached to a rigid ring of the same material clamped to the telescope frame. Push-pull screw adjustments are provided for the optical parts.

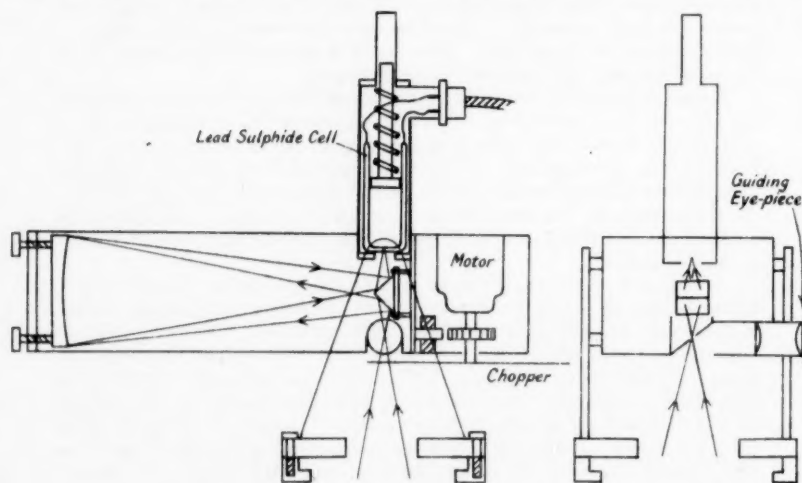


FIG. 1.—Optical system.

The hole in the guiding mirror corresponds to about $30''$ of arc. It has so far been possible to detect infra-red radiation only from bright stars. Consequently, even when the star is centred in the hole, the light scattered by the rim is sufficient for guiding. The accuracy obtained is only just sufficient, however, and this simple arrangement would not work for fainter stars. Another criticism of the optical system is that there is no field ("Fabry") lens or mirror

to image the telescope aperture on the cell. It seemed undesirable to attempt such improvements until the first programme had shown whether a worthwhile infra-red sensitivity would be realized. The chopper wastes half the incident radiation. This loss could be avoided if the radiation were switched between two independent sensitive areas of the cell, for example, by a reflecting chopper disk. The difference in size between the two sensitive areas of the present cell makes it unsuitable for this treatment.

2. Electronics

It is thought that a detailed description of those circuits which follow established practice would be out of place. The discussion will be mainly concerned with showing where special precautions and arrangements are needed. Fig. 2 shows the general arrangement, and the full circuits are shown in Figs. 3-6.

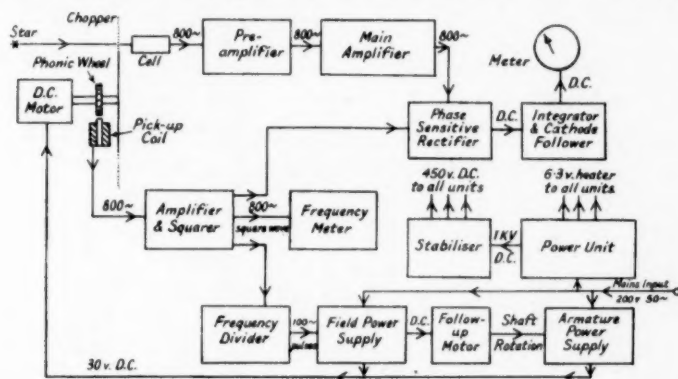


FIG. 2.—General arrangement of photometer.

(1) *Detector*.—The detector is a lead sulphide photo-conductive cell having sensitive areas 3 mm. \times 1 mm., and 10 mm. \times 1 mm. The sensitivity is strongly localized in "hot spots", which are sufficiently small for the focusing of the star on to the cell to be rather critical. One of these spots in the smaller area gave the greatest response and was used in all the observations. The cell was the best of some dozen tested on the telescope. It had also been tested in an earlier spectrometric investigation, and found to be several times less sensitive than the best cells then available. Cells vary in their behaviour on cooling; the present one improves very little and has therefore been used uncooled. The spectral response is shown in Fig. 8a. The equivalent noise power at the peak response is 4×10^{-12} watts.

The response of lead sulphide and telluride cells is almost independent of frequency up to a certain value, depending on the individual cell, beyond which it falls. The noise power is roughly inversely proportional to the frequency. The signal-to-noise ratio therefore has a maximum for a frequency at which the response has fallen somewhat. It is to take advantage of this maximum that the radiation is modulated by a chopper disk. The optimum frequency should be determined for each cell; but it has been customary to use a standard value of 800 cycles, which is about right for most sulphide cells. This value has been used in the present work. The sensitivity of the cell is only slightly greater at its optimum frequency of 1200 cycles.

There is also an optimum excitation current, which was 30 microamp. for the present cell, and this value has been used throughout.

(2) *Preamplifier*.—The main electrical equipment is too heavy to be carried on the telescope and is placed on the floor of the dome. The cable run from there

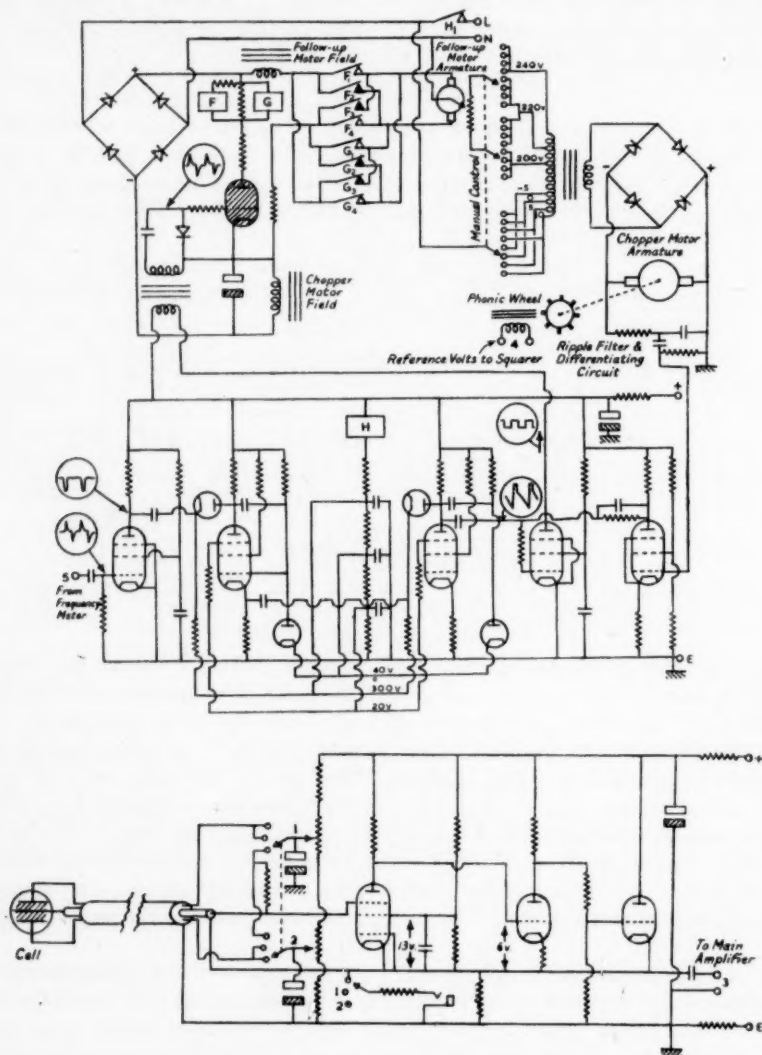


FIG. 3.—Preamplifier and chopper motor control.

to the Newtonian focus is about 8 metres long. The capacity of a screened load of this length connected directly to the cell would attenuate the signal heavily. A preamplifier is therefore needed to match the cell to the cable.

The resistance of lead sulphide cells is usually 10^5 to 10^6 ohms. Telluride cells, especially when used in cooled cavities, may go as high as 10^9 ohms. To

allow high-resistance cells to be tried out, the preamplifier input is taken to an acorn pentode used as an electrometer tube (1). The tube must be protected from changes in D.C. level of the cell output, arising from the applied excitation.

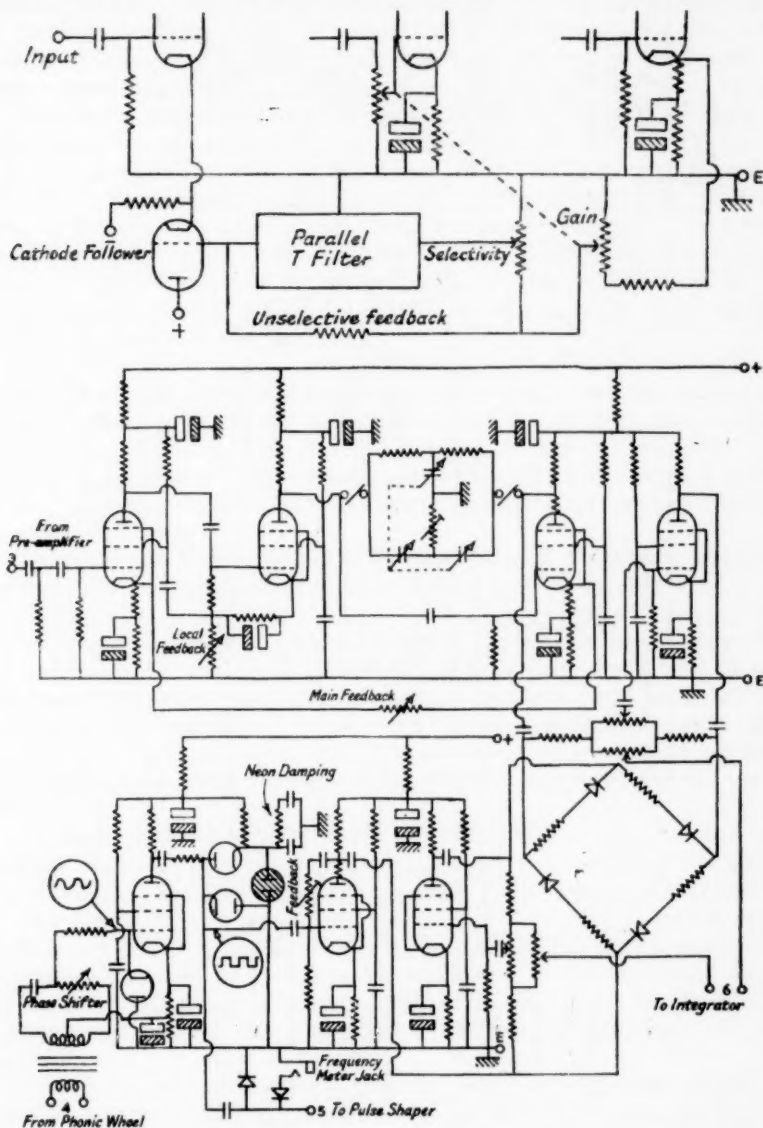


FIG. 4.—Main amplifier, reference amplifier and phase sensitive rectifier.

Top : improved feedback arrangement.

To do this with a series condenser would require a grid leak of 10^{10} ohms. This has been avoided by using direct coupling and compensating for changes in level by feedback to the cathode of the tube. This cathode follower arrangement also

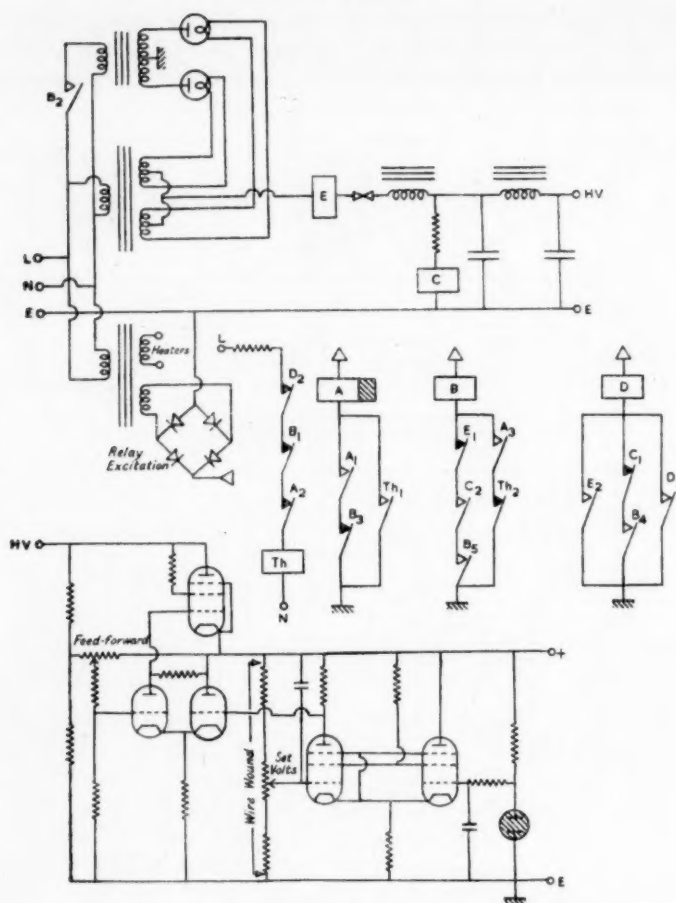


FIG. 5.—Power supply, stabilizer and protection circuits.

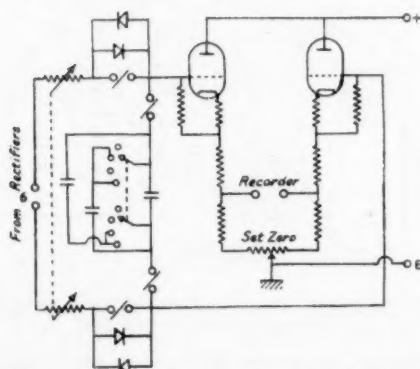


FIG. 6.—Output integrator and cathode follower.

gives the low output impedance necessary to feed the screened cable to the main amplifier. The electrometer tube cannot be used as a cathode follower directly, since the control grid is separated from the cathode. Instead, the action is obtained by using two auxiliary tubes connected as a D.C. amplifier (Fig. 3). As the cathodes carry signal potentials, the transformer exciting the heaters must be well screened to prevent hum and interference getting in through the heater-cathode capacity.

Because the impedance level may be high, the capacity and leakage of the cable connecting the cell to the preamplifier must be small. The insulation is polythene, and a fine wire (No. 44 S.W.G.) is used for the lead carrying the signal. This wire is surrounded by a shield connected to the cathode of the input tube. Some of the effects of capacity and leakage are thereby reduced. The whole is surrounded by an outer shield which is earthed. Serious microphony occurs unless the inner wire is fixed rigidly by fusing it into the polythene. This effect persists when no steady voltage exists across the cable, and seems to imply an electric polarization of the polythene.

The two sensitive areas of a three-electrode cell can be used in push-pull; or the two sides can be excited separately by switching a feed resistance in place of the unused side of the cell, and this arrangement has been used in all the observations. It is important to select the feed resistor for low-current noise. Cracked carbon resistors have been found satisfactory. Wire-wound resistors give little noise but are bulky for values exceeding 100 K Ω . Composition resistors are usually too noisy.

The equivalent noise resistance of the preamplifier is 3 M Ω and it seems from the open circuit time constant that the input resistance exceeds 10^{10} Ω . The equivalent noise resistance of a cell at optimum excitation is commonly some twenty times its actual resistance. The noise factor should therefore be good for cell resistances down to 500 K Ω , below which the efficiency will fall. It seems that the present design has gone too far toward high impedance levels and that a compromise with more usual circuits should be sought, capable of covering the whole range of cell resistance. Lower resistance cells have been tested on the main amplifier for which the equivalent noise resistance is 75 K Ω and the leak 2 M Ω .

(3) *Main amplifier*.—Fig. 4 shows the circuit used. Gain control is by feedback from the cathode of the second stage to the screen of the first. Selectivity is provided by a tunable "parallel T" filter giving negative feedback between the anodes of the second and third stages. To maintain stability of gain, the filter is adjusted so that the feedback has a non-zero minimum at the tuning frequency. There is also overall feedback between the cathodes of the first and last stages. This is normally reduced until it has little effect, but if wide-band working is desired, the filter is switched out and this feedback used to control the gain.

This circuit has been described because it was used in the observations, but it has since been found more convenient to use the circuit shown at the top of Fig. 4 connected between the first and third cathodes. The filter is here adjusted to give a true null, and local feedback is not used. The arrangement depends on the practicability of large gain reduction factors with the feedback circuit in this position, provided the usual precaution is taken of making the frequency response of one stage much narrower than that of the rest of the feedback loop (2).

It has the advantage that the selectivity and gain controls are almost independent. It is desirable to gang the gain control to an attenuator in the amplifier so that the gain reduction factor does not depend on the gain setting.

(4) *Phase sensitive rectifier*.—The final stage of the main amplifier feeds an anode follower phase splitter, and the resultant push-pull signal is applied to a phase sensitive rectifier as shown in Fig. 4. Spurious outputs are minimized if the push-pull action is maintained during overloads. To this end, a resistance of about one-fifth of the anode load is placed in series with the anode of the output valve, so that this valve overloads before the anode follower.

The reference voltage for the rectifier is derived from a phonic wheel on the same shaft as the chopper. It is amplified, squared, and applied in push-pull to the rectifier using an anode follower phase splitter. If the reference voltage is not in phase with the signal, the desired output is reduced but the noise is unaffected. A phase shifter is therefore needed. The circuit shown has been found simpler than the mechanical shifters commonly used.

The reference voltage can be switched off and two opposite arms of the phase sensitive rectifier open-circuited, converting it into an ordinary detector. In the absence of signal, the output is then a measure of the noise in the pass band of the main amplifier. Some such means of determining the noise level is invaluable in the adjustment of the apparatus for best sensitivity.

In this context the important property of a phase sensitive rectifier is that, if the reference frequency is F , an output of frequency f can be caused only by an input of frequency $F \pm f$. Smoothing after the rectifier is therefore as effective in reducing noise as selectivity in the preceding amplifier. In this way the bandwidth can be made as small as we please, whereas the practicable selectivity of an amplifier is limited. Moreover, with a very selective amplifier it is difficult to keep the chopper frequency within the pass band.

In contrast, a rectifier without phase discrimination intermodulates the noise input so that the output at each frequency depends on the whole input spectrum. It is found that if the input bandwidth B is much larger than the output bandwidth b , and if the signal is smaller than the noise in B , then the signal-to-noise power ratio is proportional to $B^{-1}b^{-1}$, and the signal output varies as the square of the input. As the signal increases, the transfer relation becomes linear and the signal-to-noise power tends to the more favourable law of proportionality to b^{-1} , which applies to the phase sensitive rectifier. This is because the signal and not the noise then largely determines when the rectifier conducts. The improvement is less valuable for taking place when the signal-to-noise ratio is already high. In a phase sensitive rectifier the times of conduction are determined by the reference voltage. It may be noticed that the signal and reference are applied symmetrically; it is the larger of the two which in fact acts as reference. Its control over the conduction may be seen to be complete if at every instant the reference exceeds the sum of the signal and output voltages. Square-wave reference is used because it is most favourable to this condition. The foregoing relations are widely known, but I have not found them described in the literature.

It is not easy to maintain a phase sensitive rectifier adjusted so that it attenuates spurious noise components more than about 100 times in voltage. The input bandwidth should therefore not exceed the output bandwidth by more than the square of this factor, 10^4 . We have seen, however, that the input

bandwidth should not be too small. A value of 50 c./s. has been found suitable in the present work.

(5) *Output circuits.*—Fig. 6 shows the integrator and output cathode followers. Time constants up to 20 seconds are provided. The signal is read on a milliammeter or pen recorder. The back-to-back rectifiers which can be switched into the signal path are Westectors type WX 6. These present a high impedance to noise, but when a large signal is applied they break down and permit the smoothing condensers to come quickly to nearly full charge. The resistance and time constant then again increases. For the same degree of noise smoothing, readings can be taken several times as fast as with a linear resistance. The curvature of the characteristics of these rectifiers must not be large enough to cause appreciable intermodulation between noise components.

To check the overall linearity, four pea-lamps are used, placed in the optical path of the telescope and excited in series by current stabilized with a ballast tube. When any lamp is switched out of circuit, a similar dummy lamp screened from the cell is switched in instead (Fig. 7). With this arrangement the brightness of each lamp varies by less than 1 part in 1000 when the others are switched. No deviations from linearity were found greater than the experimental error of less than 1 part in 100; the criterion being that the deflection caused by a number of lamps should be the sum of the deflections they give separately. Observations on actual stars of the effect of stopping down the telescope confirm this result.

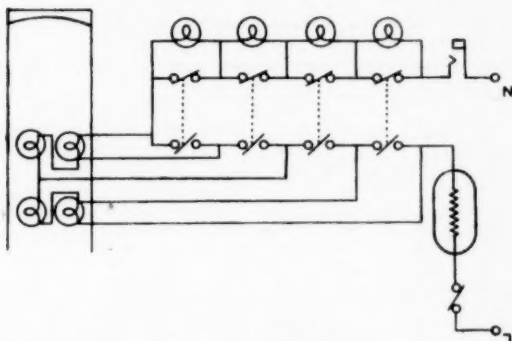


FIG. 7.—Calibrator.

(6) *Chopper motor control.*—The chopping frequency can conveniently be kept within the pass band of the main amplifier by locking the motor to the 50 c./s. mains. At the time the apparatus was built, no suitable synchronous motor could be obtained. A 32-volt D.C. motor was therefore servo-synchronized. Although the arrangement is of interest for some infra-red work, in the type of apparatus we are considering it seems to have no special advantages over the synchronous motors now available. It will therefore not be described; the circuit is shown in Fig. 3, for completeness and because it is not entirely separable from the other parts of the apparatus.

The control system may lock the motor at any one of a number of speeds such that the chopping frequency is a harmonic of the 50 c./s. mains. A frequency meter is therefore provided to help in the selection of the required harmonic

(7) *Power supply.*—A 1 KV. $\frac{1}{2}$ amp. power supply, which was available, has been used, although it is unnecessarily large. The voltage is reduced to 500 in a stabilizer using parallel 807 series valves. A neon tube followed by a long time constant is used as the voltage standard. The stabilizer is rather crude but it has proved satisfactory for the present work.

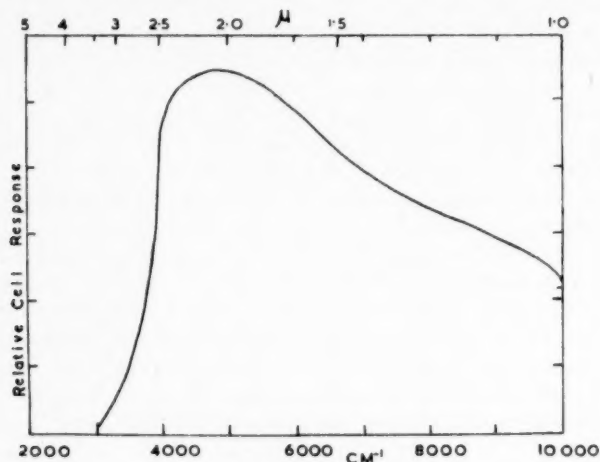


FIG. 8 a.—Spectral response of cell.

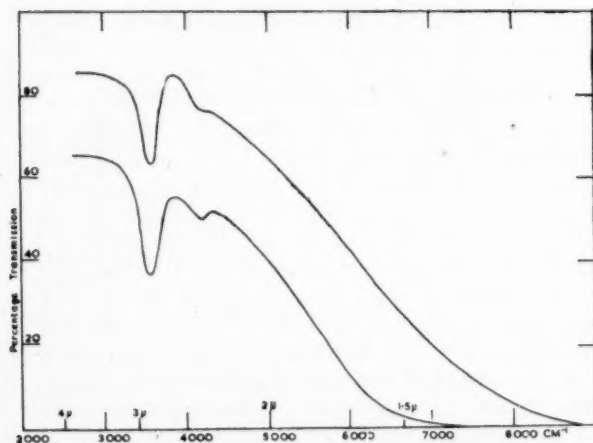


FIG. 8 b.—Spectral transmission of mica filters.

The power supply has comprehensive protection circuits. These delay the switching on of the high voltage until the cathodes of the mercury vapour rectifiers have warmed up. If the mains fail momentarily at any time, the high voltage is switched off for the full delay time. Protection is also provided against overload or open-circuited bleeder chain. Upon a fault developing, the supply is switched off permanently until the relays are cleared by interrupting the mains input. This system has saved the apparatus from damage on several occasions.

(8) *General*.—A voltage gain of about 10^7 is available in the main amplifier. If hum and undesired feedback are to be avoided, care must be taken with the earthing and screening of each stage. An excellent description of the principles involved has been given by Zepler (3). The method of screening which has been most convenient in the present work is to use metal boxes snap-fitting over each stage, the screen running across the middle of the valve-holder. Inductances are difficult to screen at audio-frequencies, and have therefore been avoided in the signal circuits.

Carefully designed earthing and screening are especially necessary when parts of the apparatus are separated by long cables, since, for example, a small gap in a screen may leave a length of cable effectively unshielded. One specific problem may be mentioned. If the only earth connection between one chassis and another is the outer of a screened cable carrying signal and this cable is unplugged, the chassis will be raised to the potential of the plate supply. There must therefore be additional earthing by the cable which carries the positive line of the power supply; but circulating currents may then be induced in the loop formed by this double earthing and spoil the screening. These currents may be controlled by placing a resistance, usually some 50 ohms, in series with the safety earth.

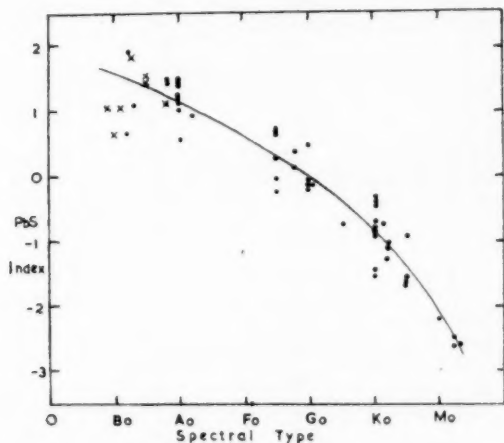


FIG. 9.—Lead sulphide index and spectral type.
Points represent normal stars; crosses, stars of type Be (see text).

Since telescopes and often observing platforms are earthed, it is especially important in astronomical apparatus to make sure that a breakdown will blow a fuse before any chassis can become "live". Three-pin mains wiring is essential. Plugs with "live" pins must be avoided by using "female" connectors where appropriate.

3. Observations

Observations were begun on the brightest and reddest star available, which was Arcturus. As the adjustment of the apparatus was improved and experience gained, a programme could be worked out. Stars of south declination are not well seen from Cambridge, and a peculiarity of the telescope mounting made it difficult to work further north than 50° declination. As Fig. 9 was built up, it

was used as a guide to the limiting visual magnitude. For some very red stars, the limit was set by the guiding arrangements rather than the infra-red sensitivity. Within these limitations the observing list is fairly complete.

The inaccessibility of circumpolar stars made it necessary to use as standard a group of stars that could be compared each with its easterly neighbour, until the Earth had moved far enough round its orbit to enable the last member of the sequence to be compared with the first. The sequence chosen was β Andr, α Auri, β Gemi, α Boot, α Lyra, β Pegs. When the measurements round this ring had been closed, the accumulated error was distributed equally between the comparisons. Fainter stars were compared with the standard sequence. The zero of magnitude has been chosen to make the colour index against visual magnitudes vanish for the type Go.

In addition to these observations with the cell unscreened, the brighter stars have been measured, using two filters of different thicknesses split from the same block of selected biotite mica. The spectral transmissions are shown in Fig. 8*b*.

The results are presented in Table I. The visual magnitude and spectral type are taken from Schlesinger (4).

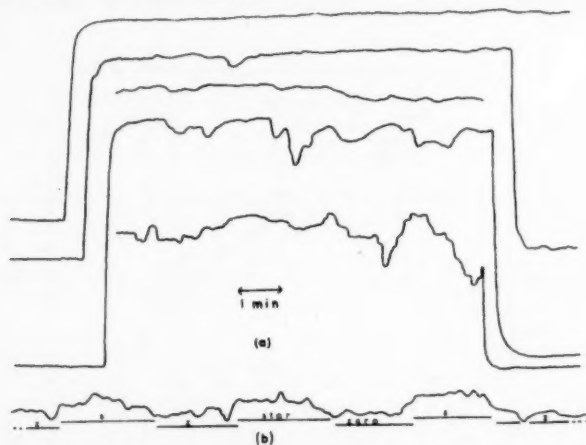


FIG. 10.—(a) Pen tracings showing variation in atmospheric extinction. (b) Lalande 21185.

(1) *Procedure, atmospheric effects and accuracy.*—The procedure in the classical radiometric investigations appears to have been to observe star A at a certain zenith distance taking ten deflections and zeros, then in succession the programme stars B, C, etc., returning to A after some hours when its zenith distance had altered, and from the change in deflection deducing a “zenith extinction for the night”. The ten deflections on each star were reduced according to formulae based on expansion in power series of the fluctuations disturbing the measurement. Although, except for blue stars, rather similar spectral ranges are important for lead sulphide and for thermal detectors, it was found that such procedures were not appropriate in the present work.

In Fig. 10*a*, reproduced from pen recordings, the upper trace shows the noise level on the deflection produced by the calibrator lamps. The others show typical variations in the apparent intensity of stars under conditions of atmospheric transparency ranging from excellently steady to very patchy. Such fluctuations

TABLE I

Star	m_v	mp_{PbS}	$mp_{\text{PbS}} - m_v$	Mica Ratios*		Spect.
α Andr	2.15	3.28	1.13			Aop
β Andr	2.37	0.15	-2.22	0.45	0.28	Mog
γ Andr	2.28	1.36	-0.92	0.35	0.25	Kog
δ Andr	3.49	2.41	-1.08	0.46		K2g
α Arie	2.23	1.17	-1.06	0.45	0.20	K2g
α Auri	0.21	0.10	-0.11	0.35	0.18	Gog
β Auri	2.1-2.2	3.10	1.0			Aop
ϵ Auri	3.3-4.1	3.25†	-0.05	0.25	0.10	F5pc
η Auri	3.28	4.4	1.1			B3c
ζ Auri	3.94-5.6	2.43‡	-1.51	0.39	0.24	Ko, B1c
ι Auri	2.90	1.60	-1.30	0.28	0.19	K2g
θ Auri	2.71	4.2	1.5			Aop
α Boot	0.24	-0.67	-0.91	0.36	0.20	Kog
α C Min	0.48	1.13	0.65	0.23	0.12	F5
α Cass	2.1-2.6	1.58	-0.8	0.36	0.24	Kog
δ Ceph	3.7-4.4	3.96	-0.09			Go
ζ Ceph	3.62	2.13	-1.49	0.40	0.20	Koc
α Cygn	1.33	2.25	0.92	0.20		A2p
β Cygn	3.2	2.30	-0.9	0.38	0.16	Ko, Ao, B9g
γ Cygn	2.32	2.42	0.10			F8pc
δ Cygn	2.97	4.4	1.43			Ao
ϵ Cygn	2.64	1.94	-0.70	0.34	0.23	Kog
β Drac	2.99	2.75	-0.24			Go
α Gemi	1.5	2.80	1.3			Ao
β Gemi	1.21	0.89	-0.32	0.31	0.15	Kog
γ Gemi	1.93	3.39	1.46			Ao
ϵ Gemi	3.18	2.45	-0.73			G5c
η Gemi	3.2-4.2	1.24	-2.5	0.42	0.22	M2g
μ Gemi	3.19	0.59	-2.60	0.39	0.22	M3g
ξ Gemi	3.40	3.98	0.58			F5
ζ Herc	3.00	3.48	0.48			Go
η Herc	3.61	3.25	-0.36			Ko
μ Herc	3.48	4.1	0.62			G5
π Herc	3.36	2.39	-0.97			K5
α Leon	1.34	2.75	1.41	0.19	0.02	B8
γ Leon	2.3	1.55	-0.75	0.33	0.18	K1
ϵ Leon	3.12	2.95	-0.17			Gopc
α Lync	3.30	1.69	-1.61	0.39	0.22	K5g
α Lyra	0.14	1.33	1.19	0.21	0.04	Ao
γ Orio	1.70	3.62	1.92			B2
α Pegs	2.57	3.13	0.55			Ao
β Pegs	2.61	-0.05	-2.66	0.51	0.30	M2g
γ Pegs	2.87	3.56	0.69			B2
α Pers	1.90	2.13	0.23	0.30	0.11	F5c
β Pers	2.2-3.5	3.27§	1.1	0.07		B8
γ Pers	3.08	2.84	-0.24	0.28		F5, A3c
α Taur	1.06	-0.60	-1.66	0.50	0.31	K5g
β Taur	1.78	3.23	1.45			B8
θ U Maj	3.26	3.63	0.37			F8p
ψ U Maj	3.15	2.66	-0.49			Ko
μ U Maj	3.21	1.52	-1.69	0.39	0.19	K5

* Fraction of intensity passed by the two mica filters.

† ϵ Auri at max.‡ ζ Auri. Unchanged in eclipse.§ β Pers at max.|| β Andr and β Pegs. Variable.

always made it necessary to bracket each observation of a star A between two observations of the comparison B; usually the double bracket $A_1B_1A_2B_2$ was observed and the brightness ratio taken as $\{(A_1 + A_2)/4B_1\} + \{A_2/(B_1 + B_2)\}$. The changes in transparency made speed in completing the bracket important for accuracy. Therefore only three deflections and zeros were normally taken in each observation. They were reduced by forming the simple mean, since reduction formulae can be justified only by reference to the spectrum of the fluctuations disturbing the measurement, which was not determined. The mica filter measurements were intended mainly as a check on the effective wave-length of the cell, and are the less reliable because of the loss of intensity in the filter and because they could not be allowed to slow appreciably the taking of the brackets. It has appeared qualitatively that visual and lead sulphide extinctions are well correlated, in agreement with measurements made with a horizontal light path at ground level (5).

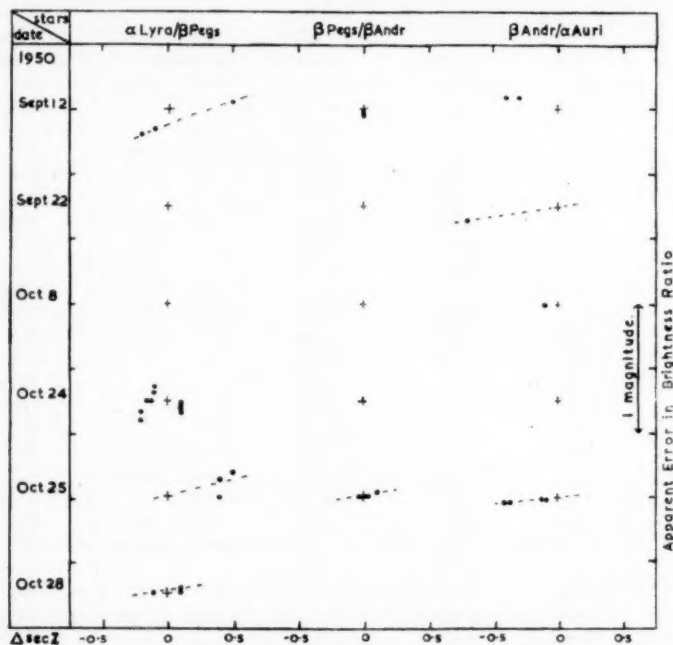


FIG. 11.—Variation of extinction with zenith distance. The points represent individual measurements, and the crosses the magnitude difference derived from all the observations.

An investigation was made of the effect of zenith distance on intensity, and the results are plotted in Fig. 11. When stars are compared, only relative extinctions can be determined. Each column of the figure refers to one pair of stars, and each row to a single night. The points show, with arbitrary zero, the observed difference in magnitude between the two stars as a function of the difference in the secants of their zenith distance, $\Delta \sec z$, at the time of observation. The crosses at $\Delta \sec z = 0$ show, with the same zero, the difference in magnitude estimated from all the observations. The values of $\sec z$ were found from a

clinometer on the telescope (6), or by circles of equal $\sec z$ drawn on an equatorial stereographic net (7). Since, in most azimuths, the telescope will not reach values of $\sec z$ greater than 1.6, special planning was needed to obtain values of $\Delta \sec z$ as high as in the diagram. Even without any intent to keep the difference small, convenience would ensure that in ordinary work $\Delta \sec z$ would usually be smaller than 0.2, since the mounting becomes increasingly difficult to manoeuvre for $\sec z$ greater than 1.3.

The points seem as consistent with a $\sec z$ extinction law as with any other, and indicate a zenith extinction of about 0.2 magnitudes on all nights. The extinction is perhaps 0.05 to 0.1 magnitudes greater for Vega than for the other stars. This differential extinction would be expected, since the effective wave-length is shorter the hotter the star. When the transparency is poor, Vega consequently appears faint compared with other stars, and the proportion of its energy passed by the filters is increased. In light mist this proportion for the thin mica filter was found to be 0.25 compared with its normal value for Vega of 0.19.

Despite the regularities shown by Fig. 11 it seems that the concept of zenith extinction has little meaning in the climate of Cambridge, except as a rough average. The transparency often changes rapidly, and indeed it is rare to observe for a whole night without cloud intervening; the small range of $\Delta \sec z$ shown for some of the nights is due to such interruption. Moreover the figure shows that errors may occur which exceed the maximum correction for zenith distance possible with the present telescope, and that these may persist for hours without change of sign. It was verified, by readjustment for various orientations of the telescope, that no such error was introduced by a flexure of the optical system. Comparisons over large distances, and therefore especially of the standard sequence, are unreliable because of these errors unless repeated on several nights; repetitions on the same night are of little value. Except in special circumstances, therefore, stars were compared only at similar zenith distances and no attempt was made to apply a correction.

It was often impossible to detect even considerable unsteadiness of the extinction by visual inspection of the sky, and latterly a record of the kind shown in Fig. 10 has been taken at the beginning of each period of work. Moonlight and twilight do not interfere with infra-red detectors; and, by revealing any thin cloud obscuring the star being measured, their presence can increase accuracy and enable observations to be made in weather that would otherwise be unsuitable.

The stars listed have been observed on from one to eight occasions, sometimes using different standard stars. The internal consistency indicates a mean square error of 0.09 magnitudes for a single comparison. This estimate is based on all the data, including faint stars and observations made while the technique was being developed. More repetitions have been made for stars observed when the atmospheric extinction was less steady, so that the final accuracy is to some degree equalized and corresponds to about two observations per star.

The standard sequence was observed when conditions were especially steady, and each comparison was repeated sufficiently often to reduce the mean square error to 0.02 magnitudes. The first set of observations, made over a period of about a year while the sequence was being chosen, closed with the intolerable error of 0.35 magnitudes. The sequence was repeated and, to reduce as far as possible errors due to any variability of the stars, it was completed in a few months

by taking advantage of the long winter nights. The differences in magnitude found from the two sets of observations are as follows:—

Star	α Boot	α Lyra	β Pegs	β Andr	α Auri	β Gemi	α Boot
Type	Ko	Ao	M2	Mo	Go	Ko	Ko
Δm	-0.02	-0.02	0.12	0.24	0.04	0.01	0.27

The zero of Δm is arbitrary. The values are uncorrected for closing error; therefore the differences shown are cumulative, and one star (α Boot) is listed twice. If the differences for β Pegs and β Andr were due to errors of measurement, the probability of the cumulative difference returning to a small value, as it does in the two succeeding columns, would be less than 0.001. It seems therefore that these two stars are slowly variable, and this is not unlikely in view of their late spectral type. The cumulative divergence from α Boot to β Gemi is only 0.03 magnitudes, and this represents excellent agreement between the two sets of observations. There is serious disagreement, however, in the direct comparison of β Gemi and α Boot. The fault is certainly in the earlier set of observations, and it accounts for the majority of the closing error. The erroneous comparison was based on only two nights, 1950 March 22 and 24, but the agreement both within each night and between the two was almost perfect. The angular separation of β Gemi and α Boot is wider than for any other consecutive pair, and it is suggested that the error was caused by haze over the town of Cambridge, the centre of which is about a mile east of the observatory. An anticyclone was developing at the time, and a weak trough passed through and gave cloud on March 23.

The second series closed with an error of 0.16 magnitudes. The probability of this being caused by the random errors is 0.06, and it is consistent with the suggestion that the transparency may be systematically lower in the east. From the Gog Magog Hills a bank of smoke and haze, which might well cause such an effect, can often be seen coming from the town and drifting eastwards on the prevailing wind.

In the final reduction of the standard sequence, the mean of both series of observations has been used, omitting only the earlier comparison of β Gemi and α Boot. But the two supposedly variable stars β Pegs and β Andr have been assigned the magnitudes they were observed to have at the epoch when they were used as standards. It is at present necessary to use as standards stars which are bright to lead sulphide, and these are likely to be late-type giants which tend to be variable. The objections to this use of such stars are minimized if the above precaution is taken.

(2) *Sensitivity and scope.*—The signal to “peak to peak” noise ratio is ≈ 150 for stars of first lead sulphide magnitude (as defined below) for a deflection time of about 10 seconds. As this is using the non-linear integrator described above, it is not possible to say exactly what the bandwidth is. The fluctuations caused by the atmospheric effects described in Section 3 (1) begin to be exceeded by the noise level of the cell for PbS magnitudes fainter than 3.5. The faintest PbS magnitude that can be detected is about 6. Fig. 10*b* shows the deflection produced by Lalande 21185 magnitude $m_v = 7.6$ $m_{PbS} \approx 5.5$. The scope of the present apparatus with a 36-inch telescope at about sea-level is thus, for red stars, rather similar to that of a thermocouple with a 100-inch telescope on a mountain site.

It has been pointed out that the present chopping arrangement introduces a certain loss in sensitivity. It may be possible to reduce the number of times the radiation is reflected and to improve the infra-red reflectivity of the coatings on the mirrors, since the present ones were intended for visual wave-lengths. By these means, the sensitivity can probably be increased by a factor of between 2 and 4, the lower figure being more likely. Further improvements will depend on using more sensitive cells. I have measured lead sulphide and telluride cells eight times as sensitive as the present cell (9), and these would be better by a factor of 2-5 if the area could be reduced to that required in stellar work. A further factor of 2-5 can be obtained by using the cells in cooled cavities (10, 11). Thus we may hope for a total improvement of ≈ 100 times compared with the present apparatus by using simultaneously these methods which have been shown to be separately practicable. This represents a close approach to fundamental limits. The chief obstacle is the availability of suitable cells. The making of cells with the required properties is still fortuitous, and the chance of being able to select such exceptional cells is reduced by several circumstances. Cells are seldom made with areas as small as is desirable for stellar work. Much development has been based on tests which are designed to simulate some practical use and bear little relation to the overall potentialities, which can be assessed only if the sensitivity is measured as a function of wave-length. Since cells must be used in cooled enclosures when the highest sensitivity is required, it is unfortunate that so many cells are made to meet the industrial demand for sensitivity at room temperature. This is especially so since there is evidence that comparatively simple photo-conductors perform well when cold, that the main difficulty of manufacture lies in the treatment required to give sensitivity at ordinary temperatures, and that this treatment may reduce rather than improve the sensitivity when cooled. An increase in the scientific demand for cells would do much to overcome these difficulties.

It has been shown (9) that the possible sensitivity of infra-red detectors is limited by statistical fluctuations in the thermal radiation which they receive from their surroundings, and that the performance of the best lead sulphide and telluride cells is within a factor of 2-3 of the limit for room temperature. Consider the effect of these fluctuations in disturbing the measurement of radiation from a small black-body source at temperature T_1 , in the presence of a much larger amount of radiation from surroundings at a temperature T_2 . The fluctuation in $m d\nu$, the number of quanta having frequencies between ν and $\nu + d\nu$, falling in 1 second on 1 sq. cm. of a detector is given by (*loc. cit.* equation (3.27))

$$\overline{\Delta m^2 d\nu} = \frac{2\pi}{c^2} \frac{\exp(h\nu/kT_2) \nu^2 d\nu}{\{\exp(h\nu/kT_2) - 1\}^2}, \quad (1)$$

where c is the velocity of light, h Planck's constant and k Boltzmann's constant. The number of quanta in the same frequency range radiated by 1 sq. cm. of the target in 1 second is given by (*loc. cit.* equation (3.21))

$$m d\nu = \frac{2\pi \nu^2 d\nu}{c^2 (e^{h\nu/kT_1} - 1)}. \quad (2)$$

With any optical system, the ratio of the square of the signal from the target to the mean square fluctuation from the surroundings is therefore proportional to

$$f(\nu) d\nu = \frac{m^2}{\Delta m^2} = \frac{2\pi}{c^2} \frac{(e^{x_1} - 1)^2 \nu^2 d\nu}{(e^{x_2} - 1)^2 e^{x_1}}, \quad (3)$$

where $x_1 = h\nu/kT_1$, $x_2 = h\nu/kT_2$. This formula has many uses in the design of radiation experiments; it has been derived here in order to show the frequency at which the signal-to-noise ratio is a maximum. This is found by differentiating $f(\nu)$ logarithmically and equating to zero, giving after some manipulation

$$\frac{2x_2}{1 - e^{-x_2}} - x_2 - \frac{2x_1}{1 - e^{-x_1}} + 2 = 0. \quad (4)$$

For $T_1 = T_2$, the solution is $h\nu/kT = 2$. Other solutions are readily obtained numerically by computing a table of $g(x) = x/(1 - e^{-x})$. They are plotted in Fig. 12, which therefore gives the frequency at which the target would be most

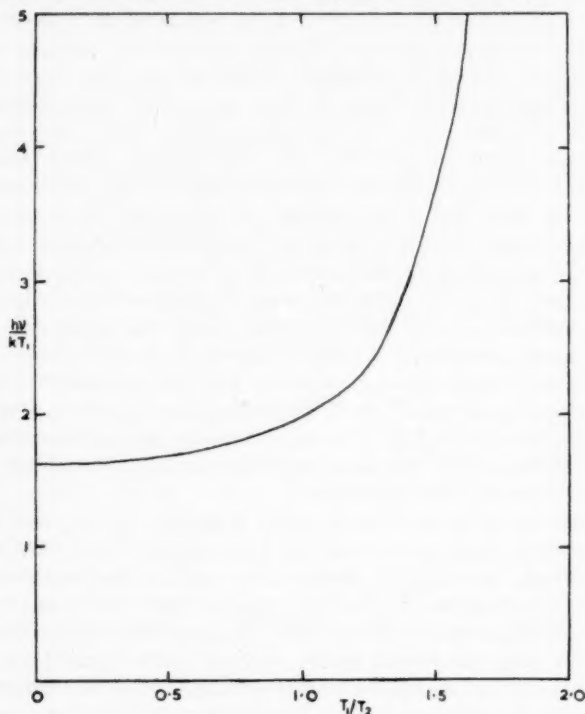


FIG. 12.—Optimum frequency for observing targets at temperature T_1 with surroundings at temperature T_2 .

easily detectable by an ideal radiation detector. At low frequencies, the magnitude of the fluctuation is independent of ν , as is well known in the radio region (see, for example, *loc. cit.* Section 4 (3)). The optimum for a cool target is therefore at the maximum of the black-body curve of the target with respect to frequency and number of quanta, which is at $h\nu/kT_1 \approx 1.60$. (The maximum with respect to energy and wave-length at $h\nu/kT \approx 5$ is the one most frequently quoted but it is often, as here, misleading.) The optimum frequency rises, as we have seen, to $h\nu/kT = 2$ when the target is at the same temperature as the surroundings of the detector, and thereafter rises quickly and diverges when $T_1 \geq 2T_2$. For in equation (4)

$$\text{Left-hand side} \geq x_2 - \frac{2x_1}{1 - e^{-x_1}} + 2,$$

and if $T_1 \geq 2T_2$, $x_2 \geq 2x_1 = 2x$ (say) and

$$\text{Left-hand side} \geq 2x - \frac{2x}{1 - e^{-x}} + 2 = 2 \left\{ 1 - \frac{xe^{-x}}{1 - e^{-x}} \right\}.$$

This can vanish only if

$$xe^{-x}/(1 - e^{-x}) \geq 1,$$

that is

$$xe^{-x} \geq 1 - e^{-x}, \quad e^{-x}(1+x) \geq 1, \quad (1+x) \geq e^x,$$

which is impossible for $x > 0$, since $e^x = 1 + x + (x^2/2!) + \dots$.

The fluctuations to which a detector is exposed can be reduced almost indefinitely by enclosing it in a sufficiently cold cavity, and it has been found possible in practice to realize a considerable improvement by this means (11). In astronomy, however, the detector is necessarily exposed to thermal radiation from the lower atmosphere and from the optical surfaces of the telescope, which will usually both be at a temperature of about 270 deg. K. An absorption of only $\frac{1}{2}$ implies a radiation of $\frac{1}{2}$, and a fluctuation of $\sqrt{\frac{1}{2}} \approx 0.6$ of the corresponding quantities for black body. It is a fair approximation therefore to assume the fluctuations have the same spectral distribution as would be given by a black body at this temperature. With this value substituted for T_2 , the foregoing analysis shows the spectral frequency at which a celestial object of temperature T_1 would be most easily detectable by an ideal detector in which the fluctuations in output are caused entirely by fluctuations in the incident radiation. But it is also a useful indication of what may be expected in practice, since the best actual detectors covering between them a wide spectral range, fall short of ideal performance by a noise factor that is less than about 6, and therefore varies comparatively little. It has been shown (*loc. cit.*) that this is true of photo-emissive and photo-conductive cells, thermal detectors and radio receivers.

It is especially to be noted that the laws of radiation are not favourable to the use of infra-red detectors for sources hotter than about 550 deg. K., that is, twice the absolute air temperature. The above treatment is too fundamental to take account of many factors which are very important practically, such as the greater relative amount of auroral and scattered atmospheric radiation at visible frequencies and the peculiarities of various types of detector. Nevertheless, it appears that except for bodies of planetary temperature, infra-red work will always be at a disadvantage in sensitivity compared with that at higher frequencies.

The divergence of the optimum for $T_1 \geq 2T_2$ does not mean that observations should really be at γ -ray frequencies. We have used the approximation that the signal is small compared with the radiation from the surroundings, and therefore neglected the noise level on the signal itself, which is an aspect of the smallness of the rate of arrival of quanta. More exact treatment (10) shows that the optimum frequency remains finite, usually in the visible region, and that it depends on the time available for the observation.

(3) *Discussion.*—The lead sulphide colour indices are plotted against spectral type in Fig. 9. The root mean square scatter, regarded as error in colour index, is 0.3 magnitudes. This exceeds the scatter attributable to error in the quantities plotted and seems therefore to be real. There is little difference if Mount Wilson spectral types are used. The stars later than G0 are unfortunately all giants or super-giants, because of observational selection. Therefore the figure would not show an absolute magnitude effect if this existed only between G0 and K5, as it does for the colour indices of Stebbins and Whitford (12). A similar scatter is

found when the lead sulphide indices are compared with the colour indices of Hall (13) and Gussow (14), and, indeed, when these are compared with each other or with the indices discussed below. Since, however, the total range of these indices is small, the value will be sensitive to local disturbance of the spectrum and to actual errors of measurement.

Fig. 13 shows that the lead sulphide indices do correlate much more closely with indices of greater total range. In the comparison with the heat indices of Pettit and Nicholson (8) close correlation would not be expected among early-type stars, since for these the radiometric intensity is mostly ultra-violet, to which the sulphide is insensitive. For other types, the mean deviation from a straight line is 0.08 magnitudes, omitting η Gemi, which is composite and variable, and μ Gemi, which is also of type gM3 and may therefore be variable. It is surprising that almost one-third of this deviation should be due to such a well observed star as α Boot, and it is possible that this star may really be exceptional. It has been said to belong to Baade's population II.

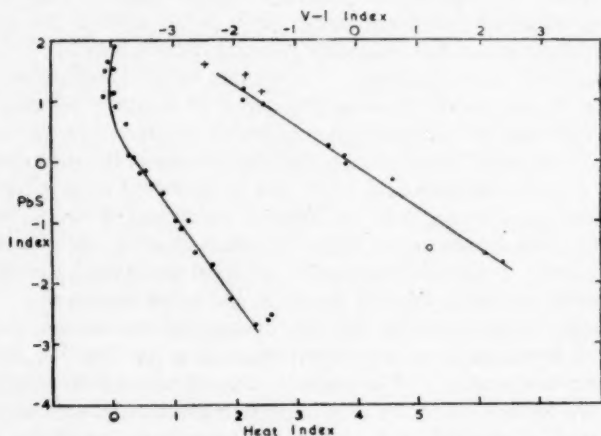


FIG. 13.—Comparison of lead sulphide index with (on the left) heat index and (on the right) the V-I index of Stebbins and Whitford. Points represent normal stars; the circle, the composite star β Cygn; crosses, the reddened stars ζ and ξ Pers, and the comparison star ϵ Pers (see text).

The spectral sensitivity of the lead sulphide cell is similar to the absorption spectrum of a water cell. A comparison has been made between the sulphide colour index and a colour index based on the intensity *absorbed* by the water cell, in the work of Pettit and Nicholson. It is found that there are no systematic differences between these two indices; therefore, the relation of stellar temperature to spectral type derived from the present work would be little more than a re-calculation of the results of Pettit and Nicholson. The mean scatter is 0.26 magnitudes, and it seems that this may be largely due to errors in the water cell measurements, since Pettit and Nicholson (according to their Fig. 2) find this amount of scatter between their water cell measurements and those of Coblentz.

For the comparison with the "V-I" index of Stebbins and Whitford's six-colour photometry (12) the mean deviation from a straight line is 0.07 magnitudes, omitting the composite star β Cygn. The number of stars common to the two programmes is too small for any but tentative conclusions to be reached;

but this close agreement is in accordance with the suggestion of recent work in the visible that suitable colour indices correlate more closely with each other than with the spectral type. If this is confirmed, the scatter relative to spectral type may be ascribed to a parameter which is different for different stars in the main sequence. There is already a suggestion that brightness is more closely related to colour than to spectrum (15).

Some peculiar stars have been examined to find whether they deviate from the normal correlations. The infra-red intensity of ϵ Auri is greater than the average for its spectral type, but only just outside the scatter of the points, and it follows exactly the normal relation with the "V-I" index. In effect, ϵ Auri behaves both in the visible and infra-red as if its spectral type were about a class "later" than is observed. This seems inconsistent with the existence of a companion of the size and absolute magnitude that has been postulated (16, 17, 18, 20). Bondi, in a private communication, indicates that according to his calculations ϵ Auri B would be expected to radiate only about $\frac{1}{10}$ of the intensity given by the mass-luminosity law, if its structure is that postulated in the Hoyle-Lyttleton theory of red giants (*M.N.*, 109, 614, 1949).

The stars ϵ , ζ and ξ Pers are represented by square crosses (+) in Fig. 13. These stars have been used by Whitford (19) in measurements of the wave-length dependence of space absorption; ζ and ξ Pers are space reddened and ϵ Pers is a normal star used as a comparison. The two reddened stars appear 0.2-0.3 magnitudes fainter in the infra-red than would be normal for their "V-I" index, as would be expected from the absorption law found by Whitford, which has a "knee" in the red. The unreddened star ϵ Pers follows the normal correlation with the "V-I" index. The following Be stars (21, 22, 23) have been measured and are represented by diagonal crosses (\times) in Fig. 9: η Taur, β C Min, α Caml, ζ Taur, χ^2 Orio, ν Gemi, κ Cass. The mean lead sulphide index of this group is 1.2 ± 0.06 , which is 0.2 magnitudes brighter in the infra-red than is normal for the average spectral type. The difference is perhaps just significant statistically. Unfortunately "V-I" indices, which would give a more critical comparison, are not available for these stars. The mica ratios of the Be stars γ Cass and β C Min seem abnormally high, respectively 0.18, 0.07 and 0.27, 1.10, corresponding to normal stars of type A5 and F3. The interpretation of these results should take into account the association of several of the Be stars investigated with nebulosity, which may modify the infra-red intensity, quite apart from any effect associated with the presence of emission lines in the spectrum. Lead sulphide measurements on these early-type stars are delicate, because of the relatively small amount of energy that is radiated in the infra-red. Therefore, although conclusions may be drawn as to the general trends of the results, the data for individual stars must be regarded as liable to revision.

Some miscellaneous experiments have been made. Scans across the Moon show variations in intensity similar to those in the visible, but apparently with smaller contrast, especially when the mica filters are used. Plans to observe the Moon in eclipse were twice frustrated by cloud. A considerable area has been scanned around the positions given for radio sources in Cygnus and Cassiopeia, but without result.

4. Conclusions

It has been shown that lead sulphide can yield a useful sensitivity in astronomy, and a technique of observation has been developed. The observations encounter the difficulties of infra-red work, combined with those which arise when widely

separated stars are compared and which have been quoted as creating the central problem of bright-star photometry. These difficulties could be segregated to some extent by measuring lead sulphide indices directly, and deriving the lead sulphide magnitudes by combining these colour indices with the technically easier visual comparisons of intensity. For this purpose the infra-red photometer would be combined with one working in the visible, which could be extremely simple because of the more favourable signal-to-noise relations in this region of the spectrum. Since it is the colour indices that have been the more useful in the previous discussion, it is unfortunate that these have had to be derived by the indirect process of comparing catalogues of visual and infra-red magnitudes. The proposed method would avoid this objection.

It was found that in making wide comparisons, more time was spent in moving the telescope than in actually making measurements. The telescope was therefore being used very inefficiently; in this respect visual observations, photography and photometry form an ascending series in the demands they make on the mounting, and a mounting which is suitable for one type of work may be inadequate for a later type, as anyone knows who has used modern techniques on an old telescope. This suggests that in a telescope intended for photometry, it would be economical to provide special facilities for rapid setting.

The value of the observations obtained is reduced by the relative neglect of bright stars in recent photometry, which results in a scarcity of data with which to compare the present measurements. It is probable however that for normal stars there is a close correlation between infra-red colour indices and the visual indices of the six-colour photometry of Stebbins and Whitford, the observed scatter agreeing closely with the estimated error of measurement. The exactness of the correlation should make it a sensitive criterion of normality. Certain stars which are space reddened, abnormal in spectrum, or binary, have been found to deviate from this relation or from the normal correlation with spectral type.

The work was undertaken to find what information could be obtained by observations in a spectral region hitherto inaccessible with sufficient sensitivity. Although it has already yielded results which are of interest in specific problems of astronomy, it seems that the chief contribution lies in the information that has been gained of methods which are likely to be fruitful in further work. In particular, it seems that it is, at this stage, more important to use every resource to increase cell sensitivity than to use a larger telescope. In this way advantage would be taken of the high manoeuvrability that a modern telescope of moderate size can have. It would be advantageous to observe in a drier climate. Particular attention should be paid to stars for which modern photoelectric colours are available for comparison with the infra-red data.

Acknowledgments

I take pleasure in acknowledging my indebtedness to Professor R. O. Redman and Dr E. H. Linfoot for their help and advice throughout the programme. I am also most grateful to my wife Mary Caroline for assisting with the majority of the observations, and to Miss B. Middlehurst, Dr D. E. Blackwell, Mr D. W. Dewhirst and Mr H. V. Stopes-Roe, who have also given much help in this way.

*The Observatories,
Cambridge :
1951 May.*

References

- (1) Gabus, G. H. and Pool, M. L., *Rev. Sci. Instrum.*, **8**, 196, 1937.
- (2) Terman, F. E., *Radio Engineers' Handbook*, 1st ed., McGraw Hill, New York, 1943, p. 398.
- (3) Zepler, E., *The Technique of Radio Design*, 2nd ed., Chapman & Hall, London, 1951.
- (4) Schlesinger, F. and Jenkins, L. F., *Catalogue of Bright Stars*, 2nd ed., Yale Univ. Obs., New Haven, 1943.
- (5) Admiralty Research Laboratory and Telecommunications Research Establishment, *Atmospheric Transmission in the 1-14 μ Region*, ARL/R4/E600, 1949.
- (6) Cousins, A. W. J., *M. Notes Ast. Soc. S. Africa*, **9**, 38, 1950.
- (7) Debenham, F., *Astrographics*, 2nd ed., Heffer, Cambridge, 1942, p. 49.
- (8) Pettit, E. and Nicholson, S. B., *Ap. J.*, **68**, 279, 1928.
- (9) Fellgett, P. B., *J. Opt. Soc. Amer.*, **39**, 970, 1949.
- (10) Fellgett, P. B., Thesis, Cambridge Univ., 1951. Also reference 9.
- (11) Watts, B. N., *Proc. Phys. Soc.*, **62**, 457, 1949.
- (12) Stebbins, J. and Whitford, A. E., *Ap. J.*, **102**, 318, 1945.
- (13) Hall, J. S., *Ap. J.*, **79**, 145, 1934.
- (14) Gussow, M., *Zs. f. Astrophys.*, **20**, 25, 1939.
- (15) Eggen, O. J., *Ap. J.*, **112**, 141, 1950.
- (16) Kuiper, G. P., Struve, O. and Strömgren, B., *Ap. J.*, **86**, 570, 1937.
- (17) Kuiper, G. P., *Ap. J.*, **87**, 213, 1938.
- (18) Hall, J. S., *Ap. J.*, **87**, 209, 1938.
- (19) Whitford, A. E., *Ap. J.*, **107**, 102, 1948.
- (20) Whitford, A. E., *Harvard Obs. Monograph*, No. 7, Centennial Symposium, 1948.
- (21) Merrill, P. W. and Burwell, C. G. *Ap. J.*, **78**, 87, 1933.
- (22) Baldwin, R. B., *Ap. J.*, **92**, 82, 1940.
- (23) Baldwin, R. B., *Ap. J.*, **94**, 283, 1941.

PROPER-MOTION DISTRIBUTION AND MEAN PARALLAXES OF THE STARS OF THE *GENERAL CATALOGUE* IN DIFFERENT GALACTIC LATITUDES AND LONGITUDES

F. Schmeidler

(Communicated by the Director of the Cambridge Observatories)

(Received 1951 June 15)

Summary

The stars of the *General Catalogue* have been grouped according to spectral type, magnitude and galactic coordinates, and frequency tables giving the distribution of the observed proper motion in both coordinates have been constructed. The dispersions in the two components of the proper motion have been calculated from Charlier's formulae of mathematical statistics. The computed dispersions, corrected for accidental observational errors, are proportional to the mean parallaxes of the corresponding group of stars. The distribution of linear stellar velocities is given by the velocity ellipsoid. The resulting mean parallaxes depend on galactic longitude, showing a maximum in the direction towards the galactic centre ($l=345^\circ$) and a minimum in the opposite direction. A total absorption of $0^m.4$ in the direction towards the galactic centre could explain the effect.

Introduction.—For a comprehensive study of the distribution and the motions of the stars, observational data covering the whole sky and complete down to any magnitude are of greatest value, and may be considered as conclusive as far as the accuracy of the data admits. The proper motions of the *General Catalogue* of B. Boss, which contains all stars brighter than 7^m , as well as a considerable number of fainter stars, should therefore give a complete picture of the system of the brighter stars. Among other possibilities they allow us to study the question whether the general features of stellar distribution depend on galactic longitude or whether there exist any irregular differences between different parts of the sky. Our data on the proper motions of the brighter stars are now largely complete, whereas earlier investigations had mostly to use observations from restricted parts of the sky which did not cover all galactic longitudes. The present paper is an attempt to investigate differences of stellar motion, and especially of mean parallaxes, in different parts of the sky.

The derivation of mean parallaxes from proper motions can be done in two different ways: one can either use the proper motions themselves, the v -components of which should on the average represent the reflected solar motion; or one can consider the apparent dispersion of the observed proper motions as a measure of the mean parallax of the particular sample of stars. An investigation of the mean parallaxes in small areas of the sphere is better based on the second method. The v -components are affected by systematic errors, depending on right ascension, declination, or magnitude; they are also influenced by galactic rotation or any other peculiarities of stellar motion. Therefore, one can expect reliable results from the v -components only if the considered stars are distributed over a sufficiently large part of the sky, so that all systematic errors depending on position are smoothed out. The dispersion, however, is entirely independent of systematic errors which, within a limited

area of sky, cause an additive quantity that has to be applied to all observed proper motions. In this way the use of the dispersion method allows us to eliminate all systematic errors and this method has therefore been used by several authors* to derive mean parallaxes of faint stars of very small proper motions. Its main difficulty lies in the fact that the observed dispersion contains the observational inaccuracy and that the correction for accidental errors can be done reliably only if these errors are small compared with the true dispersion. Owing to the high quality of the GC proper motions and their comparatively great size, this point presents little difficulty in the present work except for the faintest stars between 7^m and 8^m , where the mean error of the observed proper motions was occasionally comparable with the true dispersion. The mean parallaxes derived in this paper should therefore be little affected by any systematic or accidental errors of the proper motions.

It was intended to investigate not only mean parallaxes but also the general distribution of the observed proper motions. This distribution function is connected with the general features of the spatial density of the stars, dispersion of luminosities and stellar velocities, and it has been shown by Charlier and other Swedish authors† what kind of results can be gained from explicit distribution functions of the observed proper motions. Thus in the present work the number of stars between definite limits of $\mu_\alpha \cos \delta$ and μ_δ was counted and represented in tables of the same kind as were constructed by Charlier in *Lund Medd.*, Series II, No. 9 for the stars of the PGC. The great number of stars in the GC made a separation of spectral classes possible. After some preliminary work stars of classes B and M were rejected because they are too rare and too irregularly distributed for statistical purposes, so that there remained four spectral classes, A, F, G, K. It is not possible to publish all distribution tables explicitly, as these would require too much space; one can, however, derive from them the moments of the distribution functions, according to Charlier's methods of numerical statistics‡, which characterize the most important features of the distributions. In the present work only the moments of second order were used to derive the dispersions; in future investigations the moments of higher order also may be determined from the set of tables which now exists. The author is, of course, prepared to put his tables at the disposal of other investigators who may want to derive any further results from them.

1. *The method of deriving the distribution functions.*—The whole sphere was divided into 48 areas, selected according to galactic coordinates as detailed below, following Charlier's procedure.

Areas	Limits of galactic latitude		Range of galactic longitude per area
GA 1-2	+66°44	+90°	180°
GB 1-10	+30	+66°44	36
GC 1-12	0	+30	30
GD 1-12	-30	0	30
GE 1-10	-66°44	-30	36
GF 1-2	-90	-66°44	180

All these areas are of equal size and number 1 of a group corresponds to the area for which the longitude range starts at 0° .

* J. H. Oort, *B.A.N.*, **8**, 75, 1936. L. Binnendijk, *B.A.N.*, **10**, 9, 1943.

† C. V. L. Charlier et al., *Lund Meddelanden*, Series II, Nos. 9, 12, 35, 41, 1912-1927.

‡ C. V. L. Charlier, *Lund Meddelanden*, Series II, No. 4, 1906.

The following stars were excluded: (1) Stars fainter than 8^m ; (2) Variable stars; (3) Stars with composite spectra; (4) Second components of double stars; (5) Known members of the star-streams Hyades, Pleiades and Praesepe.

It may seem dangerous to include the stars between 7^m and 8^m , since the GC is complete only down to 7^m ; but in the final results the stars of 7^m magnitude did not show any peculiarities. The identification of the cluster members was done: for the Hyades according to Smart (*M.N.*, **99**, 168, 1939); for the Pleiades according to Hertzsprung (*Annales Leiden*, **19**, 1, 1947); for Praesepe according to Klein Wassink (*Groningen Publ.*, **41**, 1927). Ohlsson's tables* were used for converting equatorial to galactic coordinates. Stars were classified according to the area in which they are situated, to magnitude, to spectrum, and to both components of their proper motion. For stars of classes F, G, K steps of $0''.050$ in proper motion were used, for A stars steps of $0''.025$. Each star was given two numbers; the first corresponded to $\mu_\alpha \cos \delta$, the second to μ_δ . In this way, stars of classes F, G, K received the numbers 0 to 9 for every $0''.050$ of proper motion in the range $-0''.250$ to $+0''.250$. In the case of A stars the class limits are the corresponding multiples of $0''.025$.

So, for instance, the star 12959 of the GC, with the proper motion $\mu_\alpha \cos \delta = +0''.006$, $\mu_\delta = -0''.024$, was given the numbers 5, 4. Then the number of stars within all groups of proper motion was counted separately for each area, for each spectral class, and for each magnitude, and finally combined in correlation tables. The table for the K stars between 6^m and 7^m in the area GD 10 is given below as a sample.

TABLE I
Correlation table between $\mu_\alpha \cos \delta$ and μ_δ for the K stars between $6^m.0$ and $7^m.0$ in the area GD 10

μ_δ	0	1	2	3	4	5	6	7	8	9	Sum
$\mu_\alpha \cos \delta$											
0											0
1		1									1
2			1		1						2
3			1	4	1	1					7
4				6	23	7					36
5				1	15	9					25
6				1							1
7											0
8											0
9											0
Sum	0	1	2	12	40	17	0	0	0	0	72

This division of the material into 48 areas, 4 spectral classes, and 4 magnitude groups ($m < 5$, $5 < m < 6$, $6 < m < 7$ and $7 < m < 8$), gave $48.4.4 = 768$ tables of this kind.

The moments of the frequency functions for $\mu_\alpha \cos \delta$ and μ_δ were computed according to the formulae given by Charlier.† The zero-point is mid-way between 4 and 5; stars of class 4 have, therefore, $x = -0.5$, those of class 3 have $x = -1.5$, and so on. Charlier's formulae for the computation of the moments of first and second order are then:

$$\begin{aligned}\mu'_s &= \sum x^s F(x), & \mu_0 \nu'_s &= \mu'_s, \\ b &= \nu'_1, & \sigma^2 &= \nu'_2 - b^2 - \frac{1}{12},\end{aligned}$$

* T. Ohlsson, *Annales Lund Obs.*, No. 3, 1932.

† C. V. L. Charlier, *Lund Meddelanden*, Series II, No. 4, p. 15, 1906.

where $F(x)$ is the number of stars in the group x , b the mean value of the observed proper motions and σ their dispersion. The correction $-\frac{1}{12}$ must be applied to σ^2 , since the exact definition of the moments μ'_s is given by integrals which are here replaced by finite sums. This procedure for finding mean values and dispersions has been applied to both components of the proper motions. The moments of higher order were not computed, although even they may have some significance for the distribution of stellar movements.

2. *Correction for large proper motions and accidental errors.*—In the derivation of the moments of second order extremely large proper motions have too much weight, since their contribution is proportional to the square of the proper motions. It is therefore necessary to exclude some of these large motions, and this was done in the following way: Firstly, the dispersions σ_α and σ_δ were calculated without excluding any star, and then all those stars were excluded whose deviation from the mean value b exceeded the amount 3σ in either coordinate. If the frequency functions were exact Gaussian distributions, the probability of proper motions exceeding 3σ would be 0.0027, or one star in 370 would actually have a large proper motion. The number of stars per table was in almost all cases smaller than 100, and therefore even the fact that the frequency functions are not exactly Gaussian functions should not cause any large error.

The dispersions found in this way must be corrected for the accidental errors of observation. The GC gives the probable error of the proper motion in both coordinates for each star separately; the errors increase, of course, for the fainter stars. In order to find average values of probable errors, four stars were selected at random for each hour of right ascension in the GC, one star for each magnitude ($m < 5$, $m = 5, 6, 7$). This gave for each magnitude group 24 individual probable errors, the average value of which was considered to represent the general uncertainty of the GC; any possible dependence of the accidental errors on α or δ was neglected. The probable errors have to be multiplied by 1.5 in order to convert them into mean errors.

According to Schlesinger and Barney*, the probable errors of the proper motions in the GC are to be increased by 25–35 per cent and thus the average errors, found as described above, were rounded off upwards. Finally, the values given in the last line of Table II were adopted as the mean observational errors.

TABLE II
Observational errors for different magnitudes

Magnitude	$< 5^m$	5^m-6^m	6^m-7^m	7^m-8^m
Average p.e. of the GC	0".0017	0".0036	0".0061	0".0082
Finally adopted m.e.	0".003	0".006	0".010	0".015

There were no appreciable differences between the errors in $\mu_\alpha \cos \delta$ and μ_δ . It does not matter too much what assumptions are made concerning the observational errors as these were almost always small compared with the true dispersion except in the case of A stars fainter than 7^m .

3. *Numerical values for the characteristic quantities of the frequency functions.*—In this way the dispersions σ_α and σ_δ were derived for the proper-motion components $\mu_\alpha \cos \delta$ and μ_δ . They are given numerically in Tables III to VII for the four spectral classes, A, F, G, K and for each area and each magnitude group separately. For the F and G stars, the number of stars brighter than 5^m

* F. Schlesinger and I. Barney, *A.J.*, **48**, 51, 1939; **52**, 176, 1946.

TABLE III
 Dispersions in $\mu_\alpha \cos \delta$ and μ_δ for *A* stars
 [Unit $0''.025$]

Area	$m < 5^m$			$5^m - 6^m$			$6^m - 7^m$			$7^m - 8^m$		
	σ_α	σ_δ	(n)	σ_α	σ_δ	(n)	σ_α	σ_δ	(n)	σ_α	σ_δ	(n)
GA 1		1.90	1.28	(12)	1.59	0.17	(28)	0.93	0.38	(16)
2		2.01	1.24	(24)	1.75	0.64	(35)	1.24	0.45	(15)
GB 1	2.09	2.66	(10)	1.25	1.37	(7)	0.82	0.97	(24)	0.65	0.56	(22)
2	4.15	2.11	(5)	1.40	1.07	(24)	0.96	1.02	(46)	0.53	1.17	(25)
3	2.39	0.62	(8)	1.98	1.89	(15)	1.51	1.00	(38)	0.63	0.65	(32)
4	2.92	1.50	(11)	1.21	1.72	(7)	0.96	0.75	(40)	0.90	0.33	(19)
5	2.77	1.29	(5)	1.20	1.29	(17)	1.10	0.88	(40)	0.44	0.68	(19)
6	1.11	1.60	(6)	2.01	0.85	(11)	1.05	0.33	(31)	0.69	0.00	(18)
7	2.29	1.44	(5)	1.45	0.80	(9)	1.23	0.90	(43)	0.71	0.24	(23)
8		1.44	0.54	(13)	1.19	0.56	(27)	1.03	0.11	(24)
9	2.14	0.89	(7)	1.44	0.98	(9)	1.06	0.76	(37)	0.72	0.00	(21)
10	2.58	1.81	(8)	1.78	0.82	(20)	0.92	0.71	(30)	0.78	0.43	(20)
GC 1	1.57	2.89	(6)	0.82	1.11	(32)	0.77	0.64	(58)	*	*	
2	1.27	1.93	(11)	0.23	1.09	(14)	0.46	0.71	(92)	0.54	0.71	(72)
3	2.03	1.02	(6)	1.27	0.97	(18)	0.78	1.05	(65)	0.59	0.21	(72)
4	1.12	2.08	(8)	1.66	0.87	(23)	1.12	0.76	(64)	0.64	0.69	(40)
5	1.41	1.30	(13)	0.81	0.99	(18)	0.64	1.00	(57)	0.00	0.69	(39)
6		0.57	0.98	(21)	0.64	0.50	(63)	0.00	0.61	(27)
7	0.93	0.74	(5)	0.78	0.88	(18)	0.76	0.73	(58)	0.71	0.00	(23)
8		0.87	1.06	(9)	1.54	0.78	(65)	1.24	0.47	(66)
9	1.98	1.16	(5)	1.58	1.04	(19)	1.22	0.58	(67)	0.90	0.23	(121)
10		1.10	0.77	(16)	1.17	0.55	(57)	0.82	0.14	(113)
11		1.38	0.95	(14)	0.98	0.90	(60)	0.65	0.48	(94)
12	1.60	1.96	(9)	1.13	1.16	(11)	0.64	0.80	(41)	*	*	
GD 1	0.85	1.14	(7)	0.71	0.77	(20)	0.62	0.68	(66)	*	*	
2		1.15	1.20	(19)	1.00	1.00	(66)	*	*	
3	3.20	1.20	(6)	1.98	0.54	(17)	0.87	0.45	(61)	0.75	0.00	(55)
4		1.50	0.70	(12)	1.34	0.52	(62)	0.60	0.51	(48)
5		0.72	1.14	(22)	0.99	0.47	(37)	0.53	0.47	(48)
6	1.47	1.65	(7)	0.69	0.86	(21)	0.66	0.79	(47)	*	*	
7	0.68	0.68	(6)	0.60	1.00	(29)	0.58	0.76	(67)	0.48	0.63	(44)
8	0.30	1.46	(8)	0.86	2.39	(14)	0.80	0.91	(69)	0.57	0.48	(131)
9	2.71	2.70	(5)	0.93	1.06	(21)	0.74	1.23	(78)	0.65	0.68	(126)
10		2.05	1.95	(14)	1.08	1.06	(67)	0.50	0.85	(100)
11	2.01	2.04	(5)	0.82	1.20	(17)	0.92	0.76	(71)	0.55	0.59	(115)
12		1.05	1.35	(15)	0.68	0.68	(50)	0.40	0.47	(48)
GE 1	2.40	0.68	(6)	1.44	2.20	(9)	1.33	0.44	(42)	0.55	0.60	(28)
2	3.25	2.23	(5)	2.05	0.83	(12)	1.20	0.73	(40)	*	*	
3		2.34	1.18	(13)	1.60	0.45	(19)	1.03	0.60	(20)
4	3.43	2.53	(6)	1.70	1.05	(10)	1.33	0.63	(36)	0.40	0.10	(14)
5		1.44	1.03	(10)	1.07	0.95	(31)	0.84	0.30	(18)
6		2.60	1.73	(16)	0.95	0.73	(35)	0.81	1.14	(55)
7		1.42	0.94	(5)	1.29	1.04	(30)	0.51	0.67	(70)
8		2.33	1.36	(5)	1.28	1.17	(25)	1.15	0.61	(52)
9		1.61	2.46	(8)	1.28	1.39	(24)	0.55	0.71	(75)
10	1.96	1.04	(8)	1.45	1.35	(15)	1.32	0.95	(31)	0.70	0.33	(48)
GF 1		2.12	1.35	(11)	2.05	0.90	(22)	1.18	0.94	(24)
2		1.45	0.58	(8)	1.75	0.55	(19)	1.07	0.70	(32)

TABLE IV
Dispersions in $\mu_\alpha \cos \delta$ and μ_δ for F stars

[Unit $0''.050$]

Area	$m < 6^m$			$6^m - 7^m$			$7^m - 8^m$		
	σ_α	σ_δ	(n)	σ_α	σ_δ	(n)	σ_α	σ_δ	(n)
GA	1	2.44	0.92 (9)	1.94	1.08 (29)		1.41	0.94 (37)	
	2	3.22	1.06 (10)	2.16	1.33 (30)		1.42	0.98 (40)	
GB	1	2.54	1.71 (15)	1.30	1.15 (32)		0.86	1.36 (33)	
	2	3.08	4.85 (13)	1.88	1.62 (34)		0.87	1.26 (52)	
	3	1.74	2.19 (9)	1.40	1.43 (27)		1.29	0.97 (60)	
	4	2.62	1.12 (13)	1.31	1.35 (32)		0.99	1.05 (46)	
	5	2.80	1.38 (11)	1.66	1.10 (43)		0.71	0.69 (33)	
	6	1.56	0.91 (34)		1.03	0.90 (42)	
	7	2.64	1.58 (8)	2.18	1.03 (28)		1.58	1.41 (27)	
	8	3.47	1.77 (8)	2.01	1.02 (27)		1.28	1.06 (39)	
	9	3.33	3.90 (9)	1.91	1.09 (22)		1.32	0.99 (36)	
	10	3.08	1.11 (6)	0.91	0.54 (27)		1.48	0.90 (28)	
GC	1	0.48	1.64 (11)	1.13	1.33 (37)		0.84	1.23 (28)	
	2	1.45	3.78 (12)	0.69	1.55 (27)		0.71	1.36 (41)	
	3	2.93	2.11 (14)	1.36	1.07 (24)		1.05	0.96 (53)	
	4	1.45	1.73 (8)	1.30	1.57 (39)		0.88	0.95 (42)	
	5	1.00	2.03 (8)	1.03	1.41 (42)		0.57	0.90 (30)	
	6	1.73	1.81 (14)	1.19	1.26 (30)		0.92	1.54 (26)	
	7	1.64	1.70 (21)	1.07	1.26 (31)		1.34	1.35 (17)	
	8	0.96	0.56 (10)	2.20	1.05 (35)		1.39	0.67 (45)	
	9	2.25	0.62 (8)	2.29	0.93 (36)		1.61	0.76 (66)	
	10	3.52	1.47 (11)	1.67	1.01 (36)		1.23	0.55 (67)	
	11	1.41	1.16 (14)	1.23	1.69 (29)		0.71	0.78 (60)	
	12	2.06	1.74 (11)	0.85	1.13 (32)		0.85	1.08 (37)	
GD	1	2.14	2.36 (12)	1.13	1.46 (40)		0.93	0.73 (45)	
	2	1.81	2.37 (18)	1.27	1.40 (29)		0.91	0.82 (24)	
	3	1.90	2.06 (10)	1.71	0.96 (33)		1.42	0.57 (36)	
	4	2.66	2.40 (17)	1.29	0.83 (42)		1.13	0.54 (32)	
	5	1.81	1.31 (9)	1.01	0.91 (35)		1.31	1.02 (24)	
	6	1.84	1.93 (16)	1.08	1.18 (28)		0.86	1.22 (27)	
	7	1.35	1.08 (15)	0.79	1.09 (33)		1.04	1.80 (23)	
	8	1.47	1.99 (15)	0.67	1.20 (34)		0.95	1.09 (62)	
	9	1.97	2.21 (20)	1.28	1.10 (27)		0.79	1.05 (89)	
	10	1.75	2.76 (10)	1.07	1.92 (26)		0.97	0.94 (53)	
	11	1.04	1.92 (12)	1.12	1.09 (32)		0.69	0.82 (80)	
	12	2.22	2.47 (13)	0.89	0.89 (29)		0.96	0.93 (36)	
GE	1	1.81	0.94 (8)	1.66	0.92 (32)		1.37	1.14 (39)	
	2	3.64	3.64 (9)	2.24	1.11 (28)		1.03	0.69 (40)	
	3	1.96	2.49 (9)	1.69	1.17 (33)		1.63	1.48 (32)	
	4	2.57	1.30 (13)	1.31	1.00 (29)		1.96	0.90 (26)	
	5	2.64	1.75 (11)	1.06	1.59 (22)		1.17	0.79 (27)	
	6	2.26	1.48 (12)	1.13	1.41 (31)		0.89	1.26 (61)	
	7	2.39	2.55 (10)	0.78	1.97 (21)		0.92	0.92 (62)	
	8	1.53	2.53 (15)	1.79	0.86 (32)		1.12	1.07 (94)	
	9	2.78	1.72 (11)	2.35	1.66 (27)		0.87	1.08 (80)	
	10	2.29	1.62 (11)	1.59	1.15 (32)		1.12	0.85 (76)	
GF	1	2.50	3.60 (12)	1.94	1.33 (27)		1.66	0.99 (27)	
	2	0.85	1.78 (7)	1.96	1.41 (26)		1.37	0.92 (52)	

TABLE V
Dispersions in $\mu_\alpha \cos \delta$ and μ_δ for G stars

[Unit 0".050]

Area	$m < 6^m$			$6^m - 7^m$			$7^m - 8^m$		
	σ_α	σ_δ	(n)	σ_α	σ_δ	(n)	σ_α	σ_δ	(n)
GA 1	6.29	9.31	(6)	1.86	1.33	(9)	2.29	0.66	(13)
2	2.23	2.96	(6)	2.38	1.45	(13)	1.93	1.15	(28)
GB 1	5.25	5.20	(8)	1.52	2.98	(9)	1.23	2.00	(18)
2	2.93	1.06	(10)	1.54	2.98	(8)	1.92	1.68	(33)
3	1.92	1.83	(5)	2.80	1.31	(24)	1.57	0.79	(32)
4	2.35	1.32	(14)	1.31	2.09	(19)	1.21	1.15	(27)
5	1.66	0.79	(14)	1.17	1.12	(20)	1.78	1.82	(26)
6		1.46	2.04	(13)	1.93	1.35	(27)
7	2.12	1.57	(5)	2.80	1.67	(11)	2.14	1.62	(24)
8	2.34	3.56	(11)	2.75	2.58	(19)	2.44	1.53	(19)
9		3.52	1.83	(24)	2.33	1.73	(31)
10	2.16	1.86	(12)	2.05	1.28	(14)	1.72	2.04	(27)
GC 1	2.53	1.28	(7)	1.42	2.06	(20)	1.27	1.94	(25)
2	1.46	2.68	(9)	1.54	2.13	(25)	1.31	1.07	(28)
3	0.89	1.89	(6)	0.87	0.95	(20)	2.04	0.86	(23)
4		1.53	0.98	(29)	1.55	1.64	(35)
5	0.86	2.77	(8)	1.39	0.98	(31)	1.48	1.41	(28)
6	0.99	1.58	(12)	0.81	0.92	(38)	1.49	1.90	(26)
7	1.09	1.76	(13)	0.75	1.08	(32)	1.56	2.22	(25)
8	3.20	3.15	(9)	2.57	1.44	(26)	1.51	2.28	(32)
9	4.00	2.28	(7)	2.48	1.92	(24)	1.49	1.12	(39)
10	2.69	0.85	(6)	1.62	1.55	(20)	1.58	1.15	(48)
11	1.09	0.61	(9)	2.60	1.67	(21)	1.43	1.02	(39)
12	2.29	2.03	(5)	1.33	2.57	(28)	0.85	1.62	(27)
GD 1	4.20	3.56	(6)	2.21	1.89	(22)	1.52	1.31	(25)
2		1.96	2.04	(22)	0.99	1.54	(18)
3		1.59	1.37	(28)	2.46	1.86	(25)
4	1.26	1.88	(17)	1.82	1.23	(27)	1.47	1.10	(41)
5	1.38	1.08	(6)	1.78	1.53	(37)	1.83	1.49	(31)
6	2.13	1.86	(12)	0.74	1.64	(25)	1.66	1.58	(26)
7	2.51	0.96	(12)	1.33	1.09	(32)	1.25	1.42	(20)
8	1.50	1.08	(13)	1.30	1.40	(39)	1.06	1.78	(46)
9	0.77	1.03	(8)	0.73	1.21	(24)	1.43	2.06	(33)
10	1.37	1.84	(9)	2.56	2.47	(15)	1.79	2.13	(24)
11	0.92	1.29	(8)	1.05	2.01	(29)	1.58	1.51	(48)
12	1.54	1.21	(12)	0.78	0.90	(23)	1.60	1.43	(34)
GE 1	2.15	1.26	(10)	1.80	1.61	(17)	2.30	1.66	(29)
2	2.66	1.36	(8)	3.11	0.79	(15)	1.63	1.82	(21)
3	3.45	1.42	(8)	1.12	1.56	(25)	1.59	1.75	(36)
4	2.18	1.11	(12)	0.93	1.32	(26)	2.52	1.26	(26)
5	2.36	1.24	(15)	1.03	1.46	(35)	1.91	1.48	(31)
6	3.23	2.71	(6)	1.15	0.78	(39)	1.02	1.31	(51)
7	1.34	1.38	(11)	1.70	1.57	(27)	1.48	1.39	(68)
8	3.01	2.92	(5)	2.36	1.40	(27)	1.79	1.51	(70)
9	2.28	3.71	(6)	3.55	2.33	(23)	1.97	1.79	(56)
10	1.05	0.38	(5)	1.26	1.57	(34)	2.31	1.31	(46)
GF 1	1.51	0.89	(9)	2.52	1.20	(35)	1.89	1.89	(31)
2	6.08	2.01	(6)	3.00	0.79	(23)	1.45	1.70	(53)

TABLE VI
Dispersion in $\mu_\alpha \cos \delta$ and μ_δ for K stars

[Unit 0".050]

Area	$m < 5^m$			5^m-6^m			6^m-7^m			7^m-8^m		
	σ_α	σ_δ	(n)	σ_α	σ_δ	(n)	σ_α	σ_δ	(n)	σ_α	σ_δ	(n)
GA 1	0.98	0.93	(5)	0.84	0.73	(16)	1.09	0.62	(42)	0.73	0.50	(48)
2	1.67	0.40	(3)	1.84	2.45	(16)	1.08	0.55	(51)	0.78	0.62	(48)
GB 1	1.34	2.36	(12)	1.33	0.73	(25)	0.68	0.85	(58)	0.54	0.56	(49)
2		1.06	1.09	(14)	0.50	0.74	(60)	0.59	0.66	(77)
3		1.24	0.71	(20)	1.05	0.73	(46)	0.66	0.54	(75)
4		0.73	0.65	(15)	0.46	0.55	(44)	0.54	0.00	(65)
5	1.71	2.00	(10)	0.74	0.72	(10)	0.68	0.35	(42)	0.44	0.38	(46)
6	3.43	1.23	(5)	0.92	0.62	(16)	0.55	0.43	(42)	0.77	0.69	(38)
7	2.11	2.09	(6)	1.32	1.29	(13)	0.75	0.84	(62)	0.48	0.69	(41)
8		1.63	0.46	(14)	0.94	0.60	(47)	0.55	0.52	(64)
9	2.56	2.31	(5)	1.00	0.76	(19)	0.62	0.62	(47)	0.45	0.35	(52)
10	1.86	1.18	(6)	0.85	1.07	(16)	0.74	0.71	(46)	0.58	0.64	(55)
GC 1	1.43	1.56	(7)	0.76	1.12	(22)	0.51	0.86	(62)	0.24	0.68	(69)
2	0.87	0.82	(9)	1.02	1.03	(18)	0.55	1.02	(104)	0.52	0.60	(90)
3	1.29	1.47	(12)	0.77	0.53	(15)	0.61	0.68	(67)	0.66	0.76	(104)
4		0.53	0.85	(17)	0.63	0.58	(46)	0.58	0.64	(54)
5		0.50	0.71	(20)	0.49	0.68	(72)	0.34	0.16	(66)
6	1.08	1.21	(8)	0.49	0.46	(26)	0.46	0.37	(69)	0.26	0.35	(46)
7	0.72	1.27	(8)	1.09	0.92	(20)	0.57	0.62	(77)	0.43	0.56	(33)
8	1.55	1.25	(10)	1.12	0.84	(25)	0.52	0.61	(86)	0.47	0.54	(68)
9	1.83	1.19	(9)	1.23	1.19	(19)	0.62	0.43	(87)	0.49	0.27	(125)
10	1.21	1.09	(7)	1.32	0.48	(26)	0.83	0.50	(89)	0.55	0.34	(96)
11	1.54	1.37	(10)	0.74	0.22	(17)	0.69	0.61	(48)	0.41	0.31	(71)
12	1.16	2.04	(5)	0.97	0.90	(15)	0.65	0.49	(45)	0.43	0.48	(37)
GD 1	1.38	1.22	(6)	0.65	0.82	(15)	0.59	0.48	(84)	0.67	0.62	(76)
2	1.06	0.98	(10)	1.18	1.31	(20)	0.72	0.55	(67)	0.56	0.56	(67)
3	1.52	2.21	(5)	0.91	0.58	(20)	0.66	0.51	(74)	0.54	0.31	(101)
4	1.50	1.19	(14)	1.15	0.59	(10)	0.85	0.63	(63)	0.54	0.38	(68)
5	0.40	1.28	(7)	0.56	0.86	(10)	0.47	0.78	(30)	0.30	0.45	(40)
6	0.81	1.94	(8)	0.38	0.66	(15)	0.51	0.47	(52)	0.59	0.14	(24)
7	0.95	0.74	(10)	0.68	0.91	(25)	0.54	0.62	(70)	0.41	0.43	(43)
8	1.08	1.31	(12)	0.67	0.98	(31)	0.51	0.66	(96)	0.41	0.44	(147)
9	0.74	0.98	(13)	1.11	1.55	(31)	0.85	0.80	(67)	0.55	0.61	(114)
10	1.03	1.46	(14)	1.15	0.91	(34)	0.77	0.72	(72)	0.42	0.53	(95)
11	1.46	1.90	(13)	0.77	0.75	(27)	0.52	0.63	(92)	0.43	0.36	(111)
12	0.72	2.20	(11)	0.98	0.72	(27)	0.59	0.74	(58)	0.43	0.49	(60)
GE 1	1.14	0.99	(7)	0.90	0.85	(15)	0.85	0.44	(41)	0.47	0.54	(54)
2	0.89	2.54	(6)	0.91	0.65	(13)	1.01	0.78	(51)	0.82	0.59	(40)
3	1.46	0.48	(9)	0.94	0.63	(8)	0.93	0.52	(43)	0.70	0.45	(46)
4	1.50	1.22	(6)	0.84	0.20	(6)	0.81	0.42	(42)	0.49	0.46	(24)
5	1.47	1.45	(4)	0.72	1.26	(8)	0.74	0.95	(38)	0.56	0.81	(23)
6	1.48	2.17	(10)	0.78	0.93	(17)	0.53	0.89	(41)	0.57	0.51	(97)
7	0.60	2.99	(6)	0.91	0.95	(17)	0.76	0.63	(43)	0.45	0.61	(130)
8	1.44	2.17	(5)	0.65	0.74	(25)	0.90	0.52	(54)	0.62	0.43	(112)
9	1.03	0.85	(7)	0.71	1.00	(21)	0.75	0.70	(70)	0.57	0.46	(118)
10	0.64	1.55	(4)	1.38	1.44	(26)	0.75	0.63	(76)	0.61	0.59	(105)
GF 1	2.33	1.45	(9)	1.27	0.58	(16)	1.06	0.77	(42)	0.75	0.60	(42)
2	1.80	3.02	(9)	1.54	1.01	(23)	0.89	0.67	(54)	0.59	0.46	(92)

was too small and in these classes we have therefore only three magnitude groups; even for the A and K stars the number of stars brighter than 5^m was sometimes insufficient to derive the dispersions. In a few cases the apparent dispersion of the A stars fainter than 7^m turned out to be smaller than the mean error of observation, so that the true dispersion would have become imaginary; these cases are denoted by an asterisk (*) and the corresponding dispersions were omitted. The mean values b , which have been calculated also, are not given in the tables. They are very interesting because they represent the mean star-streaming; but they are affected by the full amount of all systematic errors in the proper motions of the GC and, therefore, do not contribute very reliable information as to the stellar motions in different parts of the sky.

4. *Derivation of mean parallaxes.*—The dispersion of the proper motions is proportional to the mean parallax of the particular group of stars. Let σ be this dispersion in any direction, then

$$t\bar{\pi} = 4.74\sigma,$$

where t is the dispersion of linear velocities in the same direction. The quantity t was determined by the assumption that the frequency of stellar velocities is given by a velocity ellipsoid, the smallest axis of which is directed towards the galactic pole, the greatest axis towards galactic longitude 345° in the galactic plane and the third axis to a point distant by 90°. It was assumed that the square of the ratio (intermediate axis/major axis) equals 0.5 and the square of the ratio (minor axis/major axis) equals 0.25. If ψ_i is the position angle of any component of proper motion with respect to the north galactic pole at a point with galactic coordinates (l, b) and if further (L, B) are the coordinates of the vertex, then the dispersion t_i of linear velocities in the corresponding direction is

$$t_i^2 = a^2(l_i^2 + 0.5m_i^2 + 0.25n_i^2),$$

where

$$l_i = \sin(l-L) \sin \psi_i + \sin b \cos(l-L) \cos \psi_i,$$

$$m_i = \cos(l-L) \sin \psi_i - \sin b \sin(l-L) \cos \psi_i,$$

$$n_i = -\cos b \cos \psi_i.$$

The observations give the dispersion in two coordinates, in right ascension and declination; combining them, we find

$$4.74\sqrt{\sigma_\alpha^2 + \sigma_\delta^2} = \bar{\pi}\sqrt{t_\alpha^2 + t_\delta^2}, \quad (1)$$

where the quantity

$$\begin{aligned} t_\alpha^2 + t_\delta^2 &= a^2\{l_\alpha^2 + l_\delta^2 + 0.5(m_\alpha^2 + m_\delta^2) + 0.25(n_\alpha^2 + n_\delta^2)\} \\ &= a^2[\sin^2(l-L) + \sin^2 b \cos^2(l-L) + 0.5\{\cos^2(l-L) + \sin^2 b \sin^2(l-L)\} \\ &\quad + 0.25 \cos^2 b] \end{aligned}$$

is a constant for each area, which does not depend on the position angle ψ of the proper-motion components used. For (l, b) the coordinates of the centre of the area were inserted.

For the quantity a , the mean square velocity along the greatest axis, the results given by R. E. Wilson and H. Raymond* were used. The spectral classification in their Table IV is somewhat different from the one in the present work. For the A stars the average of the groups B7-A3 and A5-F5 would give $a = 21.4$ km./sec.; it seems, however, rather improbable that the late A stars have the same high-velocity dispersion as the stars of the later types, and

* R. E. Wilson and H. Raymond, *A.J.*, **40**, 121, 1930.

indeed this is not confirmed by Nordström.* Therefore, Nordström's value of $a=17.2$ km./sec. for the A stars was given preference. In the other spectral classes these two investigations show no appreciable differences. For giant stars of type F or later, the value of a (designated σ_1 by Wilson and Raymond) does not vary significantly with spectral class and was assumed to be 26.4 km./sec., the average for types F to M. For dwarfs of class G and K the common value 47.4 km./sec. was taken. Furthermore, an assumption must be made as to the percentage of dwarfs among the late-type stars. According to P. J. van Rhijn and A. Schwassmann† only a few per cent of the K stars 4^m-7^m are dwarfs, whereas the number of dwarfs among the G stars varies between 20 per cent and 40 per cent; it was therefore assumed that one-third of the G stars are dwarfs, while all K stars were considered as giants; the few K dwarfs should have been excluded from the material when we omitted stars with proper motions exceeding three times the observed dispersion. Thus the following values for a were used.

Spectr. class	a (giants)	a (dwarfs)	Adopted percentage of dwarfs	a (final)
A	17.2	17.2
F	26.4	26.4	...	26.4
G	26.4	47.4	33	33.3
K	26.4	47.4	0	26.4

No assumption as to the percentage of dwarfs among the F stars is necessary as in this spectral class there is practically no difference between the velocity of giants and dwarfs.

5. *Results for different galactic latitudes.*—Using the formula (1) and the dispersions σ_α and σ_δ of Tables III to VII, values of mean parallaxes were derived for stars of different magnitudes and spectral classes, in all 48 areas. For types F and G the number of stars brighter than 5^m was too small to derive the parallaxes separately, and thus there are only three magnitude groups in these two classes; all stars brighter than 6^m are combined in the first magnitude group. The mean values for all areas in the same latitudes were derived and compared with van Rhijn's‡ mean parallaxes, which were calculated from his secular parallaxes by using Nordström's § values for the velocity of the Sun relative to different spectral classes. The values are taken from Table XV of Nordström's paper and are reproduced here in Table VII together with the corresponding factor which converts secular parallaxes into mean parallaxes.

TABLE VII
Solar velocity and converting factor

Spectr. class	Vel. of Sun	Con. factor
A	16.3 km/sec.	0.291
F	17.7	0.268
G	18.1	0.262
K	20.9	0.227

The present mean parallaxes and their comparison with van Rhijn's values are given in Table VIII.

* H. Nordström, *Lund Meddelanden*, Series II, No. 79, 1936.

† P. J. van Rhijn and A. Schwassmann, *Zeitschr. f. Astrophysik*, 10, 161, 1935.

‡ P. J. van Rhijn, *Groningen Publ.*, No. 29, Tables 44-47, 1918.

§ H. Nordström, *Lund Meddelanden*, Series II, No. 79, 1936.

Table VIII shows some remarkable differences between van Rhijn's parallaxes and the present ones. The agreement for the A stars is satisfactory but, in the three other classes, the present parallaxes are somewhat smaller than those of van Rhijn. The difference is of the order of 10 per cent and could be removed by changing the velocity dispersion or the solar velocity relative to the stars of these classes by 2-3 km./sec. There is, however, another point: the present parallaxes increase towards the poles much less than van Rhijn's values. This phenomenon does not necessarily indicate an error in the present parallaxes, since the Groningen parallaxes have been derived on the assumption that the ratio between the mean parallaxes at the poles and at the galactic equator is the same for all stars down to the 10th magnitude. It is quite possible that for the brighter, and consequently nearer, stars (in a given spectral class) the flattening of the galactic system is less pronounced.

TABLE VIII
Mean parallaxes in different galactic latitudes

Sp. type	\bar{m}	A, F areas $b = \pm 73^\circ$		B, E areas $b = \pm 45^\circ$		C, D areas $b = \pm 15^\circ$	
		This paper	v. Rh.	This paper	v. Rh.	This paper	v. Rh.
A	4.5	0".0177	0".0191	0".0151	0".0184
	5.7	0".0125	0".0122	126	118	102	114
	6.7	103	83	86	80	78	76
	7.5	72	60	58	59	54	57
F	5.5	0".0241	0".0327	0".0269	0".0284	0".0242	0".0249
	6.7	176	204	162	180	157	155
	7.5	128	147	122	129	122	115
G	5.5	0".0317	0".0354	0".0202	0".0290	0".0182	0".0262
	6.7	165	210	161	186	149	160
	7.5	138	154	150	134	143	117
K	4.5	0".0219	0".0250	0".0198	0".0213	0".0162	0".0191
	5.7	137	154	107	136	108	120
	6.7	90	106	81	93	78	78

The interpolation formula

$$\log \left(\frac{\bar{h}}{\rho} \right) = -1.53 - 0.10 \cos^2 2b - (0.06 + 0.04 \cos 2b + 0.09 \sin b)(m-8) + 0.005(m-8)^2 \quad (2)$$

derived by van de Kamp and Vyssotsky* for stars of all spectral classes and down to the 15th (photovisual) magnitude represents the Groningen parallaxes very well. In order to compare the present results with van de Kamp's formula (2), we have derived from Table VIII average values of the mean parallaxes for stars of all spectral classes together. The A and K stars brighter than 5^m were excluded because we have no mean parallaxes for F and G stars of this magnitude. The conversion of secular parallaxes, which are given by formula (2), into mean parallaxes was done by applying the factor 0.263, which is the average value for the four spectral classes of Table VII. The comparison of the present parallaxes with formula (2) is given in Table IX.

This comparison illustrates the result stated above, that the increase of the mean parallaxes toward the galactic poles is less pronounced in the present investigation than in the Groningen parallaxes; the residuals are positive at the galactic equator and negative at the poles. On the other hand, the residuals do

* P. van de Kamp and A. N. Vyssotsky, *A.J.*, 46, 14, 1937.

not exceed the average amount of the residuals of the actual Groningen parallaxes as compared with the interpolation formula (2).

The suggestion that the mean parallaxes of the bright stars vary with galactic latitude less than those of the faint stars may also be supported by the mean parallaxes of faint stars derived by Oort.* According to Table XIII of this paper, the ratio of the mean parallaxes at the galactic poles to those at the galactic equator is for stars of 12th magnitude equal to 2, whereas, according to formula (2), the same ratio for stars of 8th magnitude is equal to 1.6. Thus the comparatively small variation of the mean parallaxes of bright stars with galactic latitude which we have found may quite possibly be real.

TABLE IX
Mean parallaxes for stars of all spectral classes in different galactic latitudes, compared with formula (2)

<i>m</i>	<i>b</i> = ± 15°			<i>b</i> = ± 45°			<i>b</i> = ± 73°		
	log $\bar{\pi}$ (<i>m</i>)	Formula (2)	O-C	log $\bar{\pi}$ (<i>m</i>)	Formula (2)	O-C	log $\bar{\pi}$ (<i>m</i>)	Formula (2)	O-C
5.6	8.160	8.115	+0.045	8.216	8.217	-0.001	8.254	8.273	-0.019
6.6	8.004	7.978	+0.026	8.051	8.074	-0.023	8.097	8.141	-0.044
7.5	7.918	7.863	+0.055	7.972	7.953	+0.019	7.988	8.030	-0.042

6. *Results for the different areas.*—In order to find out whether the mean parallaxes of the stars differ in various parts of the sky, all 48 areas were treated separately. When representing the $\bar{\pi}(m)$ by the interpolation formula $\log \bar{\pi}(m) = a + bm$, there seems no hope of determining any possible variations of the quantity *b* by using material which covers 3-4 magnitudes only. For this reason a common numerical value of *b* was assumed for all areas and only the quantity *a* was considered as characterizing any variation of the mean parallaxes in different areas. The value of *b* was found by combining the parallaxes of Table VIII into an average for the three latitude groups, the values of Table X being derived in this way and represented by the interpolation formulae. Owing to the small number of stars the classes F and G were combined.

TABLE X
Mean parallaxes averaged for all latitude groups

Sp.	<i>m</i>	log $\bar{\pi}$ (<i>m</i>)	Formulae	O-C
A	4.5	8.214	8.232	-0.018
	5.7	8.070	8.062	+0.008
	6.7	7.950	7.921	+0.029
	7.5	7.789	7.808	-0.019
F + G	5.5	8.390	8.385	+0.005
	6.7	8.210	8.224	-0.014
	7.5	8.125	8.117	+0.008
K	4.5	8.286	8.291	-0.005
	5.7	8.107	8.092	+0.015
	6.7	7.918	7.926	-0.008
	7.5	7.790	7.793	-0.003

O-C gives the residuals against the interpolation formulae

$$\begin{aligned} \log \bar{\pi}(m) &= 8.866 - 0.141m && \text{for A stars} \\ &= 9.122 - 0.134m && \text{F + G stars} \\ &= 9.038 - 0.166m && \text{K stars} \end{aligned}$$

* J. H. Oort, *B.A.N.*, 8, 75, 1936.

As the differences of b for the three spectral groups are insignificant, a common value $b = -0.147$ was adopted for all spectral classes and all areas. This means that the mean parallaxes are supposed to be represented by

$$\log \bar{\pi}(m) = a - 0.147m$$

with the quantity a varying from area to area.

In order to derive a for all areas and all spectral classes, the quantities $\log \bar{\pi}(m) + 0.147m$ were calculated and a taken as their average value. The results are given in Table XI.

TABLE XI

The quantities a for each area and each spectral group

Area	A	F+G	K	Area	A	F+G	K
GA 1	8.907	9.263	8.848	GD 1	8.727	9.257	8.901
2	8.973	9.213	9.034	2	8.909	9.190	8.887
B 1	8.881	9.232	9.947	3	8.852	9.194	8.842
2	8.953	9.278	8.891	4	8.863	9.148	8.879
3	8.919	9.164	8.921	5	8.828	9.180	8.825
4	8.907	9.147	8.744	6	8.843	9.229	8.854
5	8.896	9.137	8.847	7	8.725	9.161	8.824
6	8.814	9.114	8.928	8	8.849	9.103	8.822
7	8.838	9.243	8.965	9	8.889	9.106	8.869
8	8.842	9.239	8.915	10	8.981	9.225	8.886
9	8.826	9.350	8.890	11	8.895	9.137	8.894
10	8.900	9.168	8.911	12	8.854	9.172	8.956
C 1	8.901	9.191	8.935	E 1	8.904	9.230	8.841
2	8.768	9.207	8.875	2	8.960	9.240	8.933
3	8.789	9.136	8.856	3	8.975	9.203	8.830
4	8.883	9.149	8.854	4	8.854	9.171	8.810
5	8.819	9.157	8.758	5	8.895	9.171	8.982
6	8.764	9.201	8.760	6	8.904	9.140	8.909
7	8.754	9.191	8.894	7	8.865	9.149	8.905
8	8.860	9.217	8.871	8	8.987	9.167	8.858
9	8.854	9.208	8.849	9	8.992	9.287	8.818
10	8.826	9.215	8.858	10	8.884	9.189	8.966
11	8.905	9.138	8.838	F 1	9.028	9.218	8.956
12	8.914	9.241	8.951	2	8.905	9.217	8.951

No systematic differences between northern and southern hemispheres are indicated, and therefore average values were derived for all areas of equal northern and southern latitudes.

TABLE XII

The quantity a in different latitudes

Areas	Latitude	A	F+G	K
C, D	$\pm 15^\circ$	8.842	9.182	8.864
B, E	$\pm 45^\circ$	8.900	9.201	8.890
A, F	$\pm 73^\circ$	8.953	9.228	8.948

The figures in Table XII can be represented by the formulae

$$\begin{aligned}
 a &= 8.889 - 0.050 \cos 2b && \text{for A stars} \\
 &9.204 - 0.050 \cos 2b && \text{F + G stars} \\
 &8.901 - 0.050 \cos 2b && \text{K stars}
 \end{aligned}$$

Finally, the residuals of the values of a for each area as compared with the mean value for the corresponding latitude were determined and then combined for each pair of areas (of the same longitude) symmetrically north and south of the Galaxy. The result is shown in Table XIII.

TABLE XIII
Deviation of a from the average value in different galactic longitudes
[Unit 0.001]

Areas	Longitude	A	F+G	K	Average	Areas	Longitude	A	F+G	K	Average
C, D	15°	-28	+42	+54	+23	B, E	18°	-8	+30	+4	+9
2	45	-4	+16	+17	+10	2	54	+56	+58	+22	+45
3	75	-22	-17	-15	-17	3	90	+47	-17	-14	+5
4	105	+31	-34	+2	0	4	126	-20	-42	-113	-58
5	135	-18	-14	-72	-35	5	162	-4	-47	+24	-9
6	165	-38	+33	-57	-21	6	198	-41	-74	+28	-29
7	195	-98	-6	-5	-36	7	234	-48	-5	+45	-3
8	225	+12	-22	-18	-9	8	270	+14	+2	-4	+4
9	255	+30	-25	-5	0	9	306	+9	+117	-36	+30
10	285	+62	+38	+8	+36	10	342	-8	-23	+48	+6
11	315	+58	-44	+2	+5						
12	345	+42	+24	+90	+52						

The figures of Table XIII show an oscillation of $\log \bar{\pi}(m)$ with galactic longitude with a maximum in the direction towards the galactic centre. This effect exists in all three spectral groups with a considerable scattering but, in the average over all spectral types, it is very clearly pronounced. A graphical representation is given in Fig. 1.

One may even represent the oscillation of $\log \bar{\pi}(m)$ by terms in $\sin l$ and $\cos l$, and the following formula for Δa of Table XIII was found satisfactory:

$$\Delta a = -0.007 \sin l + 0.028 \cos l = +0.029 \cos (l - 345^\circ) \\ \pm 4 \quad \pm 5 \quad \pm 5 \quad \pm 8^\circ$$

This would indicate that the maximum parallaxes are at $l = 345^\circ$; this is a somewhat greater value than that usually assumed for the longitude of the galactic centre. Other investigations have also shown that the apparent longitude of the galactic centre is greater for the bright stars than for the faint ones.

The mean parallaxes derived in this paper can be represented by the interpolation formula

$$\log \bar{\pi}(m) = a - 0.147m,$$

the quantity a being given in Table XI for each spectral group and each area. If also the run of a with galactic longitude and latitude is represented by an interpolation formula, we obtain

$$\log \bar{\pi}(m) = a_0 - 0.050 \cos 2b + 0.029 \cos (l - 345^\circ) - 0.147m,$$

in which the quantity a_0 is

$$\begin{array}{ll} a_0 = 8.899 & \text{for A stars} \\ 9.204 & \text{F + G stars} \\ 8.901 & \text{K stars} \end{array}$$

7. *Possible explanations of the dependence of the mean parallaxes on galactic longitude.*—The dependence of the mean parallaxes on galactic longitude requires some investigation, especially as to whether this is a real structural feature of the stellar system, or whether it is caused by some systematic error. The result can certainly not be produced by a systematic error in the proper motions of the GC,

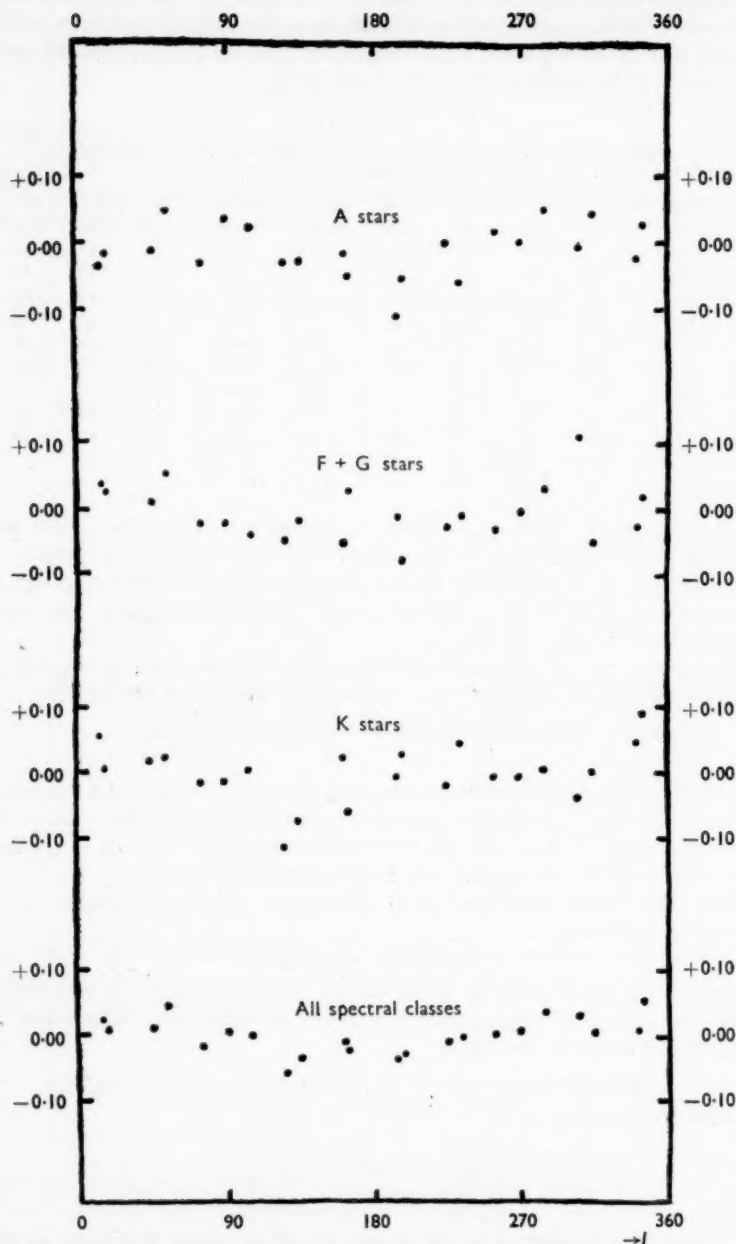


FIG. 1.—Dependence of $\log \pi(m)$ on galactic longitude.
 The curves give deviations from the average values of $\log \pi(m)$ over all longitudes.

because the mean parallaxes are derived from the dispersion of the proper motions and these are not affected by any systematic error that is practically constant within a field 30° wide. Thus no effect such as a wrong precessional constant, or galactic rotation, will produce an apparent dependence of the dispersion of proper motion on galactic longitude.

The fact that the maximum longitude of $\log \bar{\pi}(m)$ coincides exactly with the adopted longitude of the vertex (345°) could be taken as an indication that the phenomenon is a consequence of a wrong assumption concerning the vertex longitude. It is, however, easy to see from equation (1) that, if a wrong value is assumed for L , there would be a run of the mean parallaxes with $\sin^2 l$ and consequently with $\sin 2l$ instead of with $\sin l$. Nevertheless, an attempt was made to derive the dependence of $\log \bar{\pi}(m)$ on l assuming 315° for the longitude of the vertex; it was found that the numerical values of the coefficients of $\sin l$ and $\cos l$ remained unchanged, although the mean errors became slightly greater; thus even a considerably different assumption as to the position of the vertex cannot remove the dependence of the mean parallaxes on galactic longitude.

Also differences in the density of stars in space cannot be responsible for the phenomenon, because in this case the mean parallaxes should show a minimum in the direction towards the galactic centre; the more rapid decrease of stellar density in space in the direction towards the anticentre would make the average distance of stars of a definite magnitude smaller.

Only two possible explanations remain: (1) the distribution of linear stellar velocities may not exactly follow the assumed ellipsoidal law, and (2) there exists an absorption in the direction towards the galactic centre. In the first case the deviations of the stellar velocity distribution from the ellipsoidal law would have to be assumed to depend on galactic longitude. If, in the second case, the increase of the mean parallaxes towards the galactic centre is due to absorption, it would mean there is a greater absorption in this direction than towards the anticentre. One can determine this absorption difference on the hypothesis that there is only one absorbing screen. The values for $\log \bar{\pi}(m)$ show an excess of 0.058 in the direction of the galactic centre, and since one magnitude changes $\log \bar{\pi}(m)$ by 0.147, we arrive at a total absorption of $0^m.4$. It is, however, rather unlikely that there is one absorbing screen only or even a continuous uniform absorption; what we observe is probably the integrated effect of a number of irregularly distributed individual clouds which may occur in larger numbers or greater density in the direction towards the galactic centre than towards the anticentre.

In an investigation of space-reddening of the B stars, Stebbins and Huffer* found that the absorption in the galaxy depends on galactic longitude, the maximum absorption occurring in the longitude 350° . That corresponds to the maximum of the mean parallaxes of the present paper and supports the hypothesis that the derived dependence of $\log \bar{\pi}(m)$ on galactic longitude is due to absorption.

The author wishes to thank the British Council for granting him a Fellowship for one year, during which the present work was carried out. He is also indebted to Professor Redman for allowing him to work at the Cambridge University Observatories.

*University Observatories,
Cambridge:
1951 June.*

* J. Stebbins and C. U. Huffer, *Publ. Washburn Obs.*, 15, part 5, 1934.

A RADIO SURVEY OF THE CYGNUS REGION

I. THE LOCALIZED SOURCE CYGNUS (1)

R. Hanbury Brown and C. Hazard

(Communicated by A. C. B. Lovell)

(Received 1951 July 10)

Summary

A survey has been made of the Cygnus region at a wave-length of 1.89 m. using a pencil beam 2° wide. The account of this survey has been divided into two parts. Part I deals only with the observations of the intense localized source Cygnus (1). The celestial coordinates and intensity of the source are given and are compared with the measurements obtained by other observers using interferometers. The intensity of the source was observed to fluctuate and the frequency of occurrence and the degree of fluctuation are given. It is shown that the apparent mean intensity of the source is not changed by more than 2 per cent by the presence of fluctuations.

1. *Introduction.*—During the past few years the radio-frequency radiation from the region of Cygnus has been studied with particular interest by several observers. Hey, Parsons and Phillips (1) first drew attention in 1946 to irregular fluctuations in the intensity of the radio emission from this region. From their observations at 4.7 m. they concluded that these fluctuations might be due to the presence of a high-intensity variable source of small apparent angular diameter. They estimated the coordinates of the source to be R.A. 20^h 00^m, Dec. +43°, and they noted that there were possibly other active areas within 8°. Hey (2) states that their later observations suggested a diffuse source near R.A. 20^h 30^m, Dec. +38°. Surveys of this region were also made by Reber at 1.87 m. (3) and at 0.62 m. (4). His observations at 0.62 m. were made with an aerial beam-width of 4°, and they show two localized sources in the region of Cygnus (one at R.A. 20^h 40^m, Dec. +42°, and the other at R.A. 20^h 00^m, Dec. +40°). His survey at 1.87 m. was made with a beam-width of 14°, and he failed to resolve the two sources shown by his measurements at 0.62 m.

Since these early observations a source in Cygnus has been studied with interferometers by Bolton and Stanley (5), by Ryle and Smith (6), and by Stanley and Slee (7). Their observations show that there is, in Cygnus, an intense source of small angular diameter. (Stanley and Slee state that the angular diameter is less than 1' 30".) This source can be identified as the original source observed by Hey, Parsons and Phillips and as one of the sources observed by Reber at 0.62 m. It is now known to be the second brightest radio source in the sky and it will be referred to here as Cygnus (1). The fluctuations in the intensity of this source have been confirmed by many observers, and at first they were attributed to the presence of a variable component in the source; however, more recent work (9, 10, 11, 12) has shown that at least the greater part of the fluctuations can be attributed to the effects of irregularities in the ionosphere.

A detailed analysis of the surveys on 4.7 m., 1.87 m. and 0.62 m. has been made by Bolton and Westfold (13, 14), who conclude that in addition to Cygnus (1) there is a second localized source in this region whose coordinates are approximately R.A. $20^{\text{h}} 30^{\text{m}}$, Dec. $+41^{\circ}$. This second source lies in the galactic plane ($l=48^{\circ}$, $b=0^{\circ}$) and they suggest that it corresponds to a concentration of material in a spiral arm of the Galaxy. The observational evidence for this source is not satisfactory, since only one (4) of the three surveys had sufficient resolution to separate a source in this position from Cygnus (1), and the sensitivity of the equipment used in that survey was not sufficient to yield detailed contours. In view of the interesting suggestion by Bolton and Westfold it is clear that a more detailed study of the region is required using equipment of higher resolution and higher sensitivity. The region is just within the working field of the large paraboloid at the Jodrell Bank Experimental Station, and a survey has been made between the limits R.A. $19^{\text{h}} 00^{\text{m}}$ to $21^{\text{h}} 20^{\text{m}}$ and Dec. $+38^{\circ} 47'$ to $+42^{\circ} 48'$. The account of the observations can be divided conveniently into two parts: Part I of this paper deals only with Cygnus (1), while Part II deals with the region around Cygnus (1) and discusses the evidence for the second source.

2. *Description of apparatus.*—The apparatus used in this survey has been described in detail in a previous publication (15) and so only a brief description will be given here. The aerial is a paraboloid of 218 ft. diameter and 126 ft. focal length, and at a wave-length of 1.89 m. the beam-width between half-power points is 2° . The beam can be directed to declinations between $+38^{\circ}$ and $+68^{\circ}$ by tilting the mast which supports the primary feed.

The design of the receiving equipment is based on that described by Ryle and Vonberg (16), in which the power from the aerial is balanced continuously against that from a standard power generator. The calibration of the equipment for the measurement of power depends upon the standard generator, which is a temperature-limited tungsten filament diode, type C.V. 172. The receiver is tuned to 1.89 m. and has a pre-detector band-width of 2 Mc./s., a post-detector time-constant of 10 seconds and a noise factor of 3.5. The intensity of the power received is recorded on a moving chart by a standard recording milliammeter.

3. *Method of observation.*—The survey was carried out by fixing the aerial beam at a constant azimuth (approximately due south) and at a number of different elevations corresponding to declinations between $+38^{\circ} 47'$ and $+42^{\circ} 48'$. The direction of the beam was found by measuring the position of the primary feed of the aerial with a theodolite.

For each diurnal rotation of the Earth the beam swept out a strip of sky 2° wide in declination and 24^{h} in R.A., and the intensity of the power received from this strip was recorded between R.A. $19^{\text{h}} 00^{\text{m}}$ and R.A. $21^{\text{h}} 20^{\text{m}}$. The variation with right ascension of the power received at each elevation of the beam was established by making records on several successive days and by averaging the results.

4. *Results on Cygnus (1).*—The observations were taken in 1950 between August and November, and altogether 80 records of the transit of Cygnus (1) were made.

Fig. 1(a) shows a typical record taken with the aerial beam directed towards Dec. $+40^{\circ}$. The main feature of the record is the intense maximum which occurs at approximately R.A. $20^{\text{h}} 00^{\text{m}}$ and which corresponds to the transit of

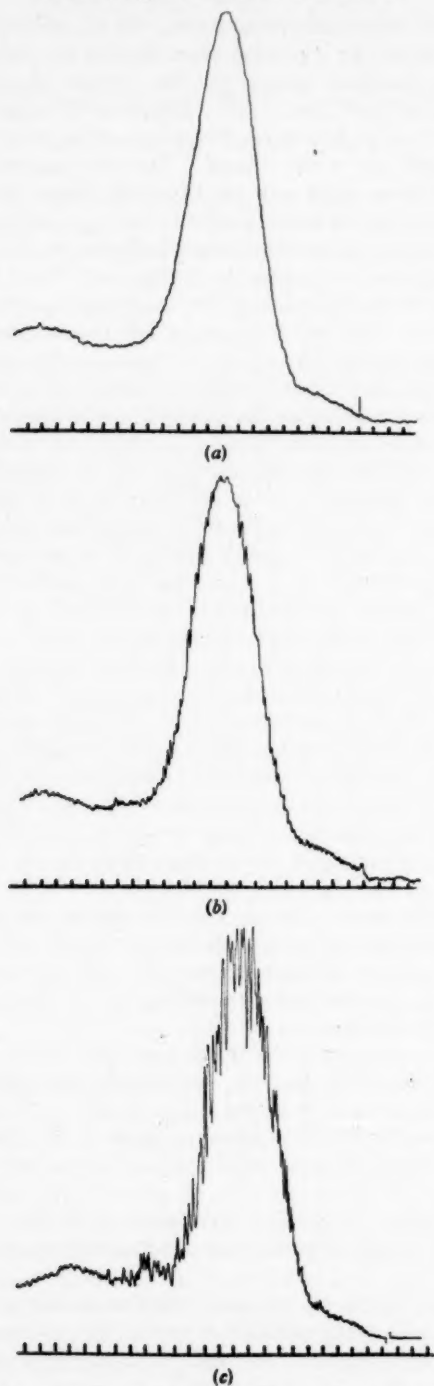


FIG. 1.—Facsimiles of single records of the transit of Cygnus (x) showing three different degrees of fluctuation.

Ordinates: Intensity in arbitrary units.
Abcissae: Right ascension (1 division = 2^m).

Cygnus (1) through the beam. The width in right ascension of this maximum corresponds to the beam-width of the aerial and therefore the source shows no measurable disk. The radiation from Cygnus (1) is superimposed on a gradient in the background radiation which is due to the approach of the beam to the galactic plane.

(i) *Fluctuations in intensity.*—The radiation from Cygnus (1) was observed to fluctuate in intensity on several occasions. Figs. 1(a), (b) and (c) show records taken on different nights and each record shows a different degree of fluctuation.* The maximum degree of fluctuation on each record has been measured, and Fig. 2 shows the frequency with which various maximum degrees of fluctuation

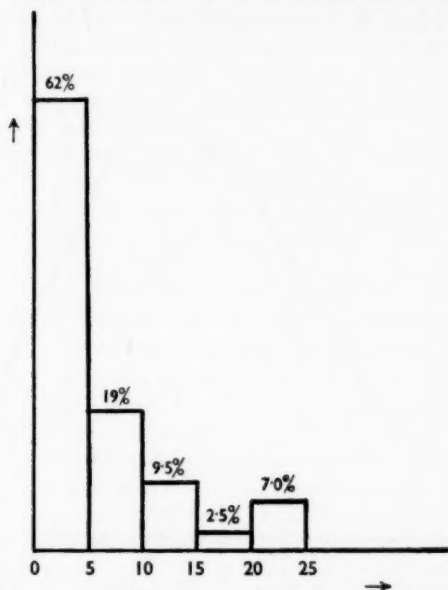


FIG. 2.—Histogram showing the maximum degree of fluctuation observed in 42 observations of the transit of Cygnus (1).

Ordinates: Number of observations, expressed as a percentage of the total number of observations.

Abscissae: Maximum degree of fluctuation observed, expressed as a percentage of the mean intensity observed at transit.

were observed. The average degree of fluctuation for a period of two minutes about the time of transit has also been measured. The mean of these average values for all the observations made in September and October was found to be about 1.5 per cent. The records used in this analysis were restricted to those in which the level of interference would permit the detection of fluctuations of 1 per cent.

The records have also been analysed with a planimeter to test if the mean power received from the source is affected by fluctuations. The analysis shows that any change in the mean power (averaged over several fluctuations) during periods of fluctuation is less than 2 per cent.

* The degree of fluctuation has been defined as the deviation from the mean intensity expressed as a percentage of the mean intensity at transit.

(ii) *Celestial coordinates.*—The coordinates of Cygnus (1) have been determined from selected records which show no interfering signals and on which the fluctuations in intensity of the source are less than 5 per cent. The declination and right ascension were determined as follows:

(a) *Declination.*—The declination of the source was found by plotting the intensity observed at transit against the angle of tilt of the aerial mast as shown in Fig. 3. The intensity of the contribution due to the source was estimated by subtracting from the total intensity, observed at the time of transit, the value of the background radiation, which was found by extrapolation of the background over the region of the source. From the results shown in Fig. 3 it can be seen that the maximum intensity was received with the mast tilted to an angle of $13^{\circ} 51' \pm 5'$. The error of $\pm 5'$ is due only to the uncertainty

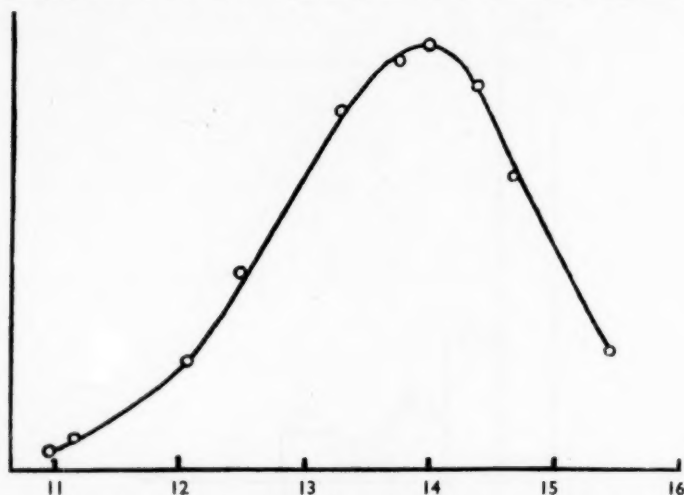


FIG. 3.—Variation of the intensity of Cygnus (1) (observed at transit) with tilt of the antenna mast. This graph is used to establish the declination of Cygnus (1) (see text).

Ordinates: Intensity in arbitrary units.

Abscissae: Degrees of tilt of the antenna mast with respect to the vertical.

in estimating the peak of the curve, since errors in the measurement of the position of the mast were negligible. In order to convert this result into a measurement of declination the relationship between the tilt of the mast and the direction of the beam must be known. The relation between the angles of tilt of the beam (α) and of the antenna mast (θ) can be represented approximately by the equation

$$\alpha = k\theta, \quad (1)$$

where α and θ are measured with respect to the axis of the paraboloid and k depends upon the parameters of the aerial system. Experiments (19) made on small paraboloids suggest that for the aerial used in this experiment the value of k is about 0.93. This value is, however, uncertain to at least ± 2 per cent and therefore for an angle of tilt of the primary feed of 14° there is an uncertainty in the direction of the beam of about $\pm 15'$. An additional error in the direction of the beam can be introduced by a displacement of the electrical centre of the primary feed of the aerial system from its mechanical centre. It is estimated that errors in the construction of the aerial may have displaced its electrical centre

2½ inches at the most from the axis of the mast, thereby introducing an error of about $\pm 10'$ in the direction of the beam.

These two effects in combination introduce a maximum uncertainty of $\pm 25'$ into the calculation of the direction of the beam when it is tilted about 14° from the axis of the paraboloid.

It was found possible to reduce these errors by observing the Great Nebula (M31) in Andromeda (15, 20), which is at approximately the same declination as Cygnus (1). The difference in the declinations of M31 and Cygnus (1) was measured by radio observations (using the value of $k = 0.93$ in equation (1)), and this difference was applied to the visual coordinates of M31 to establish the value for the declination of Cygnus (1) which is given in Table I. Since the difference in the declinations of the two sources is only about half a degree, this calibration makes the systematic errors negligible and leaves only the observational errors, which are $\pm 5'$ for Cygnus (1) and $\pm 15'$ for M31. The larger error in the case of M31 is due to the low intensity of the radiation. These two observational errors may be considered as mutually random and they combine to give an error of $\pm 16'$ in the final value of the declination.

(b) *Right ascension.*—The right ascension of Cygnus (1) was calculated from the times at which it was observed to transit the aerial beam and from measurements of the position of the primary feed. The direction of the aerial beam was found by measuring the angle of tilt of the mast in an east-west plane and by correcting this angle by means of equation (1). As this angle of tilt was always less than half a degree the error due to the uncertainty in the value of k was negligible.

There are three component errors in the final value of right ascension given in Table I: (i) the error due to the uncertainty in the position of the electrical centre of the primary feed, (ii) the error in measuring the position of the primary feed, and (iii) the error in observing the time of transit. The first of these errors is a systematic error whose value is difficult to assess. It is estimated that the electrical centre of the primary feed may be displaced up to 2 inches from the axis of the mast and that this may introduce a systematic error of about ± 20 seconds into the value of right ascension. The second and third errors are random and their effect has been reduced by averaging several observations. The final result is the weighted mean of twelve observations taken at three different mast positions and the probable error in this mean due to the two random errors alone is ± 7 seconds.

TABLE I
Coordinates of Cygnus (1)
Epoch 1950

Authority	Right Ascension	Declination
218 ft. paraboloid		
Jodrell Bank	$19^h 57^m 22^s \pm 25^s$	$+40^\circ 22' \pm 16'$
Stanley and Slee (7)	$19^h 58^m 18^s$	$+40^\circ 36'$
Ryle, Smith and Elsmore (17)	$19^h 57^m 46^s \pm 5^s$	$+40^\circ 30' \pm 7'$
Mills and Thomas (18)	$19^h 57^m 37^s \pm 6^s$	$+40^\circ 34' \pm 3'$
Bolton and Stanley (5)*	$19^h 58^m 47^s \pm 10^s$	$+41^\circ 47' \pm 7'$

* The authors understand that the result given by Bolton and Stanley (5) has now been superseded by the value given by Stanley and Slee (7). For this reason a discussion of the coordinates given by Bolton and Stanley will be omitted from this paper.

(iii) *Intensity*.—The data shown in Fig. 3 have been used to find the power received by the aerial when the source is on the axis of the beam, and this has been used to calculate the intensity of the radiation which is given in Table II. The accuracy of this value of the intensity depends upon the accuracy of the standard noise generator and upon the precision with which the aerial gain and the feeder loss are known. The standard noise generator is believed to be accurate to ± 10 per cent, the feeder loss has been measured and the errors in its value may be neglected, while the gain of the aerial has been calculated and is believed to be accurate to about ± 15 per cent.* The final value of intensity is therefore subject to a maximum error of about ± 25 per cent.

TABLE II
Intensity† of Cygnus (1)

Observer	Intensity at 3.7 m. watts/sq. metre/c.p.s.	Intensity at 1.89 m. watts/sq. metre/c.p.s.
218 ft. paraboloid Jodrell Bank Stanley and Slee (7) Ryle (21)	... 15×10^{-23} 14×10^{-23}	$5.7 \times 10^{-23} \pm 25$ per cent 7×10^{-23} 13.5×10^{-23}

5. *Discussion*.—The data given in this paper are the first detailed results on Cygnus (1) to be published as the result of measurements made with a pencil beam, and it is interesting to compare them with the results obtained using interferometers.

(i) *Coordinates*.—The coordinates of Cygnus (1) have been measured with interferometers by several observers and their results are shown in Table I, together with the result of the present work. Comparison of these results shows that all the values of declination lie within the limits of error of the result given by the pencil beam. The values of right ascension given by Ryle and by Mills and Thomas agree with that given by the pencil beam within the limits of experimental error. However, the value of right ascension given by Stanley and Slee differs from the present result by 56 seconds and it is difficult to assess the significance of this disagreement because the accuracy of their result is not stated. From an earlier paper by Bolton and Stanley (8) the accuracy of their method appears to be about ± 10 seconds in right ascension, and hence the disagreement between the two results appears to be outside the limits of the combined experimental errors.

(ii) *Intensity*.—The values of the intensity of Cygnus (1) obtained by different observers are given in Table II.

The value attributed to Stanley and Slee has been obtained from the graph in their paper, while that due to Ryle has been obtained by interpolation from his results at 1.4 m., 3.7 m. and 6.7 m.

The values of intensity at 3.7 m. given by Stanley and Slee and by Ryle agree satisfactorily and may be provisionally accepted. There is, however, a

* During some earlier work on 4.2 m. a transmitter carried by an aircraft was used to check the gain of the aerial and the result agreed closely with the calculated value.

† The intensity given is double that observed in one plane of polarization. It is assumed that the radiation is randomly polarized.

‡ The authors understand from a private communication from J. G. Bolton that a further extension of this work gives a value of 4.7×10^{-23} watts/sq. metre/c.p.s.

considerable discrepancy between their results at 1.89 m. The values given by Ryle show that the intensity remains almost constant over the range 3.7 m. to 1.4 m., while the values given by Stanley and Slee show that it falls off directly as the wave-length. The value of intensity obtained in the present work lends support to the latter conclusion.

(iii) *Fluctuations*.—The fluctuations in the intensity of Cygnus (1) have been studied in detail at wave-lengths longer than 3 m. They have, however, rarely been observed at shorter wave-lengths. The present observations show that they occur frequently at 1.89 m. but that the average degree of fluctuation has decreased compared with that observed at 3.7 m. Thus Ryle and Hewish (12) give a value for the average degree of fluctuation observed during September and October of 3.5 per cent at 3.7 m. while the value given here for the same period of the year is 1.5 per cent at 1.89 m. The decreased intensity of the source and the lower degree of fluctuation make the study of fluctuations at wave-lengths below 3 m. difficult without the use of a high-gain aerial.

Some early observers (8) concluded that the fluctuations represented an increase in the mean power from the source; later observations, however, have not supported this conclusion and have shown that the fluctuations are due to diffraction in the ionosphere. The present work shows that the mean power of the source is unchanged by the presence of fluctuations and this result supports the diffraction theory (22).

It must be noted that the receiver, due to its post-detector time constant, was unable to follow fluctuations with periods short compared with 10 seconds. The number of fluctuations which have therefore been missed cannot be estimated, since the necessary observational data do not exist. However, Little and Maxwell (11) show that the average number of fluctuations per minute observed on Cygnus (1), when in transit at upper culmination, is one per minute at 3.7 m. Their result suggests that the majority of the fluctuations will have been recorded in the present work; however, this value for the rapidity of the fluctuations cannot be extrapolated from 3.7 m. to 1.89 m. without further evidence.

6. *Acknowledgments*.—The work has been carried out at the Jodrell Bank Experimental Station of the University of Manchester. The aerial system was designed by Dr J. A. Clegg. The construction of the aerial and apparatus was made possible by financial assistance from the Department of Scientific and Industrial Research. We wish to thank Dr A. C. B. Lovell for his interest in the investigation. One of us (R. H. B.) is indebted to Messrs I.C.I. Ltd. for a research fellowship, and the other (C. H.) to the Department of Scientific and Industrial Research for a maintenance grant.

*University of Manchester,
Jodrell Bank Experimental Station,
Holmes Chapel,
Cheshire:*

1951 July 9.

References

- (1) Hey, J. S., Parsons, S. J. and Phillips, J. W., *Nature*, **158**, 234, 1946.
- (2) Hey, J. S., *M.N.*, **109**, 179, 1949.
- (3) Reber, G., *Ap.J.*, **100**, 279, 1944.
- (4) Reber, G., *Proc. I.R.E.*, **36**, 1215, 1948.

- (5) Bolton, J. G. and Stanley, G. J., *Nature*, **161**, 312, 1948.
- (6) Ryle, M. and Smith, F. G., *Nature*, **162**, 462, 1948.
- (7) Stanley, G. J. and Slee, O. B., *Austr. J. Sci. Res. (A)*, **3**, 234, 1950.
- (8) Bolton, J. G. and Stanley, G. J., *Austr. J. Sci. Res. (A)*, **1**, 58, 1948.
- (9) Smith, F. G., *Nature*, **165**, 422, 1950.
- (10) Little, C. G. and Lovell, A. C. B., *Nature*, **165**, 423, 1950.
- (11) Little, C. G. and Maxwell, A., *Phil. Mag.*, **42**, 267, 1951.
- (12) Ryle, M. and Hewish, A., *M.N.*, **110**, 381, 1950.
- (13) Bolton, J. G. and Westfold, K. C., *Nature*, **165**, 487, 1950.
- (14) Bolton, J. G. and Westfold, K. C., *Austr. J. Sci. Res. (A)*, **3**, 251, 1950.
- (15) Hanbury Brown, R. and Hazard, C., *M.N.*, **111**, 357, 1951.
- (16) Ryle, M. and Vonberg, D. D., *Proc. Roy. Soc. A.*, **193**, 98, 1948.
- (17) Ryle, M., Smith, F. G. and Elsmore, B., *M.N.*, **110**, 514, 1950.
- (18) Mills, B. Y. and Thomas, A. B., *Austr. J. Sci. Res. (A)*, **4**, 158, 1951.
- (19) Silver, S. and Pao, C. S., *Radiation Laboratory Report*, 479, 1944.
- (20) Hanbury Brown, R. and Hazard, C., *Nature*, **166**, 901, 1950.
- (21) Ryle, M., *Phys. Soc. Rep. Prog. Phys.*, **13**, 184, 1950.
- (22) Little, C. G., *M.N.*, **111**, 289, 1951.

THE VELOCITY DISTRIBUTION OF SPORADIC METEORS. I

Mary Almond, J. G. Davies and A. C. B. Lovell

(Received 1951 March 29)

Summary

The radio-echo diffraction technique has been used to measure the velocities of sporadic meteors. Directional aerial systems have enabled a selection to be made of meteors whose paths lie in great circle planes through either the apex or antapex of the Earth's way. The velocity distributions measured during three separate experiments, made between 1948 and 1950, are compared with the theoretical distributions, calculated on the assumption that the meteors are moving in random directions at the parabolic velocity limit. There is no evidence for a significant hyperbolic velocity component. The errors of measurement are estimated from an experiment made during the Geminid meteor shower of 1949 December which provided a suitable homogeneous group of velocities. The methods which enable the magnitude range of the meteors to be estimated are described and it is concluded that the results refer to meteors down to the fifth magnitude. There is no change in velocity distribution with meteor magnitude down to this limit. The extension of the work to fainter meteors will be described in Part II.

1. *Introduction.*—The origin of meteors is a subject of great controversy. Although it is now widely recognized that the shower meteors move in elliptical orbits, divergent views are held as to the orbits of the sporadic meteors. Difficulties of technique, particularly in the measurement of velocities, have so far hindered any agreement as to whether the orbits of the sporadic meteors are similar to the shower meteors, or whether an appreciable percentage move in hyperbolic orbits from an origin in interstellar space.

The observations which lead to the belief in the interstellar component fall into two categories:—

(a) Since a great number of visible meteors enter the Earth's atmosphere every day, the problem of their distribution can be treated statistically. If the meteors are assumed to move in random directions it is possible to estimate the diurnal and seasonal changes in hourly rates at any latitude for a mean heliocentric velocity. This was first done by Schiaparelli*, assuming that the meteors were moving at the parabolic limiting velocity, and by von Niessl†, who found that better agreement with the available observations could be obtained by assuming that the meteor velocities exceeded the parabolic limit. More recently, Hoffmeister‡ has continued this work, and as a result of a very

* G. V. Schiaparelli, *Sternschnuppen*, Ch. 3 (see also C. P. Olivier, *Meteors*, Ch. 16, Wilkins & Wilkins, 1925).

† G. von Niessl, *Astr. Nach.*, 93, 209, 1878.

‡ C. Hoffmeister, *Astr. Abhandlungen*, 4, No. 5, 1922; *Astr. Nach.*, No. 5302-3, 1924 (a full account is given in Hoffmeister's book *Die Meteore*, Leipzig, 1937).

large number of meteor counts in various latitudes has concluded that the velocities of the sporadic meteors are markedly hyperbolic.*

(b) The second method involves the observation of the angular velocity of individual meteors. Then, if the path of the meteor and its radiant are known, the heliocentric velocity can be obtained. The Harvard-Cornell meteor expedition† to Arizona in 1931-33 used the rocking mirror method of observation devised by Öpik‡ with spaced observers to determine the meteor paths. From the measurements on several thousand meteors Öpik concluded that the meteors were of two classes, shower and non-shower, the latter being far more numerous and possessing greatly hyperbolic velocities.

These conclusions in favour of a strong hyperbolic meteor component have been severely criticized, notably by Porter§ and by Prentice||. As regards (a) the main objection is against the assumption of a uniform distribution of meteor paths in space. In the case of the second method, the results of the Arizona expedition have been criticized because of the shortness of the base-line, and because the path lengths were estimated by assuming mean centres of radiation.

The evidence in favour of a solar-system origin for the sporadic meteors has been given by Porter.§ From an analysis of 3000 observations he shows that there is no significant difference in the heights of occurrence and other properties of shower and non-shower meteors. This indicates that their velocities are similar and that the sporadic meteors move in elliptical orbits like the shower meteors. Other direct methods of velocity measurement such as the visual methods used by Prentice and Alcock§|| and the photographic techniques used by Whipple¶ give no evidence in support of hyperbolic velocities.

Hence, the conventional methods of observation appear to have led to an impasse as regards the possible existence of an appreciable interstellar meteor component. During the past few years the new radio-echo methods for the observation of meteors have been applied to this problem. As regards (a) the continuous meteor survey** has yielded new information about the distribution of meteors in space. The result of this work is being presented separately†† and will not be considered in detail here. In the case of (b) the development of the radio-echo methods for measurement of meteor velocities has provided the opportunity for a new approach to this problem. The technique developed by Davies and Ellyett‡‡ for the observation of the diffraction pattern produced

* As early as 1931, Hoffmeister (*Veröffentlichungen Sternwarte Berlin-Babelsberg*, 9, No. 1, 1931) emphasized that the velocities indicated by this type of analysis could only be regarded as "effective velocities" owing to the critical dependence on the assumed distribution of meteor directions. In a recent private communication he has shown how these visual observations can be aligned with the radio-echo results described here and with the results of the radio-echo survey of the distribution of sporadic meteor radiants (Aspinall and Hawkins, referred to below) without recourse to the assumption of a marked hyperbolic velocity component.

† H. Shapley, E. J. Öpik and S. L. Boothroyd, *Proc. Nat. Acad. Sci.*, **18**, 16, 1932.

‡ E. J. Öpik, *Tartu Obs. Publ.*, **30**, No. 5, 1940; **30**, No. 6, 1941. *Harvard Ann.*, **105**, 549, 1937. *M.N.*, **100**, 315, 1940.

§ J. G. Porter, *M.N.*, **103**, 134, 1943; *M.N.*, **104**, 257, 1944; *J.B.A.A.*, **60**, 1, 1949.

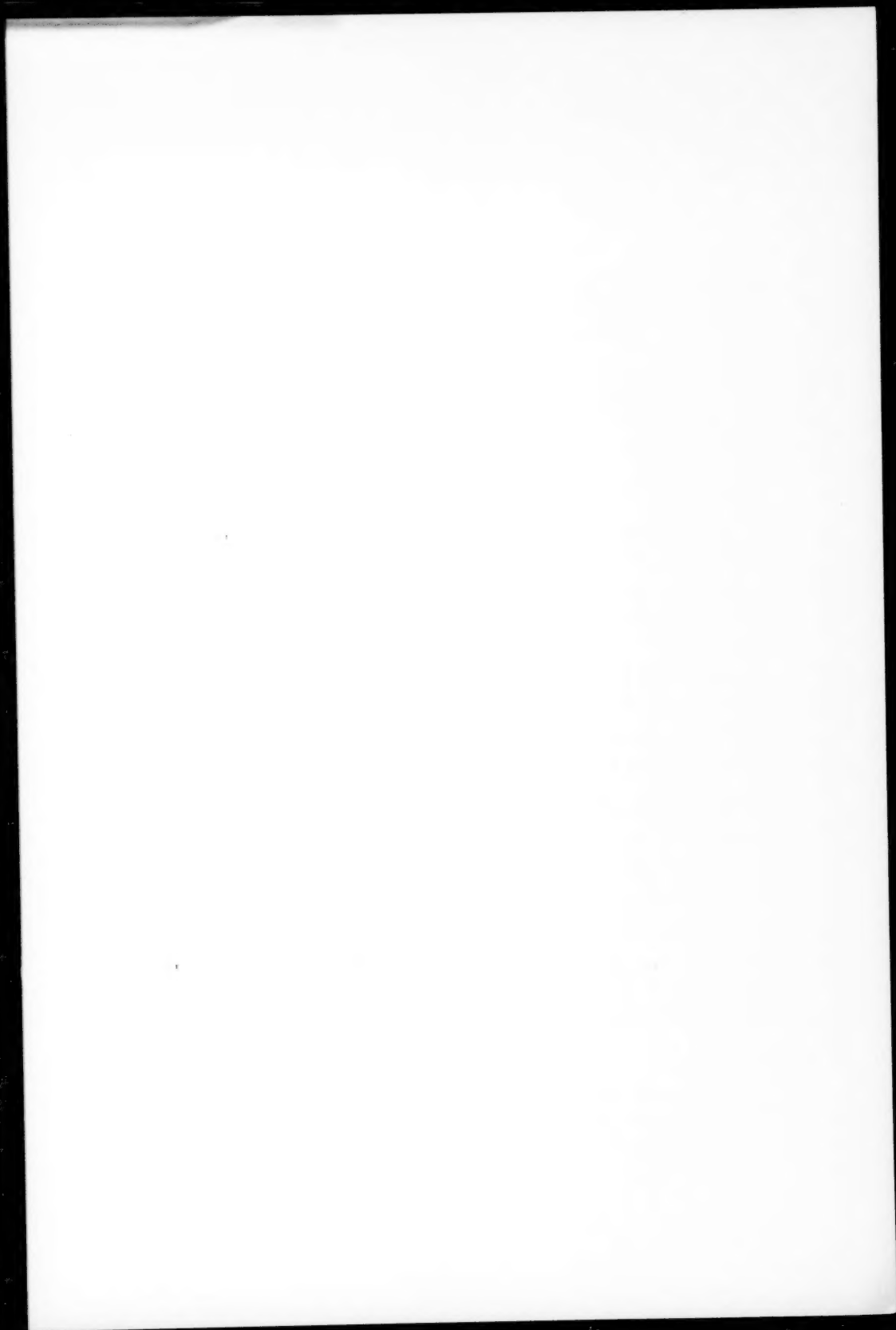
|| J. P. M. Prentice, *Phys. Soc. Rep. Prog. Phys.*, **11**, 389, 1948.

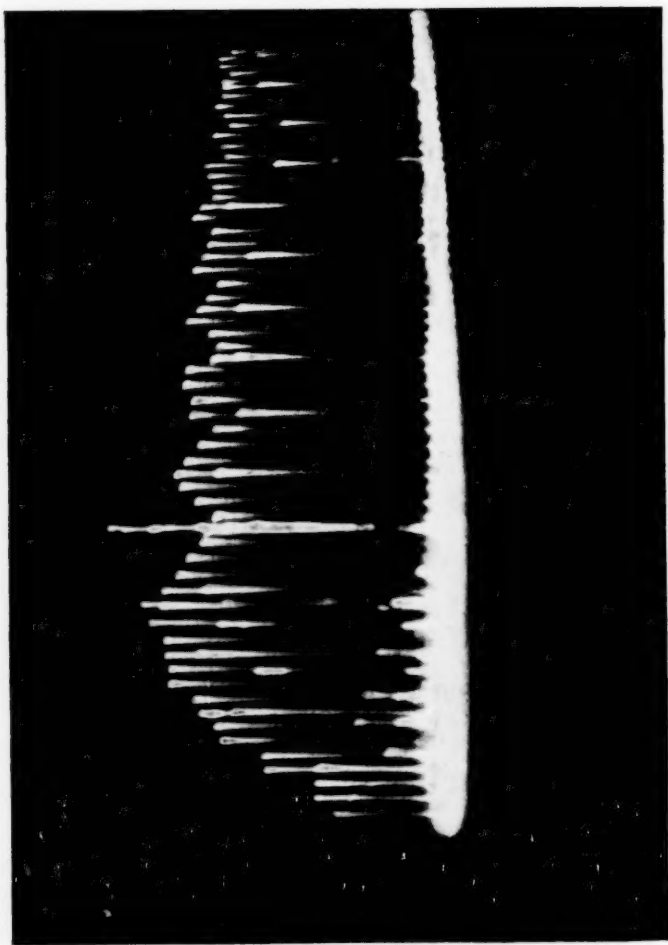
¶ F. L. Whipple, *Proc. Amer. Phil. Soc.*, **79**, 499, 1938; **82**, 275, 1940; **83**, 711, 1940; **91**, 189, 1947.

** A. Aspinall, J. A. Clegg and G. S. Hawkins, *Phil. Mag.*, **42**, 504, 1951.

†† G. S. Hawkins and A. Aspinall, in preparation.

‡‡ J. G. Davies and C. D. Ellyett, *Nature*, **161**, 596, 1948; *Phil. Mag.*, **40**, 614, 1949.





A typical diffraction photograph.

Ordinate: amplitude.

Abscissa: time.

The range of this meteor (obtained from a separate photograph) was 100 km. The velocity, calculated from the time intervals between nine maxima and eight minima, was 31.0 km./sec. The large pulse in the first minimum is produced by interference. Recorded on 1951 May 17^h 19^m 04^s. Radio wave-length 8.13 m.

by a meteor trail during its formation has now been used for the measurement of meteor velocities since 1947. The results on the shower meteors, including the newly discovered daytime meteor streams, have been described elsewhere.* These results confirm that the shower meteors have velocities below the parabolic limit. In this paper we describe the work which has been carried out on the velocity distribution of the sporadic meteors, a short note on which has already been published.† In addition, the velocity measurements on the Geminid meteor shower 1949 December 10–14 are described for comparison.

2. *Apparatus and method of velocity measurement.*—The radio apparatus was essentially similar to that described previously.‡ The transmitter radiated 600 pulses per second, each of $10\ \mu\text{sec.}$ duration. Since the separation between pulses corresponds to only 250 km. in range, it was necessary to double every fourth pulse so that ranges could be measured to 1000 km. without ambiguity. Two wave-lengths have been used: 4.16 m. and 8.13 m. The parameters of the two equipments were as follows:

Wave-length	λ	4.16 metres	8.13 metres
Peak transmitter power	P	20 kW.	30 kW.
Aerial beam width	Azimuth	$\pm 6^\circ.5$	$\pm 12^\circ$
to half power		$\pm 14^\circ$	$\pm 7^\circ$
Aerial power gain over isotropic source	G	50	25
Receiver noise level	ϵ_0	5.7×10^{-14} watts	1.3×10^{-13} watts

The 4 m. aerial system consisted of a steerable array, which was used with its beam at a fixed elevation of 10° but directed at various azimuths. The 8 m. aerial system was fixed to produce a beam at an elevation of 10° with its main axis in an easterly direction (azimuth 90°).

Common transmit-receive systems were used in each case and the received signal was fed through a conventional high-sensitivity receiver to a special recording instrument as described by Davies and Ellyett.§ The operation of this instrument was initiated automatically by the radio echo from the meteor trail and photographs showing the Fresnel zone formation were obtained as illustrated in Plate II. The time interval between successive pulses is known accurately, hence the interval between successive maxima and minima can be measured. The range of the echo is measured from a companion photograph, thus the Fresnel zone dimensions and the velocity of the meteor can be calculated.

The overall sensitivity of the apparatus to meteors of various magnitudes is discussed in Section 8. The yield of velocities from the records is discussed in Section 9 and the errors of measurement in Section 7.

Three series of experiments have been carried out with this apparatus (i) during the autumn mornings of 1948 with the 4 m. equipment and steerable array, (ii) during the autumn mornings of 1949 with the 8 m. equipment and fixed array, (iii) during the spring evenings of 1950 with the 8 m. equipment and fixed array. These are described separately below.

* J. G. Davies and J. S. Greenhow, *M.N.*, **111**, 26, 1951.

† M. Almond, J. G. Davies and A. C. B. Lovell, *The Observatory*, **70**, 112, 1950.

‡ J. P. M. Prentice, A. C. B. Lovell and C. J. Banwell, *M.N.*, **107**, 155, 1947. A. C. B. Lovell, C. J. Banwell and J. A. Clegg, *M.N.*, **107**, 164, 1947.

§ J. G. Davies and C. D. Ellyett, *loc. cit.*

3. *The first apex experiment; autumn 1948.*—In this first series of experiments the 4 m. equipment was used with the steerable array, adjusted to favour the recording of the high-velocity meteors. With the aerial beam pointed horizontally in an easterly direction, echoes are obtained from meteors whose radiants lie near the great circle passing approximately overhead, and cutting the horizon in the north and south. At 06^h the apex of the Earth's way lies on this great circle, and in the autumn months at a high altitude. Since the measured velocity of a meteor depends on the elongation of its radiant from the apex, as well as on its heliocentric velocity, the largest number of high velocities will be recorded under these conditions.

The experiment was made between 1948 September 18 and December 18 in the early morning hours, with the aerial beam adjusted so as to keep the apex on the circle of echo. Full details of the experiment with the limits of watch and aerial azimuths are given in Table I. In 230 hours' observation, 67 velocities were measured. The times and details of these measurements are given in Table II. The number distribution of velocities is shown in Fig. 1.

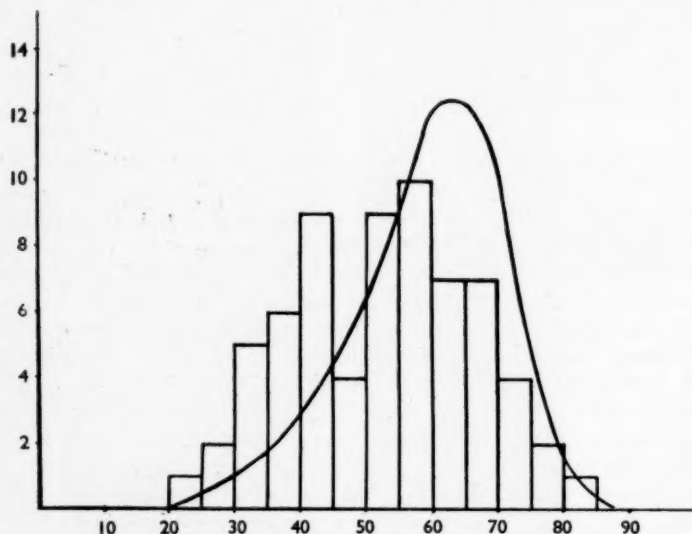


FIG. 1.—The measured velocity distribution (histogram) for the first apex experiment; autumn 1948. The theoretical distribution, calculated on the assumption of uniformly distributed parabolic meteors, is shown in the smooth curve. The theoretical curve is normalized to the equivalent number of observations.

Ordinate: number of meteors.

Abscissa: velocity in km./sec.

It will be seen that this experiment failed to give any clear evidence for the existence of an appreciable hyperbolic component, and it became necessary to compare the shape of the distribution with that to be expected from theoretical considerations. On the assumption that the meteors are moving in parabolic orbits and in random directions, a theoretical distribution can be calculated, taking into account the shape of the aerial beam and the altitude of the apex. The details of these calculations will be published separately.*

* J. A. Clegg, in preparation (Pt. III of this series).

This theoretical velocity distribution has a peak at about 60 km./sec., and a complete cut-off at 72 km./sec. For the purpose of comparison with the experimental results, the errors of measurement have been combined with this curve in the manner described in Section 7. The resulting theoretical distribution is shown as a smooth curve in Fig. 1 for comparison with the measured velocity distribution. It will be noticed that the high-velocity tail of the distribution is no greater than is to be expected from the errors of the experiment.

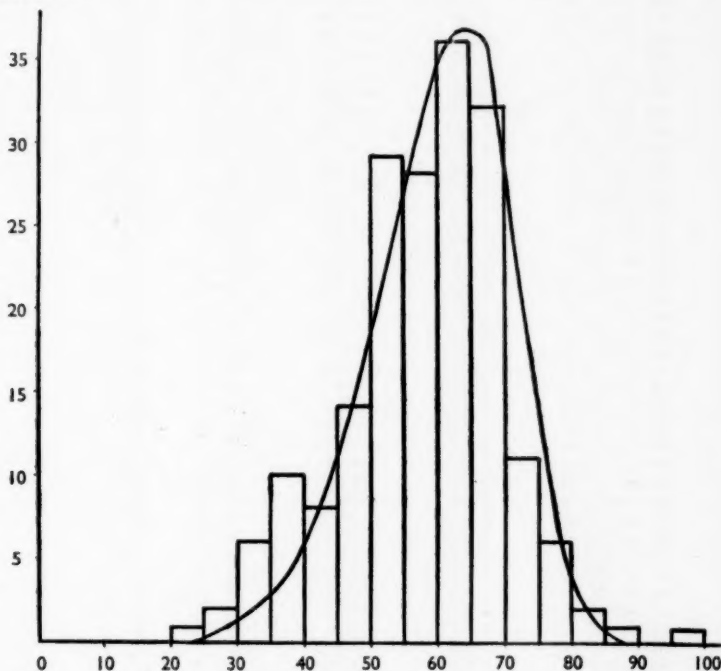


FIG. 2.—The measured velocity distribution (histogram) for the second apex experiment; autumn 1949. The theoretical distribution, calculated on the assumption of uniformly distributed parabolic meteors, is shown in the smooth curve. The theoretical curve is normalized to the equivalent number of observations.

Ordinate: number of meteors.
Abscissa: velocity in km./sec.

However, in investigating the rate of decay of echo amplitude, it was found that the mean duration of echoes of a given velocity group decreases with increasing velocity.* The time taken for the amplitude of an echo to fall to half its maximum value becomes of the order of the time required to traverse the zones of the diffraction pattern for velocities greater than about 80 km./sec., and hence the possibility that the observed high-velocity cut-off was due to this cause could not be excluded. The experiment was therefore repeated with this limitation removed.

4. *The second apex experiment; autumn 1949.*—It is known that the duration of the radio echoes from meteor trails is proportional to λ^2 .† The experiment

* A. C. B. Lovell, *Science Progress*, **38**, 22, 1950.

† A. C. B. Lovell, *Phys. Soc. Rep. Prog. Phys.*, **11**, 389, 1948.

TABLE I

Details of apex experiment; autumn 1948
(Wave-length 4.16 m.)

Date 1948	Limits of watch U.T.	Total time*	Aerial azimuth† (E. of N.)	Number of echoes	Hourly rate	Number of velocities
	h m h m	h m	° °			
Sept. 18	04 55-10 00	5 05	75-171	66	13.0	3
20	08 28-11 45	3 17	149-190	26	7.9	1
21	08 35-11 45	3 10	149-190	5	1.6	0
22	07 10-11 45	4 35	129-184	37	8.1	0
24	07 02-11 45	4 43	129-184	16	3.4	0
25	06 13-09 10	2 57	103-151	7	2.4	0
27	07 33-11 47	4 14	140-184	6	1.4	0
28	07 15-11 35	4 20	129-184	8	1.8	0
29	07 35-11 40	4 05	129-184	30	7.3	3
30	03 47-11 45	7 43	35-184	49	6.3	1
Oct. 1	07 18-11 45	4 27	129-184	24	5.4	1
2	05 05-09 32	3 34	75-165	19	5.3	0
4	07 22-10 46	3 24	165-171	18	5.3	2
5	07 25-10 45	3 20	129-177	42	12.6	0
6	07 43-11 30	3 47	129-180	24	6.3	0
7	07 16-11 42	4 26	129-180	20	4.5	1
8	07 23-10 14	2 51	129-170	36	12.6	1
12	07 13-11 45	4 32	129-181	20	4.4	0
13	09 45-11 45	2 00	170-180	5	2.5	0
14	07 21-11 42	4 21	129-174	23	5.3	0
15	07 13-11 35	4 22	129-184	13	3.0	1
16	06 12-11 00	4 48	90-166	25	5.2	0
18	07 50-11 35	3 45	129-183	9	2.4	0
22	06 37-11 57	4 45	90-185	54	11.4	1
23	04 28-10 29	5 07	90-170	55	10.7	3
25	06 01-11 45	5 44	90-177	49	8.5	2
26	08 10-11 44	3 34	150-184	21	5.9	2
27	06 05-11 45	5 10	90-184	36	7.0	0
28	05 57-11 42	5 45	90-180	35	6.1	6
29	05 10-11 15	5 50	90-170	45	7.7	5
30	05 42-11 25	5 43	90-170	79	13.8	8
Nov. 1	09 28-12 10	1 59	159-189	9	10.4	0
2	05 15-11 25	5 32	75-180	53	9.6	4
3	05 37-10 40	5 03	90-170	56	11.1	4
4	09 00-12 00	3 00	170-181	8	2.7	0
5	09 47-11 53	2 06	170-180	5	2.4	0
6	08 24-10 51	2 21	150	19	8.1	0
7	05 21-10 43	1 37	90-170	26	16.1	1
11	06 35-10 00	3 25	90-160	20	5.9	1
12	05 07-11 00	5 53	90-160	9	1.5	2
13	06 28-10 00	2 16	90-160	11	4.9	0
14	05 05-07 50	2 35	90-120	9	3.5	0
17	04 00-11 28	5 55	50-150	47	8.0	1
18	04 15-11 12	5 07	50-170	36	7.0	0
20	09 56-11 21	1 25	50	12	8.5	0
24	05 07-10 52	4 52	90-160	20	4.1	2
26	05 04-09 00	1 56	90-140	4	2.1	0
27	05 15-07 30	2 15	90-120	10	4.4	0
30	05 38-11 00	5 22	90-170	14	2.6	1
Dec. 2	06 00-10 47	4 47	90-142	11	2.3	0
4	05 12-10 43	5 31	90-170	28	5.1	0
5	05 05-10 30	5 05	90-165	10	2.0	0
7	05 00-10 00	5 00	90-160	33	6.6	3
9	05 28-07 10	1 42	90	15	8.8	3
17	04 55-11 00	5 47	90	47	8.1	3
18	05 20-10 16	4 41	90	30	6.4	1
	Totals	230 36		1444	6.3	67

* The total time here and in Tables III and V is sometimes less than the interval shown in the previous column owing to breakdowns or for other reasons.

† The aerial azimuth was increased progressively at approximately 30-minute intervals between these limits in order to maintain the apex on the circle of echo.

TABLE II

Data for velocity measurements during apex experiment; autumn 1948

Date 1948	Time U.T.	Velocity ($V \pm dV$) km./sec.	Range (R) km.	Amplitude (A) (Signal to noise ratio)	$\gamma = AR^{3/2}/G$ (R in units of 95 km.)	Electron line density (α) $\times 10^{11}$ electrons/ cm. path
	h m					
Sept. 18	08 05	66.0 ± 1.1	365	8.7	1.7	3.8
18	09 14	53.4 ± 4.2	415	5.3	1.2	2.7
18	09 25	42.3 ± 4.8	390	8.1	1.7	3.8
20	08 53	53.3 ± 0.03	340	7.4	1.4	3.2
29	08 15	34.6 ± 2.2	185	8.8	6.3	14.1
29	08 35	41.4 ± 4.1	260	8.6	2.0	4.5
29	08 35	65.3 ± 1.6	320	11.0	2.1	4.7
30	04 56	58.2 ± 2.8	305	10.3	1.9	4.3
Oct. 1	10 35	51.8 ± 1.5	230	10.8	3.1	7.0
4	07 52	26.9 ± 0.8	360	7.3	1.5	3.4
4	09 38	44.7 ± 0.08	295	10.8	2.0	4.5
7	07 35	49.2 ± 2.1	235	17.0	4.0	9.0
8	08 53	63.0 ± 4.5	265	10.8	2.2	5.0
15	07 24	62.0 ± 1.5	290	5.5	1.0	2.3
22	10 55	43.0 ± 2.1	200	8.9	4.9	11.0
23	06 30	77.5 ± 6.4	420	10.4	2.5	5.7
23	06 32	55.7 ± 2.7	330	7.0	1.3	2.9
23	08 36	40.7 ± 4.4	275	11.5	2.2	5.0
25	08 01	61.5 ± 3.5	400	10.0	2.2	5.0
25	10 17	51.8 ± 2.2	510	9.2	4.0	9.0
26	08 32	66.2 ± 3.3	220	10.8	3.6	8.1
26	11 38	64.3 ± 2.0	220	10.0	3.3	7.4
28	06 31	75.5 ± 1.8	420	9.0	2.2	5.0
28	07 09	36.9 ± 2.6	210	13.0	5.7	12.9
28	08 29	32.4 ± 2.7	440	5.0	1.4	3.2
28	08 33	33.5 ± 1.2	370	16.0	3.3	7.4
28	08 39	57.5 ± 2.2	215	8.0	3.0	6.8
28	08 45	54.0 ± 4.2	180	12.0	9.2	20.7
29	06 52	55.7 ± 4.3	395	8.0	1.7	3.8
29	07 37	58.4 ± 4.6	180	6.0	4.6	10.4
29	07 43	31.8 ± 4.5	400	20.0	4.4	9.9
29	09 03	45.5 ± 4.6	215	7.5	2.8	6.3
29	10 36	72.4 ± 1.8	380	6.0	1.2	2.7
30	06 02	64.0 ± 1.9	220	6.0	2.0	4.5
30	06 06	66.3 ± 2.0	300	6.0	1.1	2.5
30	06 24	58.1 ± 3.2	515	12.0	5.2	11.7
30	06 43	74.2 ± 4.2	380	11.0	2.3	5.2
30	08 05	68.2 ± 5.0	540	5.0	2.8	6.3
30	08 54	52.5 ± 4.0	420	10.0	2.4	5.4
30	09 00	44.7 ± 2.1	420	8.0	2.0	4.5
30	11 01	57.3 ± 5.5	385	11.0	2.3	5.2
Nov. 2	06 46	25.0 ± 2.5	195	6.4	4.0	9.0
2	07 38	39.5 ± 2.0	420	5.3	1.3	2.9
2	08 05	71.5 ± 4.4	315	6.2	1.1	2.5
2	09 33	80.5 ± 2.9	275	7.0	1.3	2.9
3	05 53	42.9 ± 3.9	230	11.6	3.3	7.4
3	06 29	56.8 ± 6.9	320	7.9	1.5	3.4
3	08 41	57.1 ± 3.2	235	15.0	4.0	9.0
3	08 43	46.9 ± 5.5	335	7.5	1.4	3.2
7	09 57	24.1 ± 4.5	195	9.3	5.8	13.1
11	07 10	37.1 ± 4.1	180	10.5	8.1	18.2
12	08 13	54.2 ± 1.1	300	11.0	2.0	4.5
12	10 08	35.7 ± 3.6	270	13.8	2.7	6.1
17	08 12	39.9 ± 4.9	380	9.3	1.9	4.3
24	06 14	41.8 ± 3.1	375	8.5	1.8	4.0
24	07 19	67.9 ± 5.6	360	7.0	1.4	3.2
30	09 12	74.6 ± 4.6	365	6.9	1.4	3.2
		58.2 ± 4.5	415	9.3	2.2	5.0
Dec. 7	No clock	61.8 ± 5.0	240	10.8	2.7	6.1
		48.1 ± 5.0	515	8.8	4.0	9.0
9	05 46	50.0 ± 2.6	360	9.2	1.8	4.0
9	06 10	52.9 ± 5.0	130	5.9
9	06 19	31.4 ± 1.5	170	6.4	5.8	13.1
		39.7 ± 1.5	325	6.0	1.1	2.5
17	No clock	67.2 ± 0.8	365	12.5	2.5	5.7
		41.9 ± 6.2	380	11.1	2.3	5.2
18	08 33	60.0 ± 1.3	400	5.5	1.2	2.7

TABLE III
Details of apex experiment; autumn 1949
 (Wave-length 8.13 m.)

Date 1949	Limits of watch U.T.	Total time	Number of echoes	Hourly rate	Number of velocities
		h m			
Oct. 10	05 03-07 10	2 07	80	38	12
11	05 29-06 49	1 20	61	46	1
14	05 08-06 24	1 16	9	7	1
28	05 14-07 00	1 46	98	55	14
29	05 16-07 12	1 56	157	81	10
31	04 59-06 41	1 42	119	70	7
Nov. 1	04 54-06 46	1 52	89	48	4
2	04 55-07 00	2 05	105	50	4
4	05 15-05 53	0 38	15	24	0
6	05 59-07 00	1 01	14	16	1
9	04 48-06 13	1 25	47	33	0
11	04 53-07 08	2 15	123	55	7
12	04 04-06 55	2 51	109	38	7
14	05 10-05 37	0 27	23	51	0
15	04 55-06 00	1 05	74	68	0
18	04 52-06 03	1 11	240	203	14
19	05 03-06 36	1 33	218	141	6
24	04 49-05 50	1 01	83	82	1
25	04 57-06 25	1 28	108	74	8
26	05 10-07 15	2 05	38	18	3
29	05 07-06 10	1 03	126	120	6
Dec. 2	05 08-05 42	0 34	50	88	0
3	05 04-07 30	2 26	10	5	1
6	05 11-05 55	0 44	66	90	2
9	05 26-07 12	1 46	107	71	10
10	06 15-07 11	0 56	128	137	7
11	06 02-07 12	1 10	235	201	13
12	06 06-07 02	0 56	229	245	25
13	06 05-06 39	0 34	134	236	12
14	06 49-06 58	0 09	51	340	6
20	05 17-07 28	2 11	99	45	5
Totals		43 33	3045	70	187

was therefore repeated on a wave-length of 8.13 m. In this case the duration of the radio echo from a given trail will be increased by a factor of four. According to the data on duration from the 4 m. measurements*, a meteor in the velocity range 80-90 km./sec. would have a duration of 0.02 seconds to half-amplitude. On 8 m., however, the duration would be 0.08 seconds. Thus any instrumental cut-off due to duration limitation would be raised to the neighbourhood of 140 km./sec.

The characteristics of the apparatus have been given in Section 2. In this experiment the aerial system was fixed in an easterly direction, but since the hours of observation were restricted to between about 05^h and 07^h this did not produce any serious change in the observed velocity distribution.

The details of the experiment, which was carried out between 1949 October 10 and December 20, are given in Table III. In 43.5 hours of observation 187 velocity measurements were made. The times and details of these measurements are given in Table IV, and the number distribution of velocities in Fig. 2. The smooth curve in Fig. 2, once again calculated on the basis of meteors moving with parabolic velocities and random directions, with the errors of measurement superimposed, shows excellent agreement with the observed distribution.

The above observations were continued during the Geminid epoch since the characteristics of the aerial were such as to preclude the recording of Geminid

* J. A. Clegg (unpublished).

TABLE IV

Data for velocity measurements during apex experiment; autumn 1949

1	2	3	4	5	6	7
Date 1949	Time U.T.	Velocity ($V \pm dV$) km./sec.	Range (R) km.	Amplitude (A) (Signal to noise ratio)	$\gamma = AR^{3/2}/G$ (R in units of 95 km.)	Electron line density (α) $\times 10^{11}$ electrons/ cm. path
	h m					
Oct. 10	05 34	62.4 \pm 4.0	380	10.0	5.9	6.0
10	05 35	59.5 \pm 4.5	320	15.0	8.8	9.0
10	05 36	69.0 \pm 5.5	380	3.0	1.8	1.8
10	06 03	62.4 \pm 6.9	355	7.0	4.1	4.2
10	06 13	60.4 \pm 3.6	385	11.0	6.5	6.6
10	06 29	57.6 \pm 3.9	350	10.0	5.9	6.0
10	06 33	61.1 \pm 4.5	350	10.0	5.9	6.0
10	06 43	66.6 \pm 4.4	490	4.0	2.4	2.5
10	06 52	58.8 \pm 4.0	360	4.0	2.4	2.5
10	06 58	46.8 \pm 5.3	365	5.0	2.9	3.0
10	07 09	48.6 \pm 3.9	400	9.0	5.3	5.4
10	07 10	52.9 \pm 3.1	405	10.0	5.9	6.0
11	06 17	60.6 \pm 4.8	600	5.0	6.1	6.2
14	05 39	65.4 \pm 6.5	420	5.0	2.9	3.0
28	05 15	53.9 \pm 3.1	420	4.0	2.4	2.5
28	05 22	67.4 \pm 3.6	660	8.0	13.3	13.6
28	05 29	74.2 \pm 3.6	890	5.0	> 50.0	> 51.0
28	05 31	49.2 \pm 3.5	450	8.0	4.7	4.8
28	05 43	76.3 \pm 8.8	570	8.0	8.1	8.2
28	05 50	70.2 \pm 8.1	410	6.0	3.5	3.5
28	05 50	60.8 \pm 3.1	525	5.0	3.5	3.5
28	05 54	67.3 \pm 4.4	395	Sat.	> 12.0	> 12.2
28	05 58	39.3 \pm 2.8	155	6.0	4.4	4.5
28	06 01	61.6 \pm 4.1	310	6.0	3.9	4.0
28	06 06	46.5 \pm 4.0	315	8.0	5.1	5.2
28	06 42	67.9 \pm 2.7	495	Sat.	> 12.0	> 12.2
28	06 45	66.9 \pm 4.8	395	Sat.	> 12.0	> 12.2
28	06 46	42.8 \pm 1.8	400	5.0	2.9	3.0
29	05 24	68.1 \pm 8.0	365	10.0	5.9	6.0
29	05 48	66.4 \pm 2.7	615	9.0	11.5	11.7
29	06 04	54.2 \pm 4.9	395	6.0	3.5	3.5
29	06 06	49.0 \pm 2.6	330	5.0	2.9	3.0
29	06 18	74.4 \pm 4.4	650	10.0	16.1	16.4
29	06 24	62.7 \pm 7.0	345	10.0	5.9	6.0
29	06 28	68.8 \pm 3.1	405	10.0	5.9	6.0
29	06 31	74.3 \pm 5.4	385	9.0	5.3	5.4
29	06 50	52.5 \pm 1.9	350	Sat.	> 12.0	> 12.2
29	06 58	70.6 \pm 5.3	595	8.0	9.4	9.6
31	05 08	57.5 \pm 5.2	490	Sat.	> 12.0	> 12.2
31	05 26	59.2 \pm 6.4	350	10.0	5.9	6.0
31	05 36	23.7 \pm 1.5	160	6.0	4.5	4.6
31	06 06	79.9 \pm 10.9	375	7.0	4.1	4.2
31	06 07	59.8 \pm 6.2	360	6.0	3.5	3.5
31	06 32	68.9 \pm 4.4	425	7.0	4.1	4.2
31	06 32	64.0 \pm 4.4	430	6.0	3.5	3.5
Nov. 1	04 57	69.4 \pm 4.1	455	8.0	4.7	4.8
1	05 53	69.4 \pm 8.7	455	5.0	2.9	3.0
1	06 11	57.2 \pm 3.2	375	8.0	4.7	4.8
1	06 30	70.2 \pm 4.6	420	9.0	5.3	5.4
2	06 05	69.3 \pm 5.2	320	3.0	1.8	1.8
2	06 12	83.3 \pm 6.9	380	5.0	2.9	3.0
2	06 29	75.6 \pm 8.5	440	4.0	2.4	2.5
2	06 59	62.1 \pm 3.9	365	4.0	2.4	2.5
6	06 56	67.0 \pm 2.9	530	12.0	8.6	8.8
11	05 02	66.3 \pm 7.1	425	10.0	5.9	6.0
11	05 31	63.2 \pm 4.3	320	8.0	5.0	5.1
11	05 50	72.7 \pm 4.1	590	9.0	10.2	10.4
11	05 57	61.0 \pm 4.3	330	9.0	5.3	5.4
11	05 59	58.2 \pm 1.5	360	9.0	5.3	5.4
11	06 19	38.2 \pm 1.8	315	8.0	5.2	5.3
11	07 08	48.6 \pm 1.0	355	8.0	4.7	4.8

TABLE IV (contd.)

1	2	3	4	5	6	7
Date 1949	Time U.T.	Velocity ($V \pm dV$) km./sec.	Range (R) km.	Amplitude (A) (Signal to noise ratio)	$\gamma = AR^{3/2}/G$ (R in units of 95 km.)	Electron line density (α) $\times 10^{11}$ electrons/ cm. path
	h m					
Nov. 12	04 20	68.7 \pm 4.4	320	8.0	5.1	5.2
12	04 21	65.7 \pm 4.7	415	9.0	5.3	5.4
12	06 07	65.2 \pm 2.9	360	9.0	5.3	5.4
12	06 10	53.8 \pm 2.0	585	8.0	8.9	9.0
12	06 28	50.5 \pm 5.5	370	9.0	5.3	5.4
12	06 50	82.4 \pm 5.0	700	6.0	13.4	13.6
12	06 51	53.2 \pm 4.1	525	7.0	4.8	4.9
18	04 58	43.0 \pm 2.0	325	8.0	5.0	5.1
18	05 03	59.6 \pm 6.2	590	8.0	9.1	9.3
18	05 06	58.7 \pm 2.6	400	9.0	5.3	5.4
18	05 12	31.4 \pm 1.9	530	9.0	6.4	6.5
18	05 12	60.6 \pm 7.9	330	9.0	5.3	5.4
18	05 25	51.0 \pm 3.7	350	10.0	5.9	6.0
18	05 27	42.0 \pm 2.1	350	9.0	5.3	5.4
18	05 29	63.4 \pm 5.2	405	Sat.	> 12.0	> 12.2
18	05 31	64.1 \pm 6.8	410	6.0	3.5	3.5
18	05 35	43.3 \pm 3.0	150	9.0	6.8	6.9
18	05 41	60.0 \pm 3.9	315	7.0	4.5	4.6
18	05 45	54.0 \pm 3.2	340	10.0	5.9	6.0
18	05 48	71.9 \pm 11.8	410	10.0	5.9	6.0
18	05 55	45.6 \pm 2.7	440	9.0	5.3	5.4
19	05 27	54.9 \pm 5.1	380	10.0	5.9	6.0
19	05 40	96.9 \pm 12.6	615	9.0	11.7	11.9
19	05 40	30.3 \pm 1.5	555	9.0	8.2	8.3
19	05 46	65.0 \pm 3.4	445	10.0	5.9	6.0
19	06 01	55.4 \pm 2.6	415	4.0	2.4	2.5
19	06 01	62.6 \pm 8.0	390	10.0	5.9	6.0
24	05 34	43.9 \pm 4.0	360	10.0	5.9	6.0
25	05 07	63.7 \pm 2.5	575	9.0	9.5	9.7
25	05 17	65.2 \pm 6.1	540	8.0	6.2	6.3
25	05 31	68.0 \pm 5.9	700	5.0	11.1	11.3
25	05 31	34.7 \pm 2.4	380	7.0	4.1	4.2
25	05 31	37.1 \pm 3.2	290	6.0	4.6	4.7
25	05 50	54.3 \pm 5.1	320	9.0	5.6	5.7
25	05 59	57.0 \pm 3.0	425	9.0	5.3	5.4
25	06 22	29.0 \pm 2.0	375	9.0	5.3	5.4
		63.6 \pm 2.7	590	5.0	5.6	5.7
26	No clock	46.2 \pm 4.4	360	3.0	1.8	1.8
		38.4 \pm 2.7	310	4.0	2.6	2.6
29	05 09	64.1 \pm 4.0	400	9.0	5.3	5.4
29	05 42	66.8 \pm 3.0	500	7.0	4.1	4.2
29	05 54	49.4 \pm 4.3	360	8.0	4.7	4.8
29	05 57	56.0 \pm 3.2	365	6.0	3.5	3.5
29	06 03	53.6 \pm 4.8	390	9.0	5.3	5.4
29	06 06	68.6 \pm 7.5	440	5.0	2.9	3.0
Dec. 3	07 15	50.4 \pm 3.2	385	16.0	9.4	9.5
6	05 12	76.3 \pm 6.3	320	5.0	3.1	3.2
6	05 20	62.7 \pm 3.7	420	7.0	4.1	4.2
9	05 48	75.5 \pm 9.0	430	8.0	4.7	4.8
9	06 02	47.8 \pm 2.4	335	16.0	9.4	9.5
9	06 04	42.9 \pm 6.8	160	8.0	5.9	6.0
9	06 33	77.8 \pm 5.5	395	11.0	6.5	6.6
9	06 44	54.9 \pm 3.3	300	6.0	4.1	4.2
9	06 45	46.2 \pm 3.5	410	17.0	10.0	10.2
9	06 45	58.7 \pm 3.2	435	6.0	3.5	3.5
9	06 51	30.3 \pm 2.3	425	18.0	10.6	10.8
9	06 55	67.7 \pm 4.9	450	13.0	7.6	7.7
9	06 58	63.8 \pm 4.4	425	16.0	9.4	9.5
10	06 22	50.5 \pm 2.4	445	7.0	4.1	4.2
10	06 25	73.1 \pm 9.2	440	4.0	2.4	2.5
10	06 26	87.0 \pm 9.6	460	7.0	4.1	4.2
10	06 27	56.7 \pm 4.8	500	16.0	9.4	9.5
10	06 40	52.1 \pm 4.4	420	Sat.	> 12.0	> 12.2

TABLE IV (contd.)

1	2	3	4	5	6	7
Date 1949	Time U.T.	Velocity ($V \pm dV$) km./sec.	Range (R) km.	Amplitude (A) (Signal to noise ratio)	$\gamma = AR^{2/3}/G$ (R in units of 95 km.)	Electron line density (α) $\times 10^{11}$ electrons/ cm. path
	h m					
Dec. 10	07 04	27.6 \pm 2.3	365	15.0	8.8	9.0
10	07 09	51.1 \pm 5.5	430	15.0	8.8	9.0
11	06 07	35.4 \pm 3.1	175	5.0	3.8	3.9
11	06 09	65.2 \pm 4.6	320	10.0	6.3	6.4
11	06 12	52.2 \pm 7.4	210	4.0
11	06 14	55.5 \pm 6.1	455	10.0	5.9	6.0
11	06 23	62.8 \pm 2.3	440	4.0	2.4	2.5
11	06 33	58.6 \pm 3.2	410	11.0	6.5	6.6
11	06 34	50.8 \pm 2.6	310	9.0	5.3	5.4
11	06 41	59.6 \pm 6.8	575	Sat.	> 21.0	> 21.2
11	06 45	56.0 \pm 3.3	330	18.0	10.6	10.8
11	06 45	64.4 \pm 4.4	325	6.0	3.7	3.7
11	06 58	54.9 \pm 5.0	390	10.0	5.9	6.0
11	07 04	54.8 \pm 4.4	450	8.0	4.7	4.8
11	07 06	62.4 \pm 2.3	370	19.0	11.2	11.4
12	06 13	41.7 \pm 3.4	285	11.0	10.0	10.2
12	06 15	55.8 \pm 3.7	665	6.0	10.5	10.7
12	06 17	62.6 \pm 5.3	595	10.0	11.8	12.0
12	06 19	52.7 \pm 2.2	480	6.0	3.5	3.5
12	06 22	47.7 \pm 2.7	370	10.0	5.9	6.0
12	06 23	50.4 \pm 3.0	365	4.0	2.4	2.5
12	06 23	67.2 \pm 4.2	420	6.0	3.5	3.5
12	06 24	64.8 \pm 5.9	565	8.0	8.0	8.1
12	06 25	66.2 \pm 4.1	430	11.0	6.5	6.6
12	06 28	38.3 \pm 2.3	210	5.0
12	06 29	45.9 \pm 1.7	360	14.0	8.3	8.4
12	06 29	54.7 \pm 1.7	440	15.0	8.8	9.0
12	06 29	31.2 \pm 1.9	100	5.0
12	06 31	60.9 \pm 3.7	380	9.0	5.3	5.4
12	06 33	35.9 \pm 3.4	155	6.0	4.4	4.5
12	06 36	44.6 \pm 4.0	560	12.0	11.4	11.6
12	06 37	49.0 \pm 4.8	390	5.0	2.9	3.0
12	06 38	34.5 \pm 2.0	180	5.0	4.2	4.2
12	06 38	59.7 \pm 3.5	395	14.0	8.3	8.4
12	06 39	61.0 \pm 4.2	580	6.0	6.5	6.6
12	06 41	62.1 \pm 3.1	350	13.0	7.7	7.8
12	06 43	61.7 \pm 2.5	345	Sat.	> 12.0	> 12.2
12	06 56	63.3 \pm 3.9	385	12.0	7.0	7.1
12	06 56	54.5 \pm 3.8	440	10.0	5.9	6.0
12	06 57	51.7 \pm 2.3	375	16.0	9.4	9.5
13	06 10	64.9 \pm 6.6	445	14.0	8.3	8.4
13	06 15	37.4 \pm 2.4	165	6.0	4.4	4.5
13	06 16	56.7 \pm 2.9	640	5.0	7.7	7.8
13	06 21	67.0 \pm 2.8	560	5.0	4.8	4.9
13	06 25	63.7 \pm 6.4	390	12.0	7.0	7.1
13	06 26	74.3 \pm 5.3	405	10.0	5.9	6.0
13	06 30	68.3 \pm 11.1	195	10.0
13	06 36	56.2 \pm 2.5	345	4.0	2.4	2.5
13	06 38	52.9 \pm 3.8	580	5.0	5.4	5.5
13	06 38	67.4 \pm 6.2	620	11.0	14.7	15.0
13	06 39	59.4 \pm 3.5	370	7.0	4.1	4.2
13	06 39	39.2 \pm 2.7	150	6.0	4.4	4.5
14	06 55	50.7 \pm 2.8	420	20.0	11.8	12.0
14	06 56	59.5 \pm 6.1	420	17.0	10.0	10.2
14	06 56	55.3 \pm 4.3	570	10.0	10.0	10.2
14	06 56	55.0 \pm 3.2	460	10.0	5.9	6.0
14	06 57	57.8 \pm 7.7	180	8.0	6.7	6.8
14	06 58	64.2 \pm 6.4	400	9.0	5.3	5.4
20	05 19	72.6 \pm 4.8	450	7.0	4.1	4.2
20	05 44	69.8 \pm 4.1	525	9.0	6.4	6.5
20	06 00	38.8 \pm 3.3	320	6.0	3.5	3.5
20	06 04	51.7 \pm 3.2	350	16.0	9.4	9.5
20	06 19	64.2 \pm 2.9	605	6.0	7.3	7.4

meteors with the aerial in azimuth 90° between 05^h and 07^h . Table III shows, however, that the hourly rate increased considerably during this epoch. The 63 velocities measured during this period have been plotted separately in Fig. 3. The smooth curve is the theoretical distribution, calculated as previously, for the appropriate altitude of the apex on December 10-14. It is evident that these 63 velocities do not contain a significant proportion of Geminid meteors and these velocities have therefore been included in the main distribution (Fig. 2).

A further convincing proof that no limitations of technique were influencing these results was obtained by carrying out a third experiment as described below.

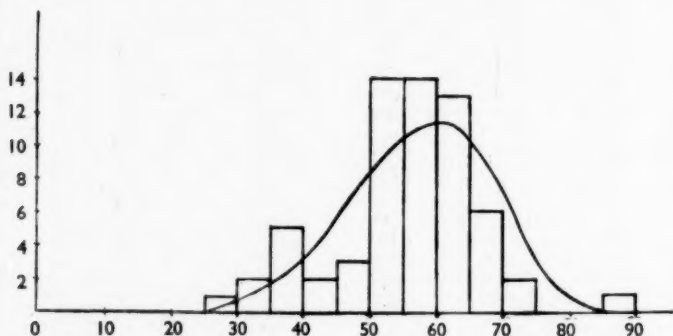


FIG. 3.—The measured velocity distribution (histogram) for the period December 10-14 during the second apex experiment 1949. The theoretical distribution, for the appropriate position of the apex at that time, calculated on the assumption of uniformly distributed parabolic meteors, is shown in the smooth curve. The theoretical curve is normalized to the equivalent number of observations.

Ordinate: number of meteors.

Abscissa: velocity in km./sec.

5. *The antapex experiment; spring 1950.*—Using the same apparatus on 8.13 metres, the previous experiment was repeated between the hours of about 15^h and 20^h from 1950 February 18 to April 29. At these times the antapex occupies the position in the sky formerly taken by the apex, and hence the velocity distribution will be the lowest possible instead of the highest. Eighty-seven velocities were measured in a total of 213 hours' observation. Table V gives details of the experiment and Table VI of the measured velocities. The velocity distribution is shown in Fig. 4, together with the theoretical distribution calculated as before on the basis of random directions of parabolic velocities. In this case a marked discrepancy occurs between the observed and theoretical results, the meteors travelling considerably more slowly than predicted. This may be due to one of two causes, or more likely to a combination of both. Either the meteors are actually travelling in markedly elliptical orbits, or their radiant are concentrated towards the plane of the ecliptic. A combination of these causes does not seem unreasonable from a comparison with cometary orbits, which fall into two classes, long and short period. The former have practically parabolic velocities, and the inclinations of their orbits are distributed at random, while the second have definitely elliptical velocities, and the inclination of their orbits is small. Thus at 06^h the atmosphere would be shielded by the Earth from meteors with orbits of low inclination and direct motion, while these would be

seen with advantage at 18^h. There has, of course, been much general evidence in support of this view from visual observations over a long period*, and more precise evidence in support has now been obtained in the continuous radio-echo survey of meteor activity referred to in Section 1.†

Since in the case of this third experiment only one meteor was observed between 60 and 70 km./sec., whereas in the previous one there were 68 meteors in this range, it is evident that the high-velocity cut-off observed is indeed a real effect, and not due to instrumental causes.

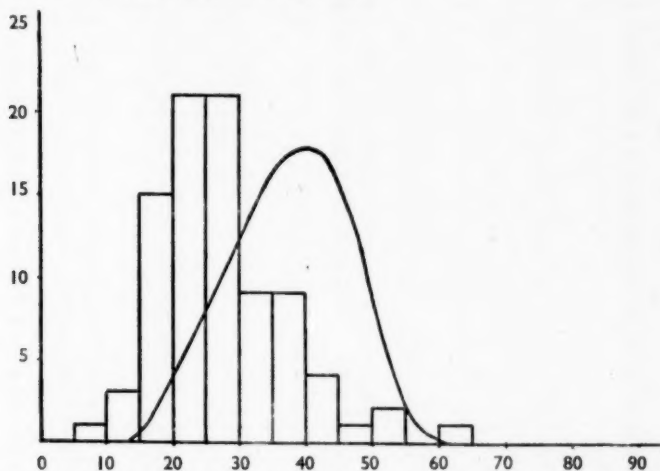


FIG. 4.—The measured velocity distribution (histogram) for the antapex experiment; spring 1950. The theoretical distribution, calculated on the assumption of uniformly distributed parabolic meteors, is shown in the smooth curve. The theoretical curve is normalized to the equivalent number of observations.

Ordinate: number of meteors.

Abscissa: velocity in km./sec.

6. *The Geminids 1949*.—In order to provide a standard of comparison and a basis for the estimation of errors, the apparatus operating on a wave-length of 8.13 metres used in the above experiments was also employed to measure the velocities of the Geminid meteors in 1949 December. The details of the experiment are given in Table VII, and of the measured velocities in Table VIII. The velocity distribution is shown in Fig. 5. In a watch totalling 5^h 49^m, 122 velocities were measured, giving a mean of 35.9 km./sec. and a standard deviation of 4.6 km./sec. The individual errors quoted are estimated from the diffraction photographs, the error depending on the number of echo pulses between the maxima and minima, and on the number of Fresnel zones observable.

7. *Experimental errors*.—The velocity measurements of the Geminid meteors referred to above have been used to estimate the error of measurement of individual velocities in the following way. In the largest group of homogeneous velocities between 34 and 38 km./sec. (Fig. 5) a total of N meteors has been selected on which the average number of independent measurements of velocity

* See, for example, W. F. Denning, *M.N.*, **47**, 35, 1886.

† G. S. Hawkins and A. Aspinall, in preparation.

TABLE V

Details of antapex experiment; spring 1950
(Wave-length 8.13 m.)

Date 1950	Limits of watch U.T.	Total time	Number of echoes	Hourly rate	Number of velocities
	h m h m	h m			
Feb. 16	16 48-19 13	2 25	5	2.1	0
17	17 47-19 30	1 43	1	0.6	0
18	16 32-18 20	1 48	3	1.7	1
21	16 27-18 40	2 13	4	1.8	0
23	15 41-18 53	3 12	10	3.1	0
24	19 12-19 50	0 38	10	15.8	0
25	16 00-19 50	3 50	36	9.4	8
27	16 00-19 52	3 52	19	4.9	0
28	16 10-17 54	1 44	4	2.3	0
Mar. 1	15 39-19 34	3 55	18	4.6	1
2	15 45-17 05	1 20	4	3.0	0
3	15 41-19 21	3 40	10	2.7	0
4	15 54-19 45	3 51	32	8.3	1
6	15 31-20 05	4 34	22	4.8	1
7	15 40-20 02	4 22	26	6.0	1
8	15 53-20 06	4 13	11	2.6	0
9	15 30-20 04	4 34	29	6.4	2
10	16 25-20 06	3 41	14	3.8	0
11	15 53-20 06	4 13	23	5.5	0
13	15 55-20 09	4 14	28	6.6	0
14	15 29-20 10	4 41	38	8.1	5
15	18 13-19 50	1 37	17	10.5	3
16	15 35-19 43	4 08	18	4.4	0
17	15 50-20 10	4 20	18	4.2	0
18	15 34-18 38	3 04	20	6.5	0
20	15 30-20 11	4 41	26	5.6	1
21	15 30-20 10	4 40	23	4.9	2
22	15 28-20 11	4 43	21	4.5	1
23	15 32-18 50	3 18	23	7.0	1
24	15 27-20 11	4 44	41	8.7	1
25	16 07-20 11	4 04	33	8.1	1
27	15 45-19 30	3 45	41	10.9	3
29	15 30-20 16	4 46	31	6.5	1
30	15 30-20 00	4 30	19	4.2	0
31	15 42-20 15	4 33	15	3.3	2
Apr. 1	16 10-20 15	4 05	11	2.7	2
3	15 35-20 10	4 35	13	2.8	1
4	15 55-20 16	4 21	36	8.3	2
5	15 36-20 13	4 37	36	7.8	1
6	15 38-20 14	4 36	43	9.3	1
7	15 53-20 16	4 23	8	1.8	0
8	16 35-20 16	3 41	41	11.1	4
10	16 14-18 00	1 46	8	4.5	0
11	15 42-20 11	4 29	73	16.2	2
12	15 53-20 11	4 18	52	12.1	2
13	15 49-20 09	4 20	61	14.1	1
14	15 47-19 55	4 08	52	12.7	5
15	16 06-18 57	2 51	16	5.6	0
17	15 08-19 26	4 18	36	8.4	3
18	15 37-19 08	3 31	57	16.2	3
19	16 49-19 45	2 56	48	16.4	2
21	15 58-19 21	3 23	42	12.4	3
22	16 20-19 32	3 12	62	19.4	0
24	16 06-19 20	3 14	58	18.0	6
25	16 03-19 26	3 23	60	17.7	2
26	16 08-19 15	3 07	50	16.0	3
27	16 12-18 14	2 02	51	25.1	3
28	16 16-19 01	2 45	42	15.3	1
29	16 16-19 45	3 29	57	16.3	4
Totals		213 06	1706	8.0	87

TABLE VI

Data for velocity measurements during antapex experiment; spring 1950

1	2	3	4	5	6	7
Date 1950	Time U.T.	Velocity ($V \pm dV$) km./sec.	Range (R) km.	Amplitude (A) (Signal to noise ratio)	$\gamma = AR^{3/2}/G$ (R in units of 95 km.)	Electron line density (α) $\times 10^{11}$ electrons/ cm. path
	h m					
Feb. 18	17 08	19.6 ± 1.9	345	9.0	5.3	5.4
25	16 28	29.5 ± 1.9	410	14.0	8.2	8.3
25	16 53	34.2 ± 1.6	490	8.0	4.9	5.0
25	16 58	19.1 ± 1.1	350	11.0	6.5	6.6
25	17 11	25.4 ± 1.2	305	13.0	8.7	8.8
25	17 59	54.3 ± 4.8	400	23.0	13.5	13.7
25	18 05	35.4 ± 1.9	455	24.0	14.1	14.3
25	18 48	33.6 ± 2.5	530	20.0	14.3	14.6
25	19 22	35.5 ± 1.3	350	23.0	13.5	13.7
Mar. 1	17 13	28.3 ± 4.3	375	8.0	4.7	4.7
4	16 21	26.5 ± 3.1	305	17.0	11.3	11.5
6	18 26	24.1 ± 1.3	395	8.0	4.7	4.7
7	15 51	29.5 ± 1.7	100	16.0	53.0	54.0
9	17 15	15.3 ± 0.7	155	10.0	7.4	7.6
9	18 30	33.5 ± 2.2	370	17.0	10.0	10.2
14	16 22	15.9 ± 1.1	300	15.0	10.3	10.5
14	17 00	29.4 ± 2.0	370	7.0	4.1	4.2
14	17 50	17.6 ± 0.6	100	12.0	60.0	61.0
14	18 40	22.6 ± 2.5	490	18.0 (Sat.)	11.0	11.2
14	18 44	40.3 ± 4.0	300	13.0	8.9	9.0
15	18 22	21.9 ± 1.8	395	12.0	7.1	7.2
15	19 26	14.8 ± 0.7	130	11.0	12.1	12.3
15	19 47	24.1 ± 1.5	140	18.0 (Sat.)	15.0	15.3
20	16 03	21.6 ± 1.8	400	10.0	6.5	6.6
21	16 38	25.4 ± 0.6	300	17.0	11.7	11.9
21	18 18	20.6 ± 1.0	310	17.0	11.3	11.5
22	20 09	25.7 ± 1.6	360	7.0	4.1	4.2
23	18 09	21.8 ± 1.2	310	13.0	8.6	8.8
24	18 08	26.9 ± 1.6	415	14.0	8.2	8.3
25	16 48	27.3 ± 1.0	360	10.0	5.9	6.0
27	16 59	12.8 ± 0.6	140	12.0	10.0	10.2
27	17 45	15.3 ± 0.4	325	7.0	4.4	4.5
27	19 24	29.8 ± 1.7	90	15.0
29	16 59	22.7 ± 2.3	160	8.0	5.9	6.0
31	17 28	33.5 ± 3.6	315	12.0	7.9	8.0
31	19 47	15.9 ± 1.1	135	10.0	8.3	8.5
Apr. 1	16 40	21.2 ± 1.8	120	6.0	8.0	8.1
1	18 18	10.7 ± 0.7	105	12.0	30.0	30.6
3	19 44	38.8 ± 1.4	600	10.0	11.8	12.5
4	16 13	42.5 ± 1.9	315	10.0	7.1	7.2
4	19 55	27.9 ± 0.6	405	8.0	4.7	4.8
5	18 55	52.5 ± 2.1	655	9.0	15.0	15.3
6	18 15	18.4 ± 0.7	90	12.0
8	18 18	31.5 ± 1.3	310	10.0	6.7	6.8
8	18 22	24.0 ± 1.1	370	8.0	5.3	5.4
8	18 35	20.9 ± 1.2	430	8.0	4.7	4.8
8	19 30	17.1 ± 1.0	380	14.0	8.2	8.3
11	17 01	29.4 ± 2.1	330	8.0	4.7	4.8
11	18 29	31.6 ± 1.4	150	14.0	16.8	17.1
12	17 31	19.0 ± 1.1	120	5.0	7.1	7.2
12	20 01	23.5 ± 1.6	170	6.0	4.6	4.7
13	17 00	25.5 ± 1.6	645	10.0	15.4	15.7
14	15 53	17.9 ± 1.2	150	6.0	4.6	4.7
14	16 23	21.6 ± 1.7	155	6.0	4.4	4.5
14	16 25	19.5 ± 0.7	110	11.0	22.0	22.4
14	No clock	18.9 ± 1.0	130	6.0	6.7	6.8
		36.9 ± 3.8	500	8.0	5.0	5.1
17	16 26	28.3 ± 1.5	105	6.0	15.0	15.3
17	16 48	46.8 ± 2.5	860	5.0
17	18 00	22.7 ± 1.6	160	6.0	4.4	4.5
18	16 19	9.8 ± 0.3	100	12.0	48.0	48.7
18	17 25	62.3 ± 4.1	330	14.0	8.7	8.8
18	No clock	29.9 ± 0.9	350	6.0	3.5	3.5
19	17 26	31.3 ± 2.7	365	5.0	2.9	3.0

TABLE VI (contd.)

1	2	3	4	5	6	7
Date 1950	Time U.T.	Velocity ($V \pm dV$) km./sec.	Range (R) km.	Amplitude (A) (Signal to noise ratio)	$\gamma = AR^{3/2}/G$ (R in units of 95 km.)	Electron line density (α) $\times 10^{11}$ electrons/ cm. path
Apr. 19	No clock	17.5 ± 0.7	170	9.0	6.9	7.0
21	16 42	36.2 ± 0.9	455	7.0	4.1	4.2
21		22.0 ± 0.7	160	9.0	6.9	7.0
21		28.8 ± 1.8	445	5.0	2.9	3.0
24		41.3 ± 3.1	325	11.0	6.8	6.9
24	No clock	21.3 ± 0.9	100	4.0	16.0	16.2
24		39.3 ± 1.3	530	13.0	8.9	9.0
24		41.8 ± 2.1	450	12.0	7.1	7.2
24		24.3 ± 1.7	540	8.0	6.4	6.5
24		35.6 ± 1.5	330	14.0	8.7	8.8
25	17 43	27.2 ± 2.0	420	12.0	7.1	7.2
25	18 38	31.9 ± 2.3	370	8.0	4.7	4.8
26	17 09	25.4 ± 1.1	100	7.0	28.0	28.5
26	17 27	26.0 ± 1.2	100	12.0	48.0	48.7
26	18 03	25.9 ± 1.2	160	5.0	4.1	4.2
27	16 38	18.3 ± 1.0	160	8.0	5.9	6.0
27	16 57	20.8 ± 1.7	100	6.0	24.0	24.4
27	18 10	36.7 ± 0.8	375	9.0	5.3	5.4
28	16 35	38.5 ± 1.5	365	6.0	3.5	3.5
29	16 19	21.8 ± 1.6	100	5.0	20.0	20.4
29	16 26	22.1 ± 1.1	100	9.0	36.0	36.6
29	16 57	30.1 ± 1.4	160	8.0	5.9	6.0
29	19 23	23.2 ± 2.4	140	7.0	5.8	5.9

TABLE VII

Details of Geminid experiment; 1949 December
(Wave-length 8.13 m.)

Date 1949	Limits of watch U.T.	Total time m	Number of echoes	Hourly rate	Number of velocities
	h m h m				
Dec. 9	02 06-03 01	55	42	46	5
10	01 56-02 42	46	137	178	14
11	01 55-02 33	38	109	172	12
12	01 53-02 28, 02 38-03 10	67	426	381	31
13	01 51-02 11, 02 18-02 23, 02 34-02 37, 02 59-03 07	36	261	435	13
14	01 50-02 24, 02 33-02 56	57	401	422	29
15	02 11-03 01	50	270	324	18
Totals		5 49	1646	283	122

per meteor was greater than three. Let the mean velocity of the n th meteor be v_n , and the separate measurements of its velocity be v_{nA} , v_{nB} , etc. Let the average number of measurements of velocity per meteor be η . Then if we write $\Delta_{nA} = v_n - v_{nA}$ the quantity $(\Sigma \Delta^2 / N\eta)^{1/2}$ is a measure of the accuracy of a single measurement, the sum being taken over the $N\eta$ measurements made. The standard deviation of the mean velocity of each meteor is then $[\Sigma \Delta^2 / N\eta(\eta - 1)]^{1/2}$.

For the sample of Geminid meteors selected these quantities are 1.75 and 1.46 km./sec. respectively. It is therefore evident that the distribution in Fig. 5 represents a true spread in the velocities of the Geminid meteors, but since the distribution must include a number of sporadic meteors, the extent of this cannot be estimated.

From the above results the mean error of measurement at any velocity can be determined. By the diffraction theory the velocity is given by $v = k\rho^{-1}R^{1/2}$, where R is the range of the echo and ρ the number of echo pulses in a given Fresnel zone,

TABLE VIII
Details of 1949 Geminids

Date 1949	Time U.T.	Velocity ($V \pm dV$) km./sec.	Date 1949	Time U.T.	Velocity ($V \pm dV$) km./sec.
	h m			h m	
Dec. 9	02 33	40.5 ± 3.3	Dec. 12	03 10	30.0 ± 2.3
9	02 34	36.6 ± 1.7	13	01 58	41.0 ± 4.5
9	02 40	30.7 ± 3.0	13	01 58	39.2 ± 2.5
9	02 42	35.4 ± 1.4	13	02 01	36.2 ± 1.4
9	02 44	35.0 ± 4.0	13	02 21	40.5 ± 2.9
10	02 14	42.5 ± 1.2	13	02 35	37.6 ± 1.3
10	02 14	38.5 ± 1.3	13	03 00	37.0 ± 1.7
10	02 19	37.9 ± 3.8	13	03 01	41.5 ± 2.8
10	02 21	33.6 ± 1.5	13	03 03	38.2 ± 1.2
10	02 25	32.2 ± 4.0	13	03 03	35.4 ± 2.0
10	02 35	42.1 ± 2.8	13	03 03	36.3 ± 1.8
10	02 36	35.8 ± 2.3	13	03 04	33.0 ± 2.3
10	02 36	35.4 ± 5.4	13	03 04	37.1 ± 2.0
10	02 36	36.5 ± 2.8	13	03 04	37.3 ± 1.7
10	02 37	44.9 ± 2.2	14	01 51	29.2 ± 0.8
10	02 39	37.2 ± 1.3	14	01 58	27.7 ± 0.5
10	02 40	34.0 ± 2.2	14	01 58	40.3 ± 1.3
10	02 41	35.2 ± 2.0	14	02 05	40.5 ± 1.7
10	02 42	36.9 ± 2.5	14	02 12	34.2 ± 1.8
11	02 03	28.2 ± 1.0	14	02 13	23.9 ± 1.0
11	02 13	35.6 ± 2.7	14	02 14	30.2 ± 1.2
11	02 15	24.4 ± 2.7	14	02 19	35.7 ± 1.5
11	02 21	33.6 ± 1.1	14	02 19	37.4 ± 1.2
11	02 21	39.9 ± 4.4	14	02 20	33.6 ± 1.5
11	02 25	32.0 ± 0.1	14	02 23	35.2 ± 2.3
11	02 26	35.2 ± 5.0			40.8 ± 1.8
11	02 26	31.5 ± 0.9			38.2 ± 1.5
11	02 27	30.4 ± 1.9			38.9 ± 1.7
11	02 29	22.4 ± 0.9			35.9 ± 0.7
11	02 31	34.8 ± 1.5			34.0 ± 1.8
11	02 33	33.2 ± 1.0			45.7 ± 3.2
12	02 09	43.2 ± 2.3			43.4 ± 2.0
12	02 14	29.6 ± 1.4			37.2 ± 2.7
12	02 16	36.4 ± 1.6			32.1 ± 1.7
12	02 19	35.6 ± 2.5	14	No clock	35.9 ± 2.1
12	02 21	36.8 ± 2.7			36.7 ± 1.4
12	02 40	26.1 ± 1.4			34.4 ± 2.0
12	02 41	34.7 ± 1.0			37.1 ± 1.5
12	02 41	45.5 ± 2.4			39.1 ± 0.9
12	02 42	39.2 ± 2.3			38.1 ± 1.3
12	02 42	29.5 ± 2.0			36.0 ± 2.0
12	02 47	37.8 ± 5.9			33.3 ± 1.1
12	02 47	33.7 ± 1.6			37.3 ± 2.2
12	02 48	36.2 ± 2.6	15	02 13	37.8 ± 2.6
12	02 48	39.1 ± 1.8	15	02 16	38.6 ± 3.0
12	02 49	47.1 ± 2.2	15	02 17	28.2 ± 1.2
12	02 50	39.1 ± 1.7	15	02 19	34.1 ± 2.7
12	02 50	35.5 ± 1.6	15	02 19	45.6 ± 1.7
12	02 53	35.6 ± 2.7	15	02 21	34.6 ± 1.4
12	02 54	36.2 ± 3.0	15	02 25	26.9 ± 1.4
12	02 56	33.6 ± 2.7	15	02 28	32.7 ± 1.6
12	02 59	39.2 ± 2.3	15	02 28	36.2 ± 3.3
12	02 59	35.1 ± 1.3	15	02 38	43.7 ± 3.4
12	03 00	34.8 ± 3.1	15	02 45	42.0 ± 1.9
12	03 02	33.0 ± 1.7	15	02 46	33.9 ± 2.7
12	03 03	24.1 ± 1.0	15	02 53	36.2 ± 2.2
12	03 04	35.7 ± 1.4	15	02 54	34.3 ± 2.4
12	03 06	49.2 ± 5.3	15	02 55	41.7 ± 3.5
12	03 08	35.5 ± 2.1	15	02 57	32.2 ± 1.2
12	03 09	38.1 ± 2.9	15	02 59	39.7 ± 2.9
12	03 09	33.1 ± 2.0	15	02 59	33.1 ± 1.1

k being a constant which includes the parameters of the apparatus. Since the mean range remains constant for different velocities, we can write for the error $\Delta v = -k\rho^{-2}R^{1/2}\Delta\rho$, where $\Delta\rho$ represents the error in estimating the value of ρ , and is constant. Thus $\Delta v = \text{const. } v^2$. Since at $v = 36 \text{ km./sec.}$ we have $\Delta v = 1.46 \text{ km./sec.}$, we can calculate the mean error in estimating any given velocity from the formula $\Delta v = 1.46v^2/36^2$, and this has been used to calculate the error function. This error function has been applied to the theoretical distributions in Figs. 1, 2, 3, 4 in order to indicate the results to be expected from the particular apparatus used in these investigations.

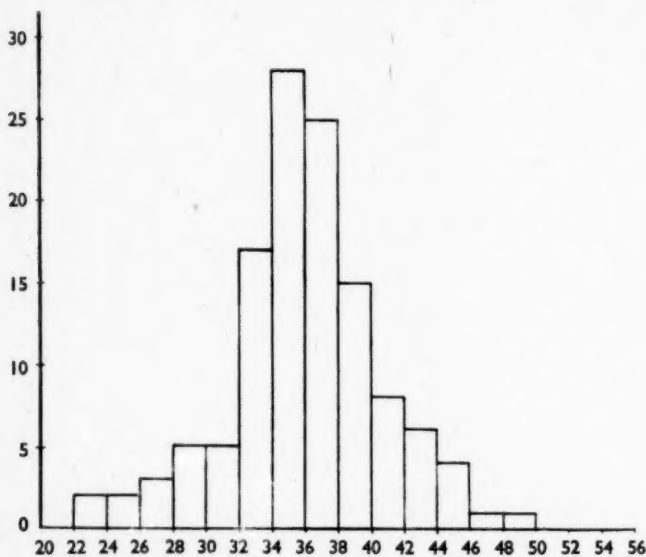


FIG. 5.—The velocity distribution for the Geminids measured during the period 1949 December 9–15.

Ordinate: number of meteors.
Abscissa: velocity in km./sec.

8. *The magnitude range of the measured meteors.*—The velocity measurements have been presented in Sections 3, 4, 5 without reference to the magnitudes of the meteors involved. Estimates of the meteor magnitudes have been made by computation of the electron densities in the meteor trails, followed by a conversion of these densities to visual meteor magnitudes. These two stages are discussed separately below.

(i) *The electron density in the trails.*—The electron density in the ionized column will increase with the brightness of the meteor, thus for given parameters of the apparatus the amplitude of the Fresnel zone pattern will serve as a measure of meteor magnitude. The conversion of the amplitude of the received signal to the electron density in the meteor trail may be made as follows.

The parameters of the apparatus involved are the wave-length λ , the peak transmitter power P , and the power gain of the aerial system G over an isotropic source. If the strength of the received signal is ϵ , then it has been shown by

Lovell* and by Lovell and Clegg† that, for a trail which is not over-dense‡, the corresponding line density α in the trail is given by

$$\alpha = \sqrt{12\pi} \left(\frac{mc^2}{e^2} \right) \frac{1}{G} \sqrt{\frac{\epsilon R^3}{P\lambda^3}} \text{ electrons/cm. path } \S,$$

where R is the range of the meteor.

The measured data for each velocity record comprise the range R and the amplitude of the first Fresnel zone A compared with the basic amplitude of the receiver noise ϵ_0 (A is the signal/noise ratio of the first zone). Thus, the above equation becomes

$$\alpha = \sqrt{12\pi} \left(\frac{mc^2}{e^2} \right) \frac{AR^{3/2}}{G} \sqrt{\frac{\epsilon_0}{P\lambda^3}} \text{ electrons/cm. path,}$$

where $AR^{3/2}$ is a factor varying with each meteor. Further, for each meteor the effective power gain G of the beamed aerial system will depend on the range R of the meteor and its azimuth with respect to the beam axis. The concept of sensitivity contours of the aerial system has been discussed by Clegg.|| Details

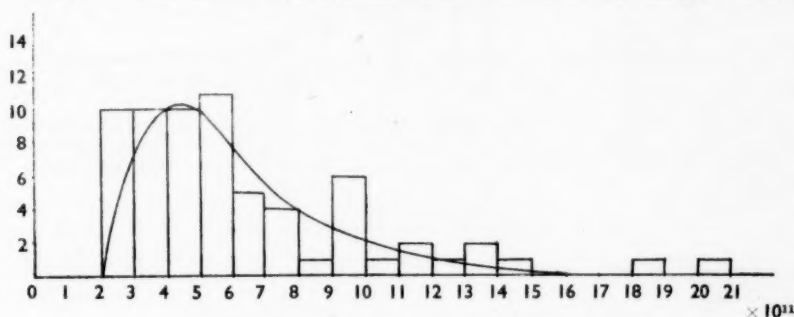


FIG. 6.—Number distribution of electron line density (α) for the 4 m. apex (1948) velocity measurements.
Ordinate: number of meteors.
Abscissa: line density α electrons/cm. path.

are given in the Appendix to this paper whereby a factor $\gamma = AR^{3/2}/G$ can be obtained for each meteor. This quantity γ is given in column 6 of Tables II, IV and VI. Column 7 gives the value of the electron line density α for each meteor calculated from the above formula using these values for γ and the values of the apparatus constants ϵ_0 , P and λ given in Section 2. The corresponding number distribution against electron density for the three experiments described in Sections 3, 4, 5 is shown in Figs. 6, 7, 8 respectively.

In order to test for any change in velocity distribution with line density, the 183 velocities for which values of α are available in Table IV have been divided

* A. C. B. Lovell, *Nature*, **160**, 372, 1947.

† A. C. B. Lovell and J. A. Clegg, *Proc. Phys. Soc.*, **60**, 491, 1948.

‡ A preliminary discussion of the problems involved if the electron density in the trail exceeds the critical density for the radio frequency used has been given by N. Herlofson, *The Observatory*, **68**, 230, 1948. In more recent private communications Herlofson has modified these calculations, as a result of which it appears that the formula given here is unlikely to be in error by more than a factor of three even when applied to over-dense trails.

§ The numerical factor in the original equation is $\sqrt{24}$. This error arose because of the use of $G\lambda^2/8\pi$ instead of $G\lambda^2/4\pi$ as the power available in a matched load connected to the aerial.

|| J. A. Clegg, *Phil. Mag.*, **39**, 577, 1948.

into three groups: $\alpha < 5 \times 10^{11}$ electrons/cm. path, comprising 65 velocities; $5 < \alpha < 7 \times 10^{11}$ electrons/cm. path, comprising 62 velocities; and $\alpha > 7 \times 10^{11}$ electrons/cm. path, comprising 56 velocities. The three distributions are given in Fig. 9, which shows that over the range of meteor sizes covered in these experiments there is no significant change in the velocity distribution

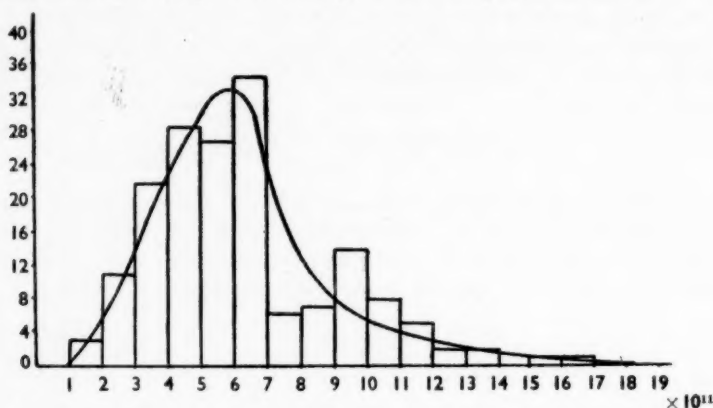


FIG. 7.—Number distribution of electron line density (α) for the 8 m. apex (1949) velocity measurements. (Eight meteors for which the only information is $\alpha > 12.2 \times 10^{11}$ electrons/cm. are not included. Two other meteors with values of $\alpha > 21.2$ and 51×10^{11} lie outside the limits of the abscissa.)

Ordinate: number of meteors.

Abscissa: line density α electrons/cm. path.

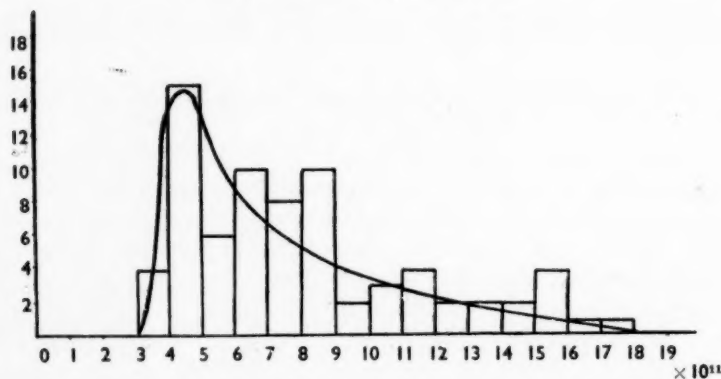


FIG. 8.—Number distribution of electron line density (α) for the 8 m. antapex (1950) velocity measurements. (Ten meteors with α values of 20.4, 22.4, 24.4, 28.5, 30.6, 36.6, 48.7, 48.7, 54.0, 61.0×10^{11} lie outside the limits of the abscissa.)

Ordinate: number of meteors.

Abscissa: line density α electrons/cm. path.

(ii) *Conversion to visual magnitudes.*—The further conversion of these electron density measurements to visual meteor magnitudes cannot be made with complete confidence owing to the uncertainties in the theories of the ionization process. A recent review has been given by Herlofson*, and the

* N. Herlofson, *Phys. Soc. Rep. Prog. Phys.*, **11**, 444, 1948.

experimental work described by Lovell and Clegg*, and by Prentice, Lovell and Banwell† indicate that his estimates are correct at least to an order of magnitude. If we accept the figures given there, the peak of the distribution curves in Figs. 6, 7, 8 lie at about third magnitude. However, recent work by Clegg‡ indicates that Herlofson's figures for the ionization produced by a meteor of a given magnitude may be too low by a factor of ten. This would shift the peak of the curves to fifth magnitude.

Unfortunately these uncertainties cannot be resolved at present and hence no precise magnitude scale can be affixed to the abscissae of Figs. 6, 7 and 8. The above discussion indicates, however, that the peaks of these distribution curves probably lie in the neighbourhood of fifth-magnitude meteors. The data presented in Fig. 9 further indicate that the velocity distributions are insensitive to the magnitude range of the meteors.

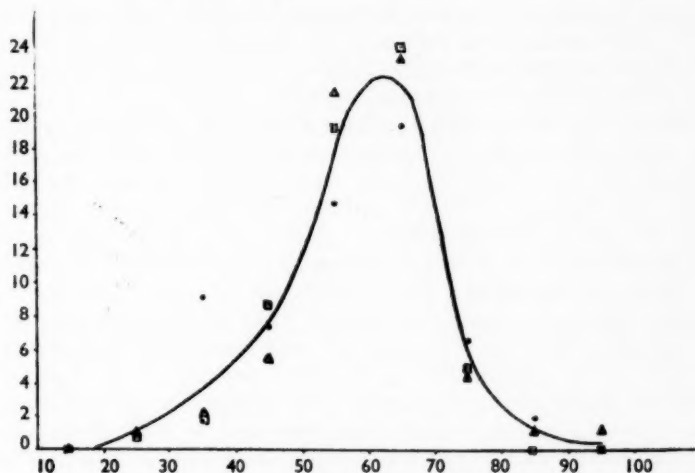


FIG. 9.—The velocity distribution for different values of line density (α) for the 8 m. (1949) apex experiment.

- $\alpha < 5 \times 10^{11}$ electrons/cm. path (65 velocities)
 - $5 < \alpha < 7 \times 10^{11}$ electrons/cm. path (62 velocities)
 - △ $\alpha > 7 \times 10^{11}$ electrons/cm. path (56 velocities)
- } All normalized to 60 total.
- distribution for all values of α .

Ordinate: number of meteors.

Abscissa: velocity in km./sec.

9. *The yield of velocities.*—It will be seen from Tables I, III, V and VII that in each of the experiments the yield of velocities has been a small percentage of the total number of echoes recorded (4.6 per cent, 6.1 per cent, 5.1 per cent and 7.4 per cent respectively). The rejections arise from several causes, the more frequent of which may be summarized as follows:—

(i) In about 40 per cent of the cases the echo amplitude is too small for satisfactory measurement.

* A. C. B. Lovell and J. A. Clegg, *Proc. Phys. Soc.*, **60**, 491, 1948.

† J. P. M. Prentice, A. C. B. Lovell and C. J. Banwell, *M.N.*, **107**, 155, 1947.

‡ J. A. Clegg (unpublished).

(ii) In about 20 per cent of the cases the range of the echo is unknown. At the high recurrence-frequencies used it is necessary to transmit every fourth pulse as a twin in order to avoid ambiguity in range measurement. If either of the components of the twin falls into one of the receiver suppression pulses the range cannot be determined.

(iii) In about 30 per cent of the cases, even although the range is known and the amplitude is satisfactory, no Fresnel zone patterns can be discerned. This arises from the turbulent conditions in the high atmosphere, which rapidly distort the meteor trail and give large fluctuations in echo amplitude as discussed by Greenhow.* In many cases the distortion is sufficient to obscure the Fresnel zone amplitude variations. It may be remarked in this connection that the continuous-wave techniques, in which a local ground wave is used as a reference phase, do much to eliminate this effect. In these cases the diffraction effect can be recorded before the meteor reaches the perpendicular reflecting point, as shown by McKinley.† In the pulse techniques used in the present work the diffraction effect can be observed only after the perpendicular reflecting point, and the distortion of the earlier parts of the trail can then have a very deleterious effect on the Fresnel zone amplitude variations.

10. *Discussion.*—The experiments described in this paper give no evidence that any appreciable numbers of meteors are moving with velocities in excess of the parabolic limit. The magnitude range covered by the experiment is somewhat uncertain, but it is believed that the major number of measured velocities lie around fifth magnitude. In any case, analysis shows that the velocity distribution is insensitive to the selection of magnitudes up to the limits measured by the apparatus. These results are in good agreement with an independent series of measurements recently made by McKinley and Millman‡ using a different radio-echo technique with a different selection of the sporadic meteors, but are in serious conflict with the measurements of Öpik§, whose rocking mirror experiments gave a marked preponderance of hyperbolic velocities.

The experiments have recently been extended to cover fainter meteors. A description of this work, together with a fuller discussion of the range of meteor magnitudes involved, will be given in Part II of this paper.

11. *Acknowledgments.*—We are indebted to several of our colleagues for their help and for valuable discussions during the course of this work, particularly to Dr J. A. Clegg and J. S. Greenhow. We also wish to express our appreciation of the interest which has been shown in the work by Professor C. Hoffmeister, Dr E. J. Öpik, Dr J. G. Porter and Dr F. L. Whipple. The research forms part of the programme of work at the Jodrell Bank Experimental Station of the University of Manchester, to which the Department of Scientific and Industrial Research has contributed substantial financial assistance. One author (M. A.) is also indebted to the Department for the award of a Maintenance Grant during the course of the work.

University of Manchester,
Jodrell Bank Experimental Station,
Holmes Chapel, Cheshire :

1951 March 28.

* J. S. Greenhow, *Phil. Mag.*, **41**, 682, 1950.

† D. W. R. McKinley (private communication).

‡ D. W. R. McKinley and P. M. Millman, *The Observatory*, **70**, 156, 1950; *Astrophys. J.*, **54**, 179, 1949; and private communications. D. W. R. McKinley, *Astrophys. J.*, **113**, 225, 1951.

§ E. J. Öpik, *loc. cit.*

Appendix

In order to calculate the most probable value of the electron density of a given meteor trail, it is necessary to know, in addition to the fixed parameters of the apparatus, the quantity $\gamma = AR^{3/2}/G$, where A is the amplitude of the received echo, R is its range, and G the power gain of the aerial in the direction of the echo. Of these the first two can be accurately measured, but it is only possible to estimate the third. It will be shown, however, that in 92 per cent of the cases the estimate will not be in error by more than a factor of two.

Clegg* has discussed the representation of an aerial beam by a set of sensitivity contours on a spherical surface at the mean height of maximum ionization, which is here assumed to be 95 km. The sensitivity of the aerial at any point on this surface is defined by $s = GR^{-3/2}$, R being measured in units of the height of the assumed surface; thus $s = 1$ corresponds to the point vertically overhead as viewed with an aerial of unit gain. For a meteor at a given range, a circle may be drawn giving the possible positions on the contour map where the echo may have occurred. A curve may now be plotted between sensitivity s and the azimuth measured from the axis of the beam. A typical curve, for a range of 400 km. on the 8·13 m. aerial system, is shown in Fig. 10a. It is now required to estimate the relative numbers seen at different points along this line, and hence the most probable value of the sensitivity.

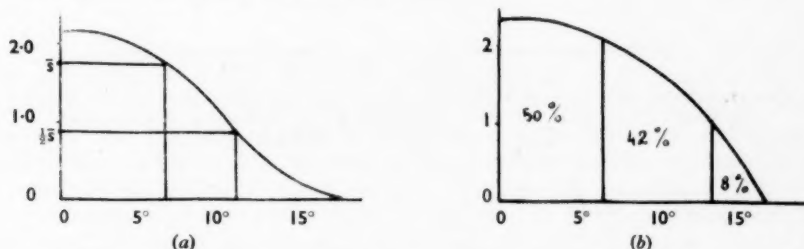


FIG. 10 (a).—A typical curve showing the relationship between sensitivity s and azimuth from the axis of the 8 m. aerial system. The example is for a range of 400 km. A complete set consists of similar curves at range intervals of 50 km.

Ordinate: sensitivity s .

Abscissa: azimuth angle from axis (degrees).

FIG. 10 (b).—The curve corresponding to 10 (a) showing relative numbers of meteors observed at different angles from the main axis of the 8 m. aerial beam.

Ordinate: relative numbers of meteors.

Abscissa: azimuth angle from beam axis (degrees).

Assuming that the distribution of number of meteors with mass obeys the law $dN = dM/M$, where dN is the number of meteors with masses between M and $M + dM$, and that the electron density (for a given velocity and zenith distance) is proportional to the mass, we have, since $\alpha = kA/s$, $dN = dM/M = d\alpha/\alpha = -ds/s$. Integration gives $N = \ln s/s_0$, where s_0 is the minimum sensitivity at which echoes yield velocity measurements. This can be obtained from the maximum range at which velocities are measured. s_0 is then the value of s on the axis of the beam at that range. Thus for meteors at a given range it is now possible to plot the relative numbers seen at different azimuths (Fig. 10b). The maximum number occurs on the axis of the beam,

* J. A. Clegg, *Phil. Mag.*, 39, 577, 1948.

and falls to zero at the angle where $s = s_0$. An azimuth angle θ can be found from this curve (measured from the centre of the beam) such that half the total number of meteors will lie within the range $\pm \theta$. The corresponding value of sensitivity (\bar{s}) may then be taken as the most probable for the range in question. It can be seen that for 50 per cent of the meteors observed, i.e. those within 7° of the beam axis, the estimate of s is within 20 per cent, and only for those meteors observed outside the limits $\pm 11^\circ$, or 8 per cent of the total number, is the estimate in error by more than a factor of two.

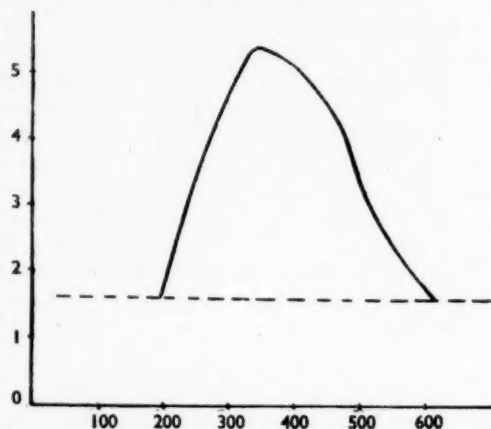


FIG. 11.—Relation between most probable sensitivity \bar{s} and range for meteors observed on the 4 m. aerial system. From these curves the values of γ are calculated for each meteor.

Ordinate: most probable sensitivity \bar{s} .
Abscissa: range in kilometres.

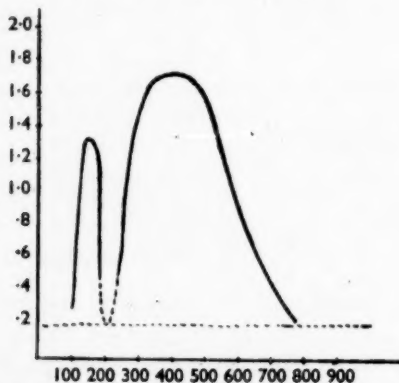


FIG. 12.—Relation between most probable sensitivity \bar{s} and range for meteors observed on the 8 m. aerial system. From these curves the values of γ are calculated for each meteor.

Ordinate: most probable sensitivity \bar{s} .
Abscissa: range in kilometres.

A graph may now be plotted between this mean sensitivity \bar{s} and range. These final curves for the 4 m. and 8 m. aerial systems are shown in Figs. 11 and 12. From these the value of γ given in column 6 of Tables II, IV and VI has been calculated from the formula $\gamma = A/\bar{s}$.

COMPUTATION OF SPECIAL PERTURBATIONS BY AN ELECTRONIC CALCULATOR

Peter Naur

(Communicated by the Director of the Observatories, Cambridge University)

(Received 1951 August 7)

Summary

The problem of special perturbations has been prepared for the electronic calculator EDSAC in Cambridge. The machine is made to perform a step-by-step integration of the equations of motion, taking the attractions of all the major planets into account, and it prints the date and the three Cartesian coordinates for each step. The various sources of errors are discussed and it is shown that the accuracy of the method applied to a minor planet is 10^{-9} astronomical units. The total time required when using this method is between 4 per cent and 10 per cent of that required when using an ordinary desk computing machine.

The desirability of high-accuracy integrations of the equations of motion for selected minor planets, taking the attractions of all the seven major planets into account, has led to an investigation of the possibility of doing this work on the electronic calculator EDSAC in the University Mathematical Laboratory, Cambridge. The problem has now been put in a general form, ready to be applied to most cases occurring in practice, and giving the desired accuracy.

The general features of the machine and the way it is operated have been described by Wilkes and Renwick (3), Wilkes (4) and Wheeler (2). For the present discussion, however, no close familiarity with the machine is necessary as long as the following facts are kept in mind. The machine shares with other high-speed machines the property that intermediate results are not recorded. Considerable care must therefore be exercised in order to make sure that the machine always acts in a controlled manner, even when exceptional situations occur. A part of this discussion will accordingly be devoted to the study of the accuracy and limitations of the procedure.

All instructions and numbers necessary to specify a problem are given to the machine in the form of paper tapes, which have been punched with holes in certain patterns, corresponding to the information. Most of the work of applying the machine to a certain problem consists in working out the instructions which the machine has to follow in order to evaluate the formulae of the problem. The result of this work is one or more tapes—the instruction or order tapes. For a general problem, like that of special perturbations, there will be additional information necessary, specifying the initial values, etc. This will have to be punched on a separate tape according to certain rules, to allow the machine to solve a particular case of the problem. The tapes are punched on teleprinter equipment, a process very similar to typing on an ordinary typewriter. They are read by the machine from a special reading mechanism, and all the information

is transferred to the memory units, where it will be ready for use when required. The reading takes place at considerable speed, so once a problem has been worked out and tested, the machine can very quickly be set to work on it again.

In normal work all numbers must lie in the range from -1 to $+1$, so that suitable scale factors must in general be applied to the variables of a physical problem. The numbers are stored as 34 binary digits and a sign, corresponding to slightly more than 10-decimal accuracy. The fact that the machine works with numbers in binary form does not present special difficulties, as the numbers are read from the tape and printed in decimal form, the conversion being performed in the machine as an ordinary computation.

Description of the process.—The equations of the problem are the Newtonian equations of motion, i.e. three second-order differential equations. As described by Gill (1), a general method for dealing with any number of simultaneous differential equations has been worked out in a convenient form for use with the EDSAC. In the present case, however, this method has not been applied. This is due to the circumstance that the equations of motion for a minor planet involve the positions of all the perturbing bodies, which must be given from tables, and it is therefore quite important to reduce to a minimum the number of points at which the equations of motion are applied. Gill's method is a fourth-order Runge-Kutta process and the derivatives are computed at three points for each step. If this method were employed, a step-length of the order 5–10 days would have to be used in order to make the neglected higher terms sufficiently small, and the derivatives would have to be computed for each second or third day. If, on the other hand, an ordinary stepwise numerical integration, working with higher differences of the variables, is used, the derivatives must be computed at one point for each step only. Furthermore, the memory of the machine is so large that in the present problem sixth-order terms can be taken into account, which permits of a step-length of the order of 20 days.

The quantities occurring in the problem are thus firstly the coordinates of the object and their differences and derivatives, secondly the coordinates of the major planets, and thirdly the auxiliary quantities used in computing the acceleration from the equations of motion. For each of these the question of scale factors must first be settled.

The coordinates of the major planets are most easily dealt with, as a factor of 10^{-2} always will make them less than 1, while still preserving the full tabular accuracy of five decimals.

It is fairly clear that a scale factor which reduces the coordinates of the object to the required range will also keep the differences, etc. within the limit. The reduction factor 10^{-2} can again be chosen, which will only exclude cases where an object is more than 100 A.U. from the Sun. In many cases, however, the distance of the object from the Sun will never exceed 10 A.U., and the programme has therefore been prepared in such a way that either of the two scale factors 10^{-2} or 10^{-1} can be used. The latter will give the higher accuracy. The question of scale factors for auxiliary quantities will be treated in connection with the method for computing r^{-2} , described below. In the discussion of the process the scale factors would in most cases give rise only to trivial changes in the expressions and can therefore be omitted. In cases where this does not hold we shall write the scale factor for the coordinates of the object 10^{-b} , where b can be given the values 1 or 2.

It will be convenient at this stage also to mention how the coordinates of the major planets are supplied to the machine. It is of course a complication that for each step of the integration 21 numbers, the coordinates of the seven major planets, must be given from tables. From the point of view of programming, however, the problem is rather simple, due to the fact that the major planets only give rise to perturbation terms, and that they act independently of each other. The coordinates of the planets can therefore be punched on one tape which is read intermittently according to the programme. When approximate coordinates of the object become available the planets are taken into the machine, one by one, and the perturbation term is built up by summing the results as the terms due to the single planets are formed. This perturbation term is then stored and used in the more accurate computations which follow. While the method has been planned with the inclusion of all the major planets in view, it will make no difference if it is desired to take only some of them into account. All planets whose data are present on the planet tape will automatically be included.

Both logically and when working on the machine the process divides itself into two parts: the start of the integration and the cycle followed by each subsequent step. On the machine a little manipulation of the tapes is necessary at the start, but once the process is under way no further attention from the operator is necessary. The machine will evaluate and print completely automatically the coordinates of the object for each step, and immediately proceed to the next.

The start of a numerical integration always presents a special problem when higher differences are involved. Various solutions have been tried in connection with the present problem, and the most convenient has been found to be one which assumes knowledge of the position of the object to be investigated at three consecutive integration points, at times t_{-1} , t_0 and t_1 , say. The positions at t_0 and t_1 must be known with full accuracy, while the accuracy at t_{-1} is less critical. When these have been read from the tape, the machine computes x_{-1}'' , x_0'' and x_1'' (and the analogous quantities for y and z —in the following we shall always regard y and z as understood) with due regard to perturbations, and then places the following numbers in the appropriate locations in the store:

$$\left. \begin{array}{l} x_1 \quad \delta x_{1/2} = x_1 - x_0, \quad \delta x_{1/2}'' = x_1'' - x_0'', \\ x_1'' \quad \delta^2 x_0'' = \delta x_{1/2}'' - x_0'' + x_{-1}''. \end{array} \right\} \quad (1)$$

An approximation to the coordinate x_2 is now obtained by

$$x_2 = x_1 + \delta x_{1/2} + x_1'' + \frac{1}{12} \delta^2 x_0''. \quad (2)$$

This is used for computing the perturbation term

$$P_{x_2} = \sum_{\text{Major planets}} w^2 k^2 m_{pl} [-(x_2 - x_{pl}) \rho_2^3 - x_{pl} r_{pl}^3], \quad (3)$$

which is placed in the store. This completes the special start computation.

We enter now the first step of the regular computation. First x_2'' is computed, using x_2 given by (2),

$$x_2'' = -w^2 k^2 x_2 r_2^3 + P_{x_2}, \quad (4)$$

from which we get

$$\delta^2 x_1'' = x_2'' - x_1'' - \delta x_{1/2}''. \quad (5)$$

We can now proceed to compute

$$x_3 = 2x_2 - x_1 + x_2'' + \frac{1}{12}(2\delta^2 x_1'' - \delta^2 x_0'') \quad (6)$$

together with P_{x_1} and x_3'' . P_{x_1} is stored for later use, while x_3'' is used to compute $\delta^4 x_1''$ according to (13) below.

An iteration cycle is now started:

$$x_2 = x_1 + \delta x_{1/2} + x_1'' + \frac{1}{12}\delta^2 x_1'' - \frac{1}{240}\delta^4 x_1'', \quad (7)$$

$$x_2'' = -w^2 k^2 x_2 r_2^{-3} + P_{x_1}, \quad (8)$$

$$\delta^2 x_1'' = x_2'' - x_1'' - \delta x_{1/2}'', \quad (9)$$

$$\delta^2 x_2'' = 2\delta^2 x_1'' - \delta^2 x_0'' + \delta^4 x_1'', \quad (10)$$

$$x_3 = 2x_2 - x_1 + x_2'' + \frac{1}{12}\delta^2 x_2'' - \frac{1}{240}\delta^4 x_1'', \quad (11)$$

$$x_3'' = -w^2 k^2 x_3 r_3^{-3} + P_{x_1}, \quad (12)$$

$$\delta^4 x_1'' = x_3'' - 2x_2'' + x_1'' - 2\delta^2 x_1'' + \delta^2 x_0''. \quad (13)$$

The aim of the cycle is to secure $\delta^2 x_1''$ and $\delta^4 x_1''$. When the cycle has been repeated three times x_2 is printed, and the next step is started by the following approximations:

$$\delta^2 x_3'' = 2\delta^2 x_2'' - \delta^2 x_1'' + \delta^4 x_1'', \quad (14)$$

$$x_4 = 2x_3 - x_2 + x_3'' + \frac{1}{12}\delta^2 x_3'' - \frac{1}{240}\delta^4 x_1''. \quad (15)$$

This value of x_4 is used to compute P_{x_4} . If we now replace the suffixes 2, 3 and 4 by 1, 2 and 3, respectively, we see that we have sufficient data to start the next iteration from equation (12).

Accuracy.—For the discussion of the accuracy obtained it is convenient to investigate the following processes separately:

- (1) the reading of the punched numbers;
- (2) the calculation of the derivatives from the coordinates;
- (3) the iteration described above.

The inaccuracy arising from the reading of numbers is due to the fact that the conversion of the decimals into binary form takes place as a regular computation, with corresponding rounding off. The possible error introduced in this way will never exceed 10^{-10} , i.e. when a scaling factor of 10^{-1} is used, one unit in the ninth decimal place of the coordinates.

In discussing the possible error introduced when computing the second derivatives from the coordinates the procedure for computing r^{-3} is important. The machine is provided with an arithmetical unit which performs addition, subtraction and multiplication, whereas the problem in question, that of calculating r^{-3} when r^2 is given, i.e. evaluation of the function $x^{-3/2}$, must be programmed in detail. Two considerations led to the method used. Firstly, it is clear that whichever way r^{-3} is evaluated the method must fail if r becomes smaller than a certain limiting distance, because quantities larger than unity will be formed. The method must be designed so that the machine stops if this happens. Secondly, the method must be constructed so as to give sufficient accuracy in the case of the Sun term, while still making the limiting distance for the planets reasonably small. In other words, the method must calculate a quantity proportional to r^{-3} , but the constant of proportionality must be different in the two cases, that of a planet and that of the Sun.

The method adopted is based on the iteration

$$y_{n+1} = 2y_n \left[\frac{3}{4} - 2^6 x^3 y_n^2 \right], \quad (16)$$

which for x lying in a certain range, including $\frac{1}{4} \leq x < 1$, converges towards the limit

$$y = \frac{1}{16} x^{-3/2} \quad (17)$$

if y_0 is suitably chosen.

The whole process works in the following way. The given quantity $10^{-b} r^2$ is shifted two binary places to the left a certain number of times, q say, so as to make

$$\frac{1}{4} \leq 10^{-2b} r^2 2^{2q} < 1. \quad (18)$$

Now the iteration is applied, giving the limit

$$y = 2^{-3q-4} 10^{3b} r^{-3}. \quad (19)$$

This number is then multiplied $1+s-q$ times by $\frac{1}{2}$, where s is a given integer, the result being the number

$$2^{-3s-7} 10^{3b} r^{-3}, \quad (20)$$

which is proportional to r^{-3} and independent of q .

The limiting distance can now be found from the condition that $q \leq s+1$, or, using (18),

$$\frac{1}{4} \leq 10^{-2b} 2^{2s+2} r^2, \quad (21)$$

$$r \geq 10^b 2^{-s-2}. \quad (22)$$

Clearly it is desirable to choose s large, but s is limited for the following reason. In order to compute

$$w^2 k^2 r^{-3}, \quad (23)$$

which is the factor to be applied to the coordinate $10^{-b} x$ when forming the acceleration term $10^{-b} w^2 k^2 x r^{-3}$, we must multiply the result of the iteration, (20), by the constant

$$10^{-3b} w^2 k^2 2^{3s+7}, \quad (24)$$

but this number must be less than 1, like all other numbers in the machine.

When applying this process to the factors r_{pl}^{-3} and ρ^{-3} the following points are of importance. The method is constructed in such a way that the number s can be given one value when dealing with the Sun terms and another when dealing with a perturbation term. Denoting these by s and p , respectively, we must now write p for s in the expressions (18) to (22). Furthermore, we must put $b=2$, as the coordinates of the major planets are always treated with the scale factor 10^{-2} . The result of the iteration is therefore

$$2^{-3p-7} 10^6 \rho^{-3} \quad (25)$$

and ρ is limited by

$$\rho \geq 10^2 2^{-p-2}. \quad (26)$$

The factor to be applied to the coordinates $10^{-2}(x-x_{pl})$ in order to give the perturbation is

$$10^{-b+2} w^2 k^2 m_{pl} \rho^{-3}, \quad (27)$$

so we must multiply (25) by

$$10^{-b-4} 2^{3p+7} w^2 k^2 m_{pl}, \quad (28)$$

which must be less than 1 for each of the planets. It will of course be the mass of Jupiter which determines the value of p . Table I gives some numerical values. If in the course of a calculation r or ρ should decrease below these limits the number $1+s-q$ will become negative and the programme has been designed so that the machine then stops.

A detailed analysis of all the processes involved in the calculation now shows that the procedure gives the full accuracy of 34 binary digits for x'' in all situations within the allowed limits.

We come now to the discussion of the iteration process defined by (2) to (15), where inaccuracies arise because a number of terms have been neglected in the expressions for x_2 and x_3 . According to the specific purpose for which they are used the coordinates must be known to different degrees of accuracy. The expression in which terms of lowest order are neglected is (2), where $\delta^2 x_0''$ takes the place of $\delta^2 x_1''$ and higher terms are neglected. The coordinates computed from (2) are used in (3), (4) and (6). The error introduced in (4) is, however, not important as it will become rectified by the iteration, and in (3) and (6) the coordinate is used only to compute the perturbation terms P_* where high accuracy is not required. The actual errors in the coordinates are seen to be of the order $\frac{1}{12}\delta^3 x''$ in (2) and

$$\frac{1}{8}\delta^3 x'' \quad (29)$$

in (6), so it is this latter quantity which must be investigated.

TABLE I

	$w=10$ days		$w=20$ days	
	$b=1$	$b=2$	$b=1$	$b=2$
s	2	6	2	5
p	8	9	7	8
r_{lim}	0.62 A.U.	0.39 A.U.	0.62 A.U.	0.78 A.U.
ρ_{lim}	0.10	0.05	0.20	0.10

In order to decide whether this error has any serious consequences we must work out the effect on the perturbation term of an error in the coordinates. From each planet we have the contribution

$$-w^2 k^2 m_{pl} (x - x_{pl}) \rho^{-3} \quad (30)$$

and the effect on P_* of an error Δx becomes

$$|\Delta P_*| < 2w^2 k^2 m_{pl} \rho^{-3} \Delta x. \quad (31)$$

The term neglected in (14) and (15) is of the order $\frac{1}{12}\delta^3 x''$. This error enters in the same way as (29), but is negligible in comparison.

Finally we come now to the approximations introduced in the expressions (7) and (11). In (7) the term

$$\frac{31}{80480} \delta^6 x_1'' \quad (32)$$

and higher terms are neglected, and in (11) $\delta^4 x_1''$ is used instead of $\delta^4 x_2''$, and higher terms are neglected. This latter error will enter partly in the iteration, where it can be neglected, as it is multiplied by small factors, and partly in (15), where it is of the same order as the term neglected in the expression. The error of most significance in the system (7) to (13) is therefore given by (32).

The quantities (29), (31) and (32) form the basis from which the accuracy of the method in any particular case can be estimated. We shall carry the numerical work through in two cases: that of circular motion and that of free fall from infinity.

Circular motion.—For the higher derivatives and differences we have in this case

$$|\delta^n x''| \approx \left| w^{n+2} \frac{d^{n+2} x}{dt^{n+2}} \right| \leq r (k w r^{-3/2})^{n+2} \quad (33)$$

and for the error (32) we get

$$\frac{31}{60480} (k w)^8 r^{-11} = 10^{-7} r^{-11} \quad (34)$$

for $w = 20$ days. From this we obtain the following limits for r , where “ n decimals” means that the error is $< 5 \times 10^{n+1}$,

$$r > \begin{cases} 1.07 \text{ A.U.} & 7 \text{ decimals} \\ 1.32 \text{ „} & 8 \text{ „} \\ 1.62 \text{ „} & 9 \text{ „} \end{cases} \quad (35)$$

The error (29) can be estimated as

$$|\frac{1}{8} \delta^3 x''| < 8 \times 10^{-4} r^{-13/2}. \quad (36)$$

The coordinates subject to this error will only enter in the factors $(x - x_{pl})$. Here the planetary coordinates x_{pl} are given to 5 decimals. An error (36) which is $< 5 \times 10^{-6}$ can therefore always be permitted, and we see that if

$$r > 2.2 \text{ A.U.} \quad (37)$$

the accuracy will always be sufficient. If $r < 2.2$ the error may, according to (31), become important if ρ becomes small, i.e. during a close approach to Venus, the Earth or Mars. As an example, let us consider a close approach to the Earth. Taking $b = 1$, which is natural for a circular orbit of radius about unity, and $w = 20$, we see from Table I that the machine will stop at approaches closer than $\rho = 0.2$. At this distance we get from (36) and (31)

$$|\Delta P_z| < 7 \times 10^{-8}. \quad (38)$$

The most important conclusion to be drawn from this discussion is that in the case of a minor planet the accuracy obtained is mostly limited by the reading of the initial values, which may introduce errors of the order of 10^{-9} A.U. The method will therefore satisfy even the requirements of the high-accuracy work on selected minor planets which is undertaken with the ultimate purpose of detecting systematic errors in the fundamental star places.

Free fall from infinity.—In this case we can take $x = r$ and get

$$w x' = -w k \sqrt{2} r^{-1/2} \quad (39)$$

and for the relevant differences

$$|\delta^3 x''| \leq 70 \sqrt{2} (w k)^5 r^{-13/2}, \quad (40)$$

$$|\delta^6 x''| \leq 138320 (w k)^8 r^{-11}. \quad (41)$$

The limits corresponding to (35) are

	$w = 10$ days	$w = 20$ days	
$r > \begin{cases} 1.5 \text{ A.U.} \\ 1.9 \text{ „} \\ 2.3 \text{ „} \\ 2.9 \text{ „} \end{cases}$	$\begin{cases} 2.5 \text{ A.U.} \\ 3.1 \text{ „} \\ 3.8 \text{ „} \\ 4.7 \text{ „} \end{cases}$	$\begin{cases} 6 \text{ decimals} \\ 7 \text{ „} \\ 8 \text{ „} \\ 9 \text{ „} \end{cases}$	(42)

and corresponding to (37) we get that $\frac{1}{8} \delta^3 x'' < 5 \times 10^{-6}$ for

$$r > \begin{cases} 2.6 \text{ A.U.} & w = 10 \text{ days} \\ 4.4 \text{ „} & w = 20 \text{ „} \end{cases} \quad (43)$$

Again we find that only during close approaches to Venus, the Earth or Mars will the terms neglected in (2) become important.

The results (42) are more important. The situation of free fall will be approached only by comets moving in highly eccentric orbits, and an accuracy of 6 decimals will generally be sufficient. But we see that although the case investigated may be an extreme one and the conditions for actual objects are likely to be less strict, great care must be taken if applying the method to objects approaching the Sun closer than 1.5 or 2 A.U.

The operation of the machine.—This is not the place to give a complete account of the practical use of the method on the machine, as a complete set of directions is available, together with the programme and tapes, in the EDSAC library in Cambridge. The following few notes about the set-up and the time taken in preparing a particular problem might, however, be of interest. Four different tapes must be ready when the machine is used: two instruction tapes, A and B, a tape giving the initial values, and the appropriate planet tape. The instruction tape B, which is about 4 feet long, is never changed, while A, 16 feet long, includes a few symbols depending on the scale factor, the interval and the number of decimals to be printed. The initial values are the three-times-three coordinates for the object. The symbols to be punched are simply the signs and decimal digits of the coordinates, and the tape can be made in a few minutes. The planet tapes are described below. Tape A is used first and is read by the machine in about one minute. After tape A the tape giving the initial values must be read, a matter of a few seconds, and then the appropriate part of the planet tape is placed in the reader. The machine now takes in the planetary coordinates for four dates, corresponding to t_{-1} , t_0 , t_1 and t_2 , evaluates the equations (1) to (3), in total a process of about two minutes, and then stops. Part B of the programme is now used and after it has been read the planet tape is again placed in the tape reader. This completes the set-up of the machine, and it will now proceed to take in parts of the planet tape and print the date and the three coordinates of the object as long as the planet tape lasts, each step taking about 45 seconds.

Besides the programme tapes mentioned, A and B, an auxiliary tape C is available, which serves the purpose of printing the higher differences and derivatives as they are held in the store. It can be applied whenever a step has been printed, and after the extra printing the integration will continue where it was interrupted. It will be particularly useful when starting an integration from a set of unperturbed coordinates surrounding an osculation point and the velocities at the osculation.

As a general rule all computations on the machine are done twice, as some protection against errors due to the machine. It was found most practical to perform the computation in runs of 20 to 30 intervals. In the first run eleven digits were printed, thus representing as closely as possible the full contents of the store. In the second only nine digits were printed. Thus when any difference between the computations became apparent it was possible to perform a third calculation from the last three points, which gave the same results in the first two runs, basing this third computation on the values from the full accuracy version.

The planet tapes.—An important factor when discussing the working economy of this method is the time necessary in punching the planet tapes. Several different procedures have been tried, the result being a method by means of which

the planet tape, including the required data for all seven major planets for 20 intervals, can be produced in less than four hours, if touch-typing is used. The tapes are punched straight from the tables of the major planets, and this time includes a double punching for checking purposes, and the interpolation of the tables for Uranus and Neptune to give 20-day intervals. The final tape is again checked by differencing, using the machine, a process which requires 12 seconds per date. A description of the method adopted for this work has been deposited in the EDSAC library. In the library will also be found the planet tape covering certain periods, as specified in Table II.

TABLE II

Planets included	Interval	Period covered
Jupiter and Saturn	20 days	1942 May 1-1944 Jan. 31
" " "	40 "	1943 Aug. 24-1948 Sept. 6
Seven major planets	10 "	1948 Oct. 6-1951 June 23
" " "	20 "	1948 Oct. 16-1957 July 1

The speed of the process.—Owing to the amount of time required in punching the planet tapes, the saving in time depends strongly on whether the required planet tapes are available, or whether they will have to be manufactured. The situation is best illustrated by considering a concrete example.

The method has been used to integrate the motion of minor planet 51 Nemausa, as a part of the work on the motion of this planet which is carried out by Mr Moeller at the Observatory, Copenhagen. The integration was started from Mr Moeller's coordinates for 1949 March 5 to April 14 and was carried as far as 1956 March. When doing the calculation by hand, aided by an ordinary desk calculating machine, one interval of 20 days requires about two hours' work, if no mistakes are made. It is here supposed that the integration has been started already. On the EDSAC about 20 intervals form a reasonable run when considering the time required. Supposing that no planet tapes are available, we get for the necessary time:

Preparation of planet tape	4 hours.
Punching of initial values	5 minutes.
Set-up of machine	4 minutes.
Integration of 20 intervals, each 45 sec.	15 minutes.
Total time for double calculation	38 minutes.
Total time for 20 intervals	4 $\frac{3}{4}$ hours.
Average total time for one interval	14 minutes.

In this case the time required when using the EDSAC is about 10 per cent of that necessary when computing by hand. This can be considered an average value, as on the one hand longer runs are possible, which will reduce the relative importance of the "set-up time", and on the other hand, occasional faults in the machine will waste time.

The situation will of course be much more favourable for the machine if several objects can be integrated over the same period, as the planetary coordinates will only have to be punched once. Integrating, for example, five objects over 20 intervals we get for the total time: 4 hours + $5 \times \frac{3}{4}$ hours = about 8 hours, and the average time needed for one object over one interval becomes less than 5 minutes, which is about 4 per cent of the time required when using hand methods.

Owing to the special arrangement of the tables of the planets, it will take a relatively shorter time to punch the tapes giving only the data for Jupiter and Saturn, and the time-saving will consequently be greater if only these two planets are taken into account. The tape giving Jupiter and Saturn for 20 intervals can actually be punched in less than 40 minutes. The time for a single step on the machine will be reduced to 33 seconds.

The method was used in this way to integrate the motion of Comet Wolf (1) over the period 1942-1950. This has been done already by Dinwoodie and also by Kamiński. A comparison with Dinwoodie's results confirms the estimates above concerning the accuracy of the method.

Acknowledgments.—It is a pleasure to thank the Director of the Mathematical Laboratory, Dr M. V. Wilkes, for permission to use the machine for this work, as well as Dr J. C. P. Miller for several valuable suggestions during the work, and Professor R. O. Redman and Mr D. H. Sadler for help in preparing the manuscript. The author also wishes to thank Copenhagen University and Rask-Oersted Fondet, Copenhagen, for the grants which enabled him to study at King's College for a year.

King's College,
Cambridge :
1951 June 22.

References

- (1) Gill, S., *Proc. Cambr. Phil. Soc.*, **47**, 96, 1951.
- (2) Wheeler, D. H., *Proc. Roy. Soc. A*, **202**, 573, 1950.
- (3) Wilkes, M. V. and Renwick, W., *Journ. Sci. Instrum.*, **26**, 385, 1949.
- (4) Wilkes, M. V., *Journ. Sci. Instrum.*, **26**, 217, 1949.

ON THE USE OF MEAN SIDEREAL TIME

R. d'E. Atkinson and D. H. Sadler

(Communicated by the Astronomer Royal)

(Received 1951 September 28)

Summary

Apparent right ascensions are at present reckoned from the computed position of the true equinox, and this computed position is also used to define sidereal time. Owing to nutation, both the right ascensions and the time so defined oscillate, and good modern clocks cannot readily indicate such time. In the observation of celestial bodies it is not the apparent right ascension itself that is involved but the hour angle, or difference between sidereal time and right ascension. It is now proposed to subtract the tabular nutation in right ascension from both these quantities, in all ephemerides. The tabulated sidereal time will then run uniformly, and the oscillations in right ascension of most celestial bodies will also be reduced. In addition to its advantages for a time service, the new arrangement will simplify a number of routine calculations. The question of a suitable name for the modified right ascension is discussed.

The tabular apparent right ascensions of all stars, as is well known, oscillate in a complicated manner on account of nutation; but it is by no means true that all of this oscillation is "real", in the sense of implying a corresponding variation in the times of transit, if uniform time is used. With an equatorial star, in fact, none of it is real in this sense; so far as nutation is concerned, the tabular oscillations of an equatorial star are purely the reflection of the oscillations of the equinox, and the apparent diurnal motion of the star itself is quite uniform except for aberration. The current practice of referring a motion which is itself demonstrably uniform to a datum which is not only known to be oscillating but whose instantaneous position is in fact not directly observable, arises from the decision to consider the true equinox as the "hour-hand" for sidereal time. This choice was made on geometrical grounds which, indeed, are still entirely valid in their own sphere; but as a result we have tabular values of right ascension and of sidereal time which not only tend to obscure the true physical state of affairs but also (though they are called "apparent") must still be corrected before they can be compared with observations based on modern clocks.

The first of these two disadvantages is not serious. There is, however, real inconvenience nowadays in working with non-uniform sidereal time. The use of the true equinox was unobjectionable as long as clocks themselves were so indifferent that uniformity could not be observationally distinguished from non-uniformity, within the range caused by nutation; but it is well known that this condition ceased to be satisfied, for the six-monthly term, as soon as the Shortt Free Pendulum came into use in 1926; with the adoption of quartz clocks one or two other terms in the nutation of the equinox have also become observable, although the main (18-year) term is still not separable here from the long-term performance of the crystal. In the operation of a time service,

one is necessarily always extrapolating the behaviour of the most uniform clock one can obtain, and in assessing its uniformity one is thus now forced to eliminate the nutation of the equinox; the tabular apparent right ascensions based on a completely fictitious "oscillating clock" would not otherwise be comparable with the observed right ascensions based on a real and highly uniform one. This correction represents a computational nuisance which certainly has no compensating advantages within the sphere of a time service; it appears doubtful whether it has any substantial advantages in any sphere, and a proposal is accordingly being submitted for discussion at the next General Assembly of the International Astronomical Union, that mean sidereal time should in future be used as the basis of apparent ephemerides.

The purpose of the present paper is to bring this proposal to general notice as far in advance as possible, so as to ensure that it may be fully considered before the actual Commission meetings. The formal wording is as follows:—

"That from an agreed date all apparent right ascensions shall be tabulated, in the ephemerides, with the nutation of the equinox (tabular 'Nutation in R.A.'), subtracted from them, and that the 'Sidereal time of 0^h' and the 'Transit of first point of Aries' shall be correspondingly tabulated without nutation, so that they increase, or decrease, uniformly."

This proposal may involve some changes in nomenclature; these, however, are not logically part of it, and they have not been included in the wording as submitted.

The proposal applies to all bodies: Sun, Moon, planets and stars. The complete nutation in R.A. of any celestial body may be divided into two parts: on the one hand, there is the quantity

$$\frac{1}{15} \tan \delta (\sin \alpha \sin \epsilon \Delta\psi - \cos \alpha \Delta\epsilon)$$

which depends on the position of the body and vanishes at the celestial equator; and on the other hand, there is the quantity

$$N = \frac{1}{15} \cos \epsilon \Delta\psi$$

(the tabular "Nutation in R.A.") which is constant over the celestial sphere at any given instant, and affects all observable bodies equally. The variable part of the nutation must obviously be applied to the individual observations in any case; this paper is concerned only with the (spatially) constant part N , and it should perhaps be stressed that in all work in which a sidereal clock is artificially kept in agreement with the "sidereal time at 0^h" (as tabulated), and is used for observing apparent places, and in all procedures (such as navigation) which reduce in principle to this, no difference will be noticed by the observer at all. The true hour angle of a body, at any given U.T., will be unaffected (as it clearly must) by the proposed change, since the nutation of the equinox enters equally into both the quantities of which it is the difference; the equation of time can be defined as a difference of hour angles, and is of course also unaffected. Observationally, the change will concern only those observatories which possess clocks of highly predictable rate.

On the computational side, however, the new procedure introduces a number of changes (mostly simplifications) which should be considered in detail. They fall under the following main headings: (a) theoretical (i.e. geometrical); (b) interpolation of tabular values by the user; (c) computation of apparent places of stars; and (d) computation of the ephemerides of the Sun, Moon and planets.

The balance is clearly favourable under the heads (b) and (c), and although it is unfavourable under (a), the number of cases which arise under this heading is relatively small.

(a) *Theoretical*.—Since no change in the tabular declinations would be admissible, the procedure now advocated means that a true equator and a mean equinox will be used simultaneously; and since the mean equinox does not lie in the true equator, the tabular coordinates are not members of the same spherical triangle.* It would not be correct, for example, to take the new kind of "right ascension" (if we may preserve the name for the moment), and the declination as tabulated at present, and to solve for longitude and latitude by standard formulae. This would be a serious objection, except that the obvious procedure will now be to add the tabular nutation in R.A. to the quantity which will be tabulated, and after that to proceed as at present. From the theoretical aspect it is thus desirable to regard the proposed tabulated quantity explicitly as apparent right ascension *minus* nutation in right ascension, and to convert to or from apparent right ascension when this is necessary. It is not necessary when the nutation cancels (as it does in hour angles); nor in the calculation of star constants, where its effect is negligible (and where, indeed, a mean right ascension for the year is as a rule sufficiently accurate); nor in some other operations where the same applies.

(b) *Interpolation*.—Several common interpolations will be simpler on the new system. In the computation of local sidereal time, for example, it is necessary at present to allow for the change in nutation in the interval since 0^h U.T.; this correction is small, but not negligible, and is definitely tiresome; indeed, its smallness makes it somewhat liable to be applied with the wrong sign if the work is only rarely done. Again, in the independent day numbers, the daily difference of f varies from 0^s.004 to 0^s.013; as will be seen below, the quantity replacing f , in the new system, will run uniformly, with a daily difference of 0^s.00841, so that interpolation to the nearest millisecond can now be fully covered by a permanent critical table with nine entries only. All tabulated "right ascensions" will also be slightly easier to interpolate.

(c) *Apparent places of stars*.—The Besselian day numbers A , B , C and D are required for declinations as well as for right ascensions, and must clearly be retained; when using them, therefore, the form of the reduction must be modified as follows. The correction to right ascension for precession and nutation is (in the standard notation)

$$\Delta\alpha = Aa + Bb + E,$$

where

$$A = \tau + \Delta\psi/\psi$$

and

$$a = m + n \sin \alpha \tan \delta.$$

* Note added October 18.—Strictly speaking, this statement does not quite do justice to the proposal. The "Apparent Transit Hour" (if we may call it that provisionally; see p. 623) can be regarded, just as any R.A. can, either as a side or as an angle of a spherical triangle in which the other two sides and two angles are right angles. Considered as an angle, it is the angle at the true pole between two hour-circles, namely the one through the mean equinox and the one through the star; considered as a side, it is the length along the true equator between the same two hour-circles (see Fig. 1). Since the apparent declination is measured up from the true equator, apparent transit hour and apparent declination are true spherical coordinates and can indeed be parts of one spherical triangle; but it is not a useful triangle, since the transit hour is not strictly part of any spherical triangle which also involves either the mean or the true longitude, nor of any triangle which also involves either the mean or the true obliquity.

The nutation of the equinox is

$$N = \frac{1}{15} \cos \epsilon \Delta\psi = m\Delta\psi/\psi + E,$$

and if we write $\Delta'\alpha$ for the correction, analogous to $\Delta\alpha$, required in the new system, then

$$\Delta'\alpha = \Delta\alpha - N = \tau m + Ap + Bb,$$

where

$$p = a - m = n \sin \alpha \tan \delta.$$

$\Delta'\alpha$ thus contains the same number of terms as $\Delta\alpha$; moreover, τm , though larger than E , increases uniformly and is easier to handle in systematic work. (E disappears altogether.) p is slightly easier to compute than a , and corresponds more closely with a' used for the declination. The evaluation of $\Delta'\alpha$ is thus simpler than that of $\Delta\alpha$.

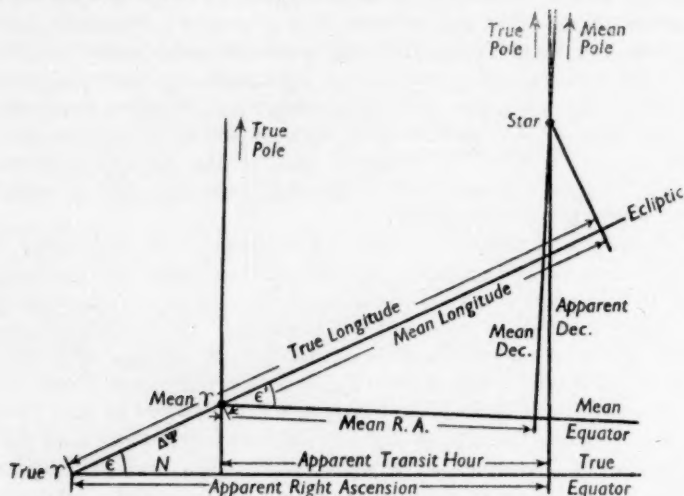


FIG. 1.—Relations between the new quantity (here called "Apparent Transit Hour"; see p. 623) and the traditional quantities. For simplicity, the luni-solar and planetary precessions have both been omitted; "mean" should thus be understood as "mean of date", i.e. eliminating nutation only.

In the case of the independent day numbers, we have

$$f = Am + E = \tau m + N,$$

and subtracting N we see that the new system will merely involve replacing f by the uniformly increasing τm , which is thus required in both methods equally. In this case, therefore, the tabular values are changed but the form of the reduction is preserved.

In both cases the argument is independent of whether the short-period terms of nutation are or are not included; the quantities A , B , $\Delta\psi$, f , N may be regarded, throughout the above discussion, as including short-period terms if required. If short-period terms are still explicitly tabulated (as at present in the *Nautical Almanac*), the term f' will disappear altogether in the new system, since it is exactly the short-period nutation of the equinox; apart from this appreciable simplification, they will be unchanged. The quantity $dx(\psi)$, used in *Apparent Places of Fundamental Stars* for applying short-period terms to the places of ten-day stars, will be modified by the omission of the term $\frac{1}{15} \cos \epsilon = 0.061$,

and will thus in the great majority of cases be much reduced numerically, with a consequent simplification of the arithmetic.

(d) *Computation of ephemerides.*—Right ascension and declination of the Sun, Moon and planets are derived geometrically from longitude and latitude, referred to the ecliptic, as given by the appropriate tables. Corrections for nutation are simple to apply in ecliptic coordinates, since they are independent of position; it is thus usual to refer the ecliptic coordinates to the true equinox before conversion to equatorial rectangular coordinates and then to right ascension and declination. It is clearly not possible to subtract the nutation in right ascension before the conversion, and it will therefore have to be explicitly subtracted from the calculated apparent right ascension afterwards, to give the proposed tabular quantity. This is a trivial addition to the amount of work involved and is, in any case, largely offset by the omission of E and f' , and by the simplifications in the calculation of mean sidereal time, the corresponding transit of the mean equinox, the quantity replacing f , and the apparent places of stars.

The question of nomenclature will have to be considered; the natural suggestion of "Mean Right Ascension" is impossible, as this term is already in use for an entirely different concept. Historically, "Right Ascension" meant "Time of rising, where risings are at right angles (to the horizon, understood)", the zero of this time being when the equinox was rising; but the historical connection was long ago broken, and the etymological justification lost, by the change from the horizon to the meridian, so that "Apparent Right Ascension" has become a purely conventional name for "Local Sidereal Time of Apparent Meridian Transit". There is thus no intrinsic reason for retaining the words "Right Ascension", and in fact all attempts to do so seem to result in inconveniently long expressions; it is therefore arguable that in this respect the change might be a radical one, clearing out the obsolete reference to the horizon and giving due weight to the meridian as well as to the perfect clock. The word "apparent", however, has a long association with aberration, and will also, now, be truly applicable to the clock-readings, so that it seems entitled to remain. These conditions could be met, for example, by calling the new quantity the "Apparent Transit Hour", with "T.H." as the (English) abbreviation replacing "R.A.". There does not appear to be a real need for a separate symbol as well; "Apparent Right Ascension" would preserve its present meaning exactly, but α could be used indifferently for "R.A." and "T.H.", except in theoretical discussions involving both, when one could be distinguished by a prime or subscript. An alternative method is not to introduce a new term, which has to be defined, but to refer to the new quantity as "Mean Sidereal Time of Apparent Transit"; this terminology, which is self-explanatory, would be abbreviated to "M.S.T. of Transit", in which the word "apparent" is deliberately omitted, since the concept of "transit" is essentially an observational one implicitly involving the "apparent" place.

The authors would welcome any suggestions or comments bearing on the desirability of making, or not making, the proposed change, and in regard to nomenclature.

Royal Observatory,
Greenwich:
1951 September 26.

Royal Greenwich Observatory,
Herstmonceux:
1951 September 26.

AMENDMENT OF THE LUNAR EPHEMERIS

D. H. Sadler

(Communicated by the Astronomer Royal)

(Received 1951 October 6)

Summary

At the Paris (1950) Conference on the Fundamental Constants of Astronomy a recommendation was adopted to amend the lunar ephemeris to bring it into accordance with the solar ephemeris, and H.M. Nautical Almanac Office was asked to report on its practicability. Such an amendment can be introduced as from the year 1961, though the necessary corrections are both complicated and lengthy; details are given for the purpose of record.

1. *Introduction.*—The ephemeris of the Moon, as given at present in all the Almanacs, is based rigorously on E. W. Brown's *Tables of the Motion of the Moon*. In order to bring the theory into approximate accord with observation, Brown (1) retained in the tables Newcomb's empirical term for which there is no theoretical justification. It is now well known that the departure of the Moon from its position, as predicted by rigorous gravitational theory, is due to the variations of the Earth's rotation; although the empirical term serves its purpose reasonably well at the present time (the discrepancy between the tabular and observed positions is about 2"), it is now clear that it will rapidly cease to do so. In any case it is desirable that the lunar ephemeris should be calculated on a rigorous theoretical basis.

Spencer Jones, in a paper (2) of outstanding importance, found that the correction required by the Moon's mean longitude, as given by Brown's tables, is

$$+4''.65 + 12''.96T + 5''.22T^2 + B - \text{the empirical term}, \quad (1)$$

where T is measured in Julian centuries of 36,525 mean solar days from 1900 January 0, Greenwich Mean Noon. B is defined as the *fluctuation* in the Moon's longitude; it is due to irregularities in the Earth's rotation and is to be determined observationally.

In the same paper, Spencer Jones determined the correction to the Sun's mean longitude, as given by Newcomb's tables, to be

$$+1''.00 + 2''.97T + 1''.23T^2 + 0.0748^*B. \quad (2)$$

This expression represents the increase in the Sun's mean longitude in the interval, ΔT , between mean solar time and the time (to be known as *ephemeris time* (3)) relative to which the solar ephemeris will agree with observation. The Moon's mean longitude increases 13.37 times as rapidly as that of the Sun and thus in time ΔT by

$$+13''.37 + 39''.71T + 16''.44T^2 + B. \quad (3)$$

* This coefficient is given in the paper as 0.0747.

The correction required to the mean longitude in Brown's tables so that the deduced position of the Moon will agree with observation in ephemeris time, is thus (1) minus (3) or

$$-8''.72 - 26''.75T - 11''.22T^2 - \text{the empirical term.} \quad (4)$$

Clemence (4) first suggested that the correction (4) should be applied to the lunar ephemeris; it enables ΔT to be determined simply by direct comparison of the observations with the ephemeris. This proposal was adopted by the Conference on the Fundamental Constants of Astronomy (Paris, 1950) and incorporated in the following recommendation (5).

"In order to bring the lunar ephemeris into accordance with the solar ephemeris the Conference recommends that Brown's *Tables of the Motion of the Moon* should be amended by removing the empirical term and by applying to the mean longitude the correction

$$-8''.72 - 26''.75T - 11''.22T^2,$$

where T is measured in Julian centuries from 1900 January 0, Greenwich Mean Noon.

H.M. Nautical Almanac Office will report on the practical implications of this recommendation."

The purpose of this paper is to present that report.

2. *General considerations.*—In his tables, Brown gives precise instructions for the application of a correction ΔL to the mean longitude (*Tables*, Section I, pp. 138, 139) and for an amendment to the empirical term (p. 140). Both sets of precepts are simple to apply and would involve little, if any, additional work in the systematic calculation of the ephemeris from the beginning. However, with the exception of a few final steps, the ephemeris of the Moon has been calculated from the tables up to the year 2000. The application of corrections to an existing ephemeris is neither so simple nor so easy to do.

A correction to the mean longitude enters directly into the true longitude and indirectly into every periodic term (including the principal "equations") into the argument of which the mean longitude enters. Differential corrections to some 23 terms, several of them quite large, would be required in the longitude alone. The alternative method, which is here adopted, is to interpolate the final ephemeris to a time $1^s.82144 \dots \Delta L''$ later than that for which it is calculated, making differential corrections to remove the effect of the consequential changes in the arguments of the solar and planetary perturbations. For $\Delta L = 50''$ (the numerical maximum up to the year 2000) there are seven significant terms in longitude and two in horizontal parallax. For the latitude most of the corrections arise through the longitude corrections in S , the argument of Table 33 in Section IV; this is one of the steps that has not yet been done, so that there is only a single significant term to be added directly to the latitude. No planetary term, not even the Great Venus Term, is large enough to require correction.

The empirical term is (deliberately) incompletely incorporated into the tables, thus leading to small dynamical inconsistencies. As explained by Brown (*Tables*, Section I, p. 44), the object was to simplify subsequent correction. A change in the mean longitude will, as we have seen, affect the arguments of all

periodic terms into which it enters. The empirical term has, in fact, been applied directly to the true longitude with differential corrections to only the three tables of largest amplitude. Brown states (p. 44) that no omitted term is so large as $0''.03$, but the correction to term 51 would appear to reach $0''.05$. This treatment prohibits effecting the removal of the empirical term in the same way as a correction to mean longitude; it must be done by the precepts given by Brown, applying differential corrections to the already computed values of $A_{11}, A_{13}, A_{15}; B_{11}, B_{13}, B_{15}$.

3. *Correction to mean longitude, ΔL .*—In addition to the final interpolation to a time $1^h.82144 \dots \Delta L''$, a consequential correction, for the effect of the increase in the Sun's mean longitude in this time,

$$0.000\,000\,363\,A(\Delta L'')(b-d) \times \frac{-\cos}{+\sin}(al+bl'+cF+dD) \quad (5)$$

is required in respect of any periodic term

$$A \frac{\sin}{\cos}(al+bl'+cF+dD). \quad (6)$$

Here $l = L - \varpi$ (Moon), $l' = L' - \varpi'$ (Sun), $F = L - \Omega$ (Moon) and $D = L - L'$ in the notation of Brown's tables.

Within the customary limits of accuracy in these tables, only terms Nos. 3, 6, 8, 15, 16, 26 and 33 need be considered in the longitude, term No. 595 in the latitude (directly), and terms Nos. 610 and 616 in the parallax. The correcting terms are given in final form in Section 5.

These periodic correcting terms are to be multiplied by $\Delta L''$, where

$$-\Delta L = 8''.72 + 26''.75T + 11''.22T^2 = G \sin g. \quad (7)$$

For any reasonably large value of G , g can be chosen to give a good fit over a large range of T ; when $G = 100''$, $g = -0^\circ.13 + 27^\circ.78T$, and the error in the representation for $0.60 < T < 1.00$ is never greater than $0''.3$.

A term

$$A\Delta L \sin \theta \quad (8)$$

may thus be represented, to adequate accuracy, by

$$-AG \sin \theta \sin g = \frac{1}{2}AG \cos(\theta+g) - \frac{1}{2}AG \cos(\theta-g). \quad (9)$$

For the terms of small amplitude it suffices to use a constant for ΔL for many years. By these means multiplications for each date may be avoided.

4. *Removal of the empirical term, E .*—In addition to the direct application of

$$-E = -10''.71 \sin e = -10''.71 \sin(240^\circ.7 + 140^\circ.0T) \quad (10)$$

to the true longitude, differential corrections, proportional to $-E$, are required to Tables 30, 31 and 32 of Section III (longitude) and Tables 15, 16 and 17 of Section V (parallax). Both Tables 30, III, and 15, V, need to be represented by two periodic terms, but the others require only one each.

By the use of the same device as with the correction to mean longitude, multiplication may be avoided at the price of doubling the number of terms. The resulting terms are listed in Section 5.

5. *List of correcting terms.*—From the operations in Sections 3 and 4, the following corrections are obtained.

(a) To the true longitude (in seconds of arc):

$$\begin{aligned}
 P = & -10.71 \sin e \\
 & -0.587 \sin (l+e) + 0.587 \sin (l-e) \\
 & -0.040 \sin (2l+e) + 0.040 \sin (2l-e) \\
 & -0.123 \sin (2D+e) + 0.123 \sin (2D-e) \\
 & -0.118 \sin (-l+2D+e) + 0.118 \sin (-l+2D-e) \\
 & -0.086 \sin (2D+g) + 0.086 \sin (2D-g) \\
 & -0.166 \sin (-l+2D+g) + 0.166 \sin (-l+2D-g) \\
 & -0.005 (6) \cos (l+2D) \\
 & -0.008 (10) \cos l' \\
 & -0.006 (8) \cos (-l'+2D) \\
 & -0.005 (6) \cos (-2l+2D) \\
 & -0.007 (9) \cos (-l-l'+2D), \quad (11)
 \end{aligned}$$

where the first nine terms arise from the removal of the empirical term. The coefficients in parentheses of the terms of small amplitude are those appropriate to the years 1980–2000, the others being for the years 1960–1980.

(b) To the latitude:

Apply P to S before using it as argument for Table 33, IV, and then apply

$$Q = -0''.013 (16) \cos (-F+2D). \quad (12)$$

(c) To the horizontal parallax (in seconds of arc):

$$\begin{aligned}
 R = & +0.0007 (8) \sin 2D + 0.0008 (10) \sin (-l+2D) \\
 & -0.0048 \cos (l+e) + 0.0048 \cos (l-e) \\
 & -0.0005 \cos (2l+e) + 0.0005 \cos (2l-e) \\
 & -0.0015 \cos (2D+e) + 0.0015 \cos (2D-e) \\
 & -0.0009 \cos (2D-l+e) + 0.0009 \cos (2D-l-e). \quad (13)
 \end{aligned}$$

R should strictly be applied to Σ_0 before being used as the argument for Table 24, V, but it may be applied directly to the horizontal parallax.

(d) The final ephemeris is to be interpolated to a time $1^h.82144 \dots \Delta L''$ later.

6. *Practicability of making the corrections.*—Even with punched-card machines the evaluation and summation of 29 periodic terms for 30,000 dates (to cover the period up to the year 2000) is no light task. It can, however, be done and the corrections can be incorporated into the lunar ephemeris as from 1961 January 1 if so desired. It is not practicable to introduce the amendment earlier, as the conversion to right ascension and declination is already completed.

This will be a convenient opportunity to introduce into the ephemeris the correction of a real error (7) in Brown's tables, recently found by Woolard in comparing the ephemeris calculated from the tables with that obtained by Eckert by the direct evaluation and summation of the individual terms on the I.B.M. Selective Sequence Electronic Calculator.

7. *Method of calculation.*—The periodic terms will be summed by a method analogous to that introduced by Brown and developed by Comrie (6). The period of each term is divided into a (small) number of parts n , in such a way that r parts are very nearly equal to the increase in the argument in $0^d.5$. The n corresponding values of the term are punched on cards and the cards arranged

(at interval r) so that consecutive cards represent the values at consecutive intervals of $0^d.5$. The process is cyclic and continuous until the error in the argument, due to the use of r/n for the half-daily motion, is as large as $\frac{1}{2}$ period/ n , when a discontinuity from part p to either part $p-1$ or part $p+1$, according to whether the error increases or decreases, is introduced. Only a few parts are required for the terms of small amplitude in (11) and (13), so that each can be continually reproduced on to date cards from a small master pack; when all the terms have thus been reproduced (a fast and cheap process), they can be summed, as required, on the tabulator. No further details are given of this process here, but it should now be clear why the multiplications were avoided. Since g and e change slowly, the same basic division into parts can be used for both terms arising in (9); the only difference is that discontinuities occur at different intervals.

The interpolation of the final ephemeris offers little difficulty and can be combined with other operations of a similar nature required in the final stages of the work.

8. *Definition and determination of B.*—It will be seen that the correction (1) has been interpreted as a combination of

- (a) a correction to mean longitude of (4), namely, ΔL —the empirical term; and
- (b) a time correction, ΔT .

The effect of this is to facilitate the future calculation of B , from the time correction ΔT obtained directly from the comparison of observation with Brown's tables as amended. As proposed by Clemence (*loc. cit.*, p. 172), B may be determined by the formula

$$1.82144 B = \Delta T - 24^s.349 - 72^s.3165 T - 29^s.949 T^2, \quad (14)$$

where ΔT is the (suitably averaged) time correction required by the amended lunar ephemeris to bring it into accord with observation. This definition of B is precisely equivalent to Spencer Jones' (*loc. cit.*, p. 542)

$$B = \text{observed mean longitude} - \text{Brown's tables} \\ + \text{the empirical term} - 4^s.65 - 12^s.96 T - 5^s.22 T^2 \quad (15)$$

provided this is interpreted as above.

The need for care in distinguishing between a correction to mean longitude and a corresponding time correction arises from the solar perturbations. For a correction of $10''$ the principal error terms are

$$0^s.0172 \cos 2D \quad \text{and} \quad 0^s.0333 \cos (2D - l) \quad (16)$$

with periods of about 15 days and 32 days respectively. Apart from the possible effect of the unsymmetrical distribution of both meridian and occultation observations throughout the lunation, these short-period terms will have no effect on B , which is necessarily an average value over a period of at least a year. The precise method of determining B in the past from (15) is therefore of little importance.

It is desirable that (14) and (15) should be used as definitions of B , without change, even if it is found in the future that, owing to accidental errors in the numerical coefficients of the corrections above, the observed corrections to the ephemerides of the Sun and Moon are not strictly proportional to their mean motions.

9. *Consequences of the amendment.*—The amendment to the lunar ephemeris must be considered in relation to the change from Universal Time, based on the actual (variable) period of rotation of the Earth, to Ephemeris Time, based on a time-unit of invariable length, namely, the length of the sidereal year at 1900.0. The argument for the ephemerides in the astronomical Almanacs will in future be ephemeris time, to correspond with the gravitational theory on which the ephemerides are based. The time-difference, ΔT , between mean solar time and ephemeris time will only be known, primarily through observations of the Moon as indicated above, several years in arrear. It may, however, be extrapolated ahead for practical purposes in the same way as the correction to the Moon's mean longitude is at present.

The positions of the Sun, Moon and planets will then be found from the Almanacs by entering the ephemerides with a time ΔT later than the U.T. for which the positions are desired. With the exception of the Moon, the differences will be insensible from the point of view of setting up instruments, etc.

For eclipses and occultations values of ΔT will be extrapolated and predictions given as closely as possible in terms of universal time. For the navigational ephemerides a similar procedure will have to be used, resulting in two ephemerides for the Moon, one with argument ephemeris time in the astronomical Almanacs, and the other with argument universal time in the navigational Almanacs. There will be no practical differences in the ephemerides for the Sun and planets.

10. *Acknowledgments.*—The Astronomer Royal and Dr G. M. Clemence have contributed much to this paper, by frequent discussions, particularly as regards the difficult question of the separation of mean longitude and time corrections; the substance of Section 8 is entirely due to Dr Clemence. I acknowledge their assistance with gratitude.

The detailed corrections to the tables have been verified, both directly and numerically, from the alternative methods mentioned above, by Dr J. G. Porter and Mr H. W. P. Richards.

*H.M. Nautical Almanac Office,
Royal Greenwich Observatory,
Herstmonceux Castle, Sussex.
1951 October 2.*

References

- (1) E. W. Brown, *M.N.*, **75**, 510, 1915.
- (2) H. Spencer Jones, *M.N.*, **99**, 541, 1939.
- (3) Recommendation No. 6 of the Paris Conference, *Bulletin Astronomique*, tome XV, fascicule 4, p. 291, 1950.
- (4) G. M. Clemence, *A.J.*, **53**, 169, 1948.
- (5) Recommendation No. 2 of the Paris Conference. See (3) above.
- (6) L. J. Comrie, *M.N.*, **92**, 694, 1932.
- (7) E. W. Woolard, *A.J.*, (in press).

ECLIPSE OBSERVATIONS OF THE STRUCTURE OF THE CHROMOSPHERE

Orren C. Mohler

(Communicated by Robert R. McMath)

(Received 1951 June 18)

Summary

Small chromospheric structures that appear in large-scale photographs of the solar eclipse 1930 October 21 have been counted. An attempt, based on the counts, to relate the small chromospheric structures to the rice grains of the solar photosphere indicates a connection between the two classes of observations.

At times of excellent seeing, the solar chromosphere exhibits an intricate, fimbriate structure that consists of very small prominences in contact with the photosphere. For brevity, these chromospheric details will be called "jets"*, but the use of this term must not be construed as a description of the shape or motion of the objects. This paper reports the observation and measurement of two characteristics of chromospheric jets on large-scale eclipse photographs. The first characteristic is indicated in a histogram (Fig. 1) showing the number of jets of a given height class, and the second is shown by a graph (Fig. 2) of the total number of jets per unit arc length of the solar limb for different position angles.

These results are based on measures of the first, second, and eighth photographs made by Marriott with the tower telescope of the U.S. Naval Observatory Eclipse Expedition to Niaufoo Island, 1930 October 21. The following list contains the pertinent details of the telescope and plates†:

Aperture of telescope: 9 inches.

Scale of image: 10.71 seconds of arc per millimetre (1 second of arc = 720 kilometres at the Sun's distance).

Emulsion: undercoat Eastman 33.
overcoat Eastman 40.

Emulsion resolving power: 35 lines per millimetre.

Separation of closest resolvable lunar features: 0.6 seconds of arc.

On Plate No. 8, the height‡ and position angle of each individual jet were measured with a transparent protractor and a diagonal scale placed in contact with the emulsion. A probable error of $\frac{1}{4}$ of a second of arc for a single estimate of height was computed from repeated measures of a group of jets. The edge of

* The term "jet" follows long-established usage. See A. Secchi, *Le Soleil*, Paris, 2, p. 38, 1877. Secchi used the word "filet" which can be translated "jet" as in "filet d'eau". See also B. Lyot, *Ann. d'Astrophys.*, 7, 47, 1944. "Spicule", introduced by W. O. Roberts, *Ap. J.*, 111, 136, 1944, apparently refers to the largest of the jets that appear in the Sun's polar regions.

† For additional information about the eclipse equipment and procedure, see R. Marriott, *P.A.*, 39, 255, 1931.

‡ Height is here defined as the extent beyond the edge of the Moon in the direction of a radius of the solar disk.

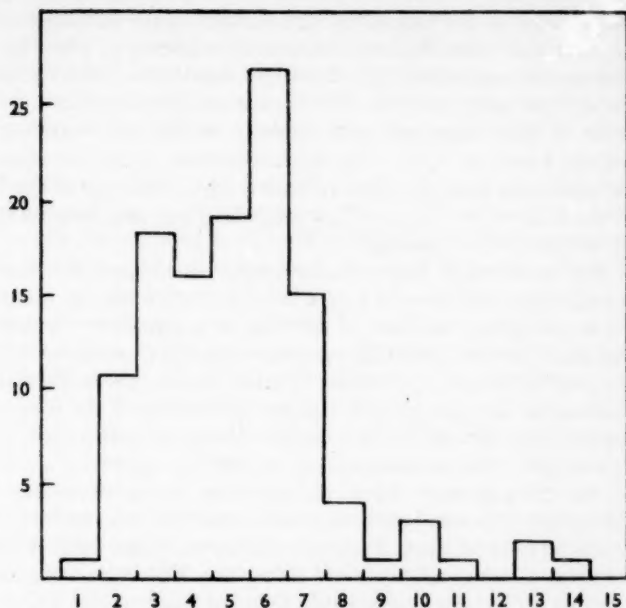


FIG. 1.—Histogram showing the number of jets for a given height class.

Ordinates: Number of jets.

Abscissae: Height—seconds of arc.

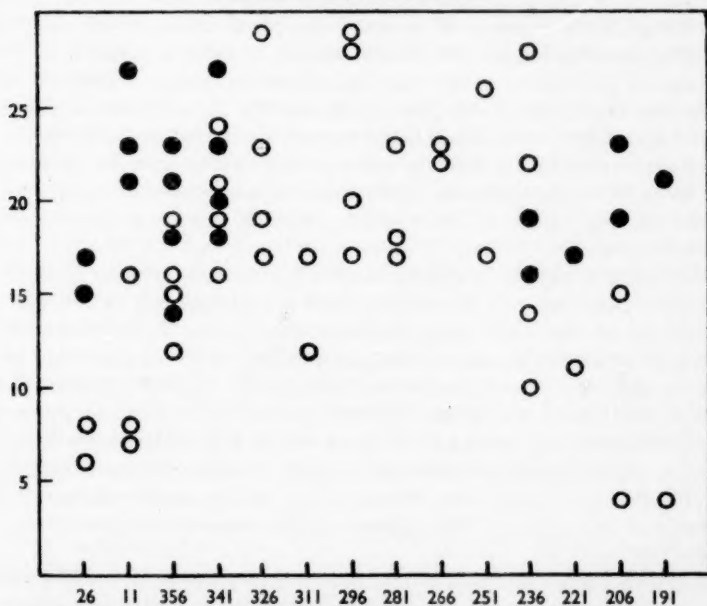


FIG. 2.—Total number of jets per unit arc length of the solar limb for different position angles.

The filled circles are corrected for the eclipse; the open circles are observed.

The position of good contact on Plate No. 8 extends from position angle 326 to 266 degrees.

the Moon was chosen as the base of the jets because of the excellent coincidence between the solar and lunar limbs at the time of exposure of Plate 8. There is a possible systematic error inherent in this origin, but the well-determined contact times for the eclipse make it certain that the error arising from any residual lack of coincidence of the lunar and solar limbs is much less than the error in estimation of the height of a jet. The heights entered in the histogram (Fig. 1) are the direct measures from the parts of Plate 8 where the edge of the Moon can be taken as the edge of the Sun. They are, therefore, true heights of the jets as projected on the plane of the sky.

Plates 1 and 2, although less perfectly timed with regard to coincidence of solar and lunar limbs, can be used with Plate 8 to determine the number of jets per unit arc length along the limb of the Sun as a function of position angle. Only the tops of all jets need be visible on a plate to make it useful for this purpose, and plates not exposed exactly at second or third contact, although of little value for height measures, can give reliable results. The edge of the lunar image on Plates 1, 2 and 8 was divided by a carefully constructed sectored disk into arcs $7\frac{1}{2}$ degrees in length. The number of jets in each $7\frac{1}{2}$ degrees of arc length was counted for the three plates. Repeat counts were made at random positions on each of the plates, but a complete duplicate count was not made on any of the three. Fig. 2 shows the number of jets per $7\frac{1}{2}$ degrees of the limb of the Sun for all position angles where measures could be made. The region of good contact on Plate 8, within which the height measures were made, extends from position angle 326 to 266 degrees. The counts at position angles 26 to 356 degrees and 236 to 191 degrees are seriously affected by the Moon eclipsing the lower chromosphere, but, since the relative positions of the limbs of the Sun and Moon can be found from a series of contact-time plates made at the eclipse, this information and the height distribution in Fig. 1 make it possible to estimate the number of jets missed in the counting where the Moon overlapped the Sun. An estimated correction of this kind is indicated by the ordinates in Fig. 2.

Fig. 1 and Fig. 2 contain all of the counts and measures made on the three eclipse plates except for a few estimates of the widths of some 20 jets. The widths seem to be so much less variable than the heights that not all jets were measured in this regard. The average width of the 20 measured jets was 1.8 seconds of arc.

The number of objects of a given height (Fig. 1) falls very sharply for heights greater than 7 seconds. This sudden decrease corresponds to the top of the chromosphere as observed under ordinary conditions. It is somewhat more difficult to interpret the gradual decrease in numbers as the heights become small. It may be that the decrease with small heights is entirely attributable to the increased difficulty of seeing the smaller objects, but it must be remembered that both the resolving power and the scale of the original photograph are quite adequate to reveal jets shorter than one second. In fact, numerous peaks of the Moon slightly smaller than one second of arc can be measured, but only one jet as small as one second of arc appears in the observable region of the Sun's limb on Plate 8.

The evidence from the three eclipse plates, shown in Fig. 2, indicates that the jets are uniformly distributed around the edge of the Sun with an average value of 3.0 jets per degree. The largest irregularities in the observed distribution, apart from those introduced by the edge of the Moon, are caused by prominences.

No object larger than 15 seconds in height was counted as a jet, and the regions where prominences occurred were recorded as having no jets.

It might possibly have been a more correct procedure to have included the prominences in the count, by considering them as very large jets, but their omission cannot have seriously changed the apparently uniform distribution of the jets.

The uniform distribution of jets around the limb of the Sun's disk (Fig. 2) indicates the possibility of a uniform distribution of jets over the surface of the Sun. If the jets are assumed to be uniformly distributed over the Sun's surface, the average number of jets per $7\frac{1}{2}$ degrees of arc along the limb of the Sun can be used to find an upper limit to the total number of these objects. The upper limit to the number of jets on the surface of the Sun is $4\pi R^2$, or 4×10^6 , where $R=171$, the number of jets per radian. This is an upper limit because it is implicitly assumed that all of the jets apparently at the limb actually are at 90 degrees from the central solar meridian.

The counts of the jets on the eclipse plates provide a basis for a critical evaluation of Secchi's* suggestion of a connection between chromospheric structure and photospheric grains. The suggestion implies an approximate agreement between the number of jets and the number of grains. There is good numerical coincidence between the average widths of the jets and Keenan's† measure of grain diameters (1.8 seconds for jet widths, 1.6 seconds for grain diameters), but Keenan's estimate of the total number of grains on the Sun, 2.6×10^6 , is more than six times greater than the upper limit to the number of jets deduced from the eclipse plates. Langley's‡ estimate of the number of grains is only one-third as large as Keenan's. In view of the difficult observations and uncertain assumptions on which both the number of grains and the number of jets depend, it is probably correct to say that the jets and grains are approximately equal in number.

Good quality spectroheliograms, particularly K_{232} photographs, often show a fine structure comparable to the grains in size and appearance. Since there is a possibility of direct observation of the connection between chromosphere and photosphere on spectroheliograms, such observations will be decisive. In a preliminary study of this sort, Hale and Ellerman§ supported "the hypothesis that the solar atmosphere consists of parallel columns of ascending and expanding gases". It is considered that the rough agreement in number and dimensions of jets and grains presented here is an additional confirmation of this idea of the structure of the photosphere and chromosphere.

It is a pleasure to acknowledge the generous cooperation of the entire staff of the Sproul Observatory during the measures (for another purpose) of the eclipse plates in 1938. Professor Ross W. Marriott was especially helpful in supplying many unpublished details of the photography of the plates and in sharing his unique knowledge of large-scale eclipse photographs.

McMath-Hulbert Observatory,
Pontiac,
Michigan:
1951 June 6.

* A. Secchi, *Le Soleil*, Paris, 2, p. 38, 1877.

† P. C. Keenan, *Ap. J.*, **88**, 363, 1938.

‡ S. P. Langley, *Amer. J. Sci.*, **7**, 87, Ser. 3, 1874.

§ G. E. Hale and F. Ellerman, *Proc. Nat. Acad. Sci.*, **2**, 108, 1916.

PHOTOELECTRIC OBSERVATIONS OF BD-3° 1413 (HD 44701), A NEW ECLIPSING BINARY

C. S. Gum

(Communicated by the Commonwealth Astronomer)

(Received 1951 September 17)

Summary

The spectroscopic binary BD-3° 1413 has been found to be an eclipsing system with a small range of 0.1 mag. A light curve has been obtained and a preliminary solution made from 326 photoelectric observations.* The rectified eclipse depths are only 0.046 and 0.029 of the total intensity, so that in order to make the solution determinate it is necessary to adopt a spectrographic estimate of the luminosity ratio.

The light curve is asymmetrical, terms in $\cos \theta$, $\cos 2\theta$, $\sin \theta$ and $\sin 2\theta$ being required to represent the light between eclipses. The rectified primary minimum appears to be slightly asymmetrical, with the descent less rapid than the ascent. There is a discrepancy between the spectrographic and photometric values of $e \cos \omega$.

The variability of BD-3° 1413 (HD 44701) was discovered by the author during the course of photometric tests on several spectroscopic binaries. The spectrographic orbit is by Pearce (1). The magnitude difference between the components has been measured by Petrie (2).

1. *Equipment and observations.*—The observations were made in the 1949–50 season with the nine-inch refractor of the Commonwealth Observatory. The photoelectric photometer used for the work consisted of a 1P21 photomultiplier tube and D.C. amplifier, and has been described by Hogg and Bowe (3). The effective wave-length of the measurements depends on the distribution of the star's radiation, the atmospheric transmission, the photo-cell response, and the telescope optics. In the absence of precise information on the telescope optics a sharp cut-off at 3700 Å. has been adopted as a rough approximation. Estimates of the other factors and the assumption of black-body radiation of 15,500 deg. for a star of type B5 lead to the value $\lambda_{\text{eff}} = 4400 \text{ Å.}$

Details of the comparison stars and variable are as follows:

	α 1950	δ	m_{IPV}	Sp	
	h	m	s		
HD 44701 (variable)	6	20.5	-3 15	...	B5n-B8n
HD 45321 (comp. 1)	6	24.1	-4 34	6.15	B3
HD 44756 (comp. 2)	6	20.9	-4 40	6.51	B9

The magnitudes of the comparison stars have been converted from the Harvard System to the International Photovisual System by means of the equation $\text{IPV} - \text{HPV} = +0.10 + 0.06C_p$, adopting Seares' values (4) for the colour index.

The number of observations used for the solution was 326; this excludes 66 which were rejected because of instrumental trouble. Any failure of the light curve to repeat itself accurately could not be established by the present work. The

* The individual observations are not reproduced here, but will be available on request from the Commonwealth Observatory.

individual observations have been assembled on a period of 1.19042 days, with the phase computed from the epoch of primary minimum, JD(hel) 2,433,340.168. Each observation consisted of five measurements on the variable made between two sets of five each on comparison star C_1 . Corrections were made for sky background and for extinction. The normal points, formed by combining ten individual observations, are shown in Table I, and are plotted together with the theoretical light curve in Fig. 1. The probable error of a normal point is ± 0.0024 mag., corresponding to ± 0.008 mag. for an individual observation.

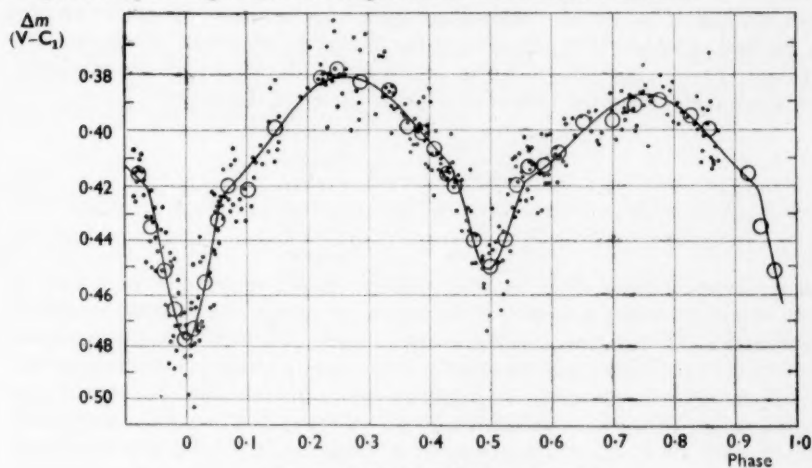


FIG. 1.—Light curve of BD -3° 1413.

• Individual observations.
 ○ Normal points.
 — Computed curve.

TABLE I
 Observed normal points

No.	Phase	Δm^*	O-C	No.	Phase	Δm^*	O-C
1	0.0136	0.4732	+0.0002	18	0.5239	0.4392	-0.0018
2	0.0308	0.4557	-0.0005	19	0.5451	0.4192	-0.0059
3	0.0523	0.4324	+0.0025	20	0.5628	0.4128	-0.0046
4	0.0706	0.4199	-0.0007	21	0.5880	0.4124	-0.0009
5	0.1026	0.4210	+0.0080	22	0.6118	0.4078	-0.0007
6	0.1476	0.3988	-0.0019	23	0.6517	0.3969	-0.0030
7	0.2228	0.3812	-0.0030	24	0.6996	0.3965	+0.0052
8	0.2489	0.3784	-0.0030	25	0.7363	0.3912	+0.0033
9	0.2881	0.3827	+0.0008	26	0.7764	0.3894	+0.0010
10	0.3342	0.3860	-0.0022	27	0.8287	0.3947	-0.0010
11	0.3650	0.3985	+0.0033	28	0.8590	0.3996	-0.0027
12	0.3891	0.4004	-0.0007	29	0.9232	0.4155	-0.0022
13	0.4078	0.4064	+0.0006	30	0.9424	0.4346	+0.0094
14	0.4302	0.4154	+0.0044	31	0.9646	0.4512	+0.0003
15	0.4435	0.4196	+0.0022	32	0.9814	0.4656	-0.0032
16	0.4732	0.4394	-0.0026	33	0.9975	0.4769	-0.0008
17	0.4989	0.4491	-0.0019				

* Δm is in the sense $V-C_1$.

2. *Period and epoch.*—Assuming a symmetrical minimum, and considering only observations within 23° of the middle of primary eclipse, a least squares solution for the period gave $P(\text{photometric}) = 1^d.19058 \pm 0.00030$ (p.e.). The spectrographic period found by Pearce (1) is $1^d.19033$. To obtain an estimate of the accuracy of this period a re-analysis of his observations has been carried out and yields $P(\text{spectrographic}) = 1^d.19036 \pm 0.00012$ (p.e.). The spectrographic observations were made 22 years ago, so that if they are used to predict the time of an eclipse in the present series the uncertainty in the predicted time is equal to about one-half of the period. Adopting Luyten's revised spectrographic elements (5), we find an epoch JD 2,425,478.605 for the conjunction with the fainter star in front. Combining this with the photometric epoch of primary minimum JD 2,433,340.168 gives the following possible values of the period:

No. of revs.	Period (days)
6603.....	1.19060
6603½.....	1.19052
6604.....	1.19042
6604½.....	1.19033
6605.....	1.19024

Those periods derived from an odd number of half cycles correspond to an occultation for primary eclipse. If the secondary component is of lower surface brightness, as is suggested by the spectral types (B5–B8), then the primary eclipse must be a transit and the periods $1^d.19052$ and $1^d.19033$ are inadmissible. A more decisive test of this point would require a modern determination of the spectrographic phase.* We are left with the two periods $1^d.19042$ and $1^d.19024$, both of which are within the probable error of the spectrographic determination. The photometric work favours the longer period $1^d.19042$, which has therefore been adopted.

The epochs of minima are

Min I JD (hel) 2,433,340.168 ± 0.002 (p.e.)

Min II JD (hel) 2,433,270.523 ± 0.003 (p.e.)

3. *Eccentricity.*—The displacement of the secondary minimum of the light curve gives $t_2 - t_1 = 0^d.5902 \pm 0^d.005 = (0.496 \pm 0.004) P$, and hence the value $e \cos \omega = -0.007 \pm 0.007$. A circular orbit is therefore not excluded by the photometric observations. Pearce's spectrographic values are $e = 0.036 \pm 0.011$, $\omega = 9^\circ \pm 13^\circ$, that is, $e \cos \omega = +0.035 \pm 0.012$. The discrepancy between the spectrographic and photometric values could possibly be accounted for by apsidal motion, but in view of similar discrepancies found in other systems (6) it seems more likely that the spectrographic values for e and/or ω are spurious. In a re-discussion of the orbit Luyten (5) has calculated elements separately for each component, as follows:

$$\gamma = +7.8 \pm 2.8, \quad e = 0.077 \pm 0.024, \quad \omega_1 = 352^\circ \pm 20^\circ \text{ (primary)}$$

$$\gamma = -9.1 \pm 5.5, \quad e = 0.051 \pm 0.030, \quad \omega_2 = 193^\circ \pm 35^\circ \text{ (secondary)}$$

He points out that the average elements $e = 0.04 \pm 0.02$, $\omega_1 = 3^\circ \pm 28^\circ$ must therefore be approximate only.

For the photometric solution the values $\omega_1 = 180^\circ$ (assumed) and $e = 0.007$ have been adopted.

* Recent spectrographic observations by J. A. Pearce (private communication) confirm the transit hypothesis for primary eclipse.

4. *Solution.*—Assuming the light between eclipses to be of the form $I = A_0 + A_1 \cos \theta + A_2 \cos 2\theta + B_1 \sin \theta + B_2 \sin 2\theta$, harmonic analysis of normal points Nos. 4 to 14 and 20 to 29 yields the values

$$A_0 = 0.9766 \pm 0.0005 \text{ (p.e.)}$$

$$A_1 = -0.0031 \pm 0.0007 \text{ ,,}$$

$$A_2 = -0.0177 \pm 0.0008 \text{ ,,}$$

$$B_1 = 0.0028 \pm 0.0006 \text{ ,,}$$

$$B_2 = -0.0025 \pm 0.0006 \text{ ,,}$$

where unit intensity was assigned to normal point No. 8. In this solution the values $\omega_1 = 180^\circ$ (assumed), $e = 0.007$ have been used for the calculation of θ . Rectified light values were computed from

$$I_R = \frac{I - A_1 \cos \theta - B_1 \sin \theta - B_2 \sin 2\theta}{A_0 + A_2 \cos 2\theta}.$$

The values of the phase θ were rectified by Merrill's method (7, 8) and the rectified normals are shown in Table II. The depths of the rectified minima are

$$I - \lambda_1 = 0.029, \quad I - \lambda_2 = 0.046.$$

The asymmetry of the light curve cannot be due to a "periastron effect", even assuming the existence of such an effect, because the spacing of the minima requires a value $e \cos \omega = -0.007$, which is too small to produce an observable asymmetry. There have been attempts to explain such asymmetries (9, 10), but in the present state of the theory no reliable method of orbital solution is available. Application of Kopal's methods (11) does not appear justified because these methods include $\sin \theta$ asymmetry only if it can be attributed to changes in tidal distortion (periastron effect). All that can be done at present is to remove the sine terms by an empirical rectification and adopt the standard methods of solution due

TABLE II
Rectified normals

θ'	I_R	θ'	I_R
5.1	0.9588	181.1	0.9740
11.3	0.9735	190.2	0.9831
19.1	0.9922	198.0	1.0002
25.8	1.0007	204.4	1.0042
37.4	0.9928	213.5	1.0009
53.7	1.0017	222.2	1.0007
80.4	1.0027	236.3	1.0028
90.2	1.0029	253.3	0.9953
104.3	0.9992	266.1	0.9971
121.0	1.0021	280.2	0.9991
132.2	0.9969	298.6	1.0009
141.0	1.0006	309.4	1.0027
147.8	0.9994	332.3	1.0021
156.0	0.9960	339.2	0.9982
160.8	0.9945	347.2	0.9763
171.8	0.9808	353.3	0.9648
		359.2	0.9557

to Russell (12). Although the uncertainty of the elements so derived may be large it was thought worth while to perform such a preliminary solution.

Since the solution from photometric observations alone is indeterminate in the case of eclipses shallower than 0.1 mag., the value $L_1/L_2 = 3.34$ (corresponding to $\Delta m = 1.31 \pm 0.24$ found by Petrie (2)) has been adopted for the luminosity ratio. The uncertainty in Δm would permit values of L_1/L_2 ranging from 2.7 to 4.2, but solutions for these extreme values do not differ essentially from the solution given in Table III. In any case the elements may be in error due to other unknown causes. The method of solution differs from the usual photometric solution in that once a value for L_1/L_2 is adopted it is necessary only to read the

TABLE III
Provisional elements of BD - 3° 1413 = HD 44701

Darkening coefficients $u_1 = u_2 = 0.6$ (assumed) $\lambda_{\text{eff}} = 4400 \text{ \AA.}$		
Period (days)	P	1.19042
Orbital eccentricity factor	$e \cos \omega$	-0.007
Rectified eclipse depths	$1 - \lambda$	0.046, 0.029
Surface brightness ratio	J_b/J_f	1.7
Adopted luminosity ratio	L_1/L_2	3.34
Maximum fractional loss of light (Unit = light loss at internal tangency)	α_0^f	0.108
Ratio of radii	α_0^c	0.125
Inclination	k	0.71
Semi-axis major of relative orbit (in A.U.)	i	62°
Longest semi-axis	$a_f + a_b$	0.054
Ratio of intermediate to longest axis*	a_1, a_2	0.34, 0.24
Ratio of polar to longest axis	b/a	0.98
Masses ($m_\odot = 1$)	c/a	0.96
Absolute bolometric magnitudes	m	9.0, 6.0
Absolute photovisual magnitudes	M_1, M_2	-2.7, -0.9
Mean densities	M_{IPV}	-1.1, +0.1
Parallax (seconds of arc)	ρ_1, ρ_2	0.16, 0.26
	π	0.0027

* Derived from the observed ellipticity factor $z = 0.032$.

depths of minima from the rectified curve to obtain values for k , α_0 and χ . A reading of the width of primary minimum at a point corresponding to a light loss of one-half enables the remaining elements r_1 , r_2 and i to be found. That it is impossible even to attempt to solve for the elements from the shape of the minimum, is due to the fact that with some χ values, read from the curve, entry could not be made in the χ tables for any degree of darkening. The rectified primary minimum appears to be slightly asymmetrical with the descent less rapid than the ascent, and both branches are somewhat less steep than required by the theoretical χ values.

The absolute dimensions were computed with the aid of Pearce's spectrographic elements :

$$m_1 \sin^3 i = 6.2, \quad m_2 \sin^3 i = 4.1, \quad a \sin i = 7.14 \times 10^6 \text{ km.}$$

No correction was made for the effect of reflection.

The ellipticities of the components obtained from the light between eclipses should agree with the values computed from the finally adopted physical

dimensions. Using Russell's methods and notation (13) it is found that setting $G_e/G_h = J_h/J_e = 1.7$ gives for the photometric ellipticity,

$$Nz = -4(A_2 - C_2)/(A_0 - C_0 - A_2 + C_2),$$

the value 0.083. Assuming $u=0.6$, $y=1$ gives $N=2.6$, and therefore an observed geometrical ellipticity $z=0.032$. The ellipticities of the components in the case of a centrally condensed model are*

$$\epsilon_1 = \frac{3}{2}(m_2/m_1)r_{1(\text{mean})}^3, \quad \epsilon_2 = \frac{3}{2}(m_1/m_2)r_{2(\text{mean})}^3.$$

Substituting the appropriate values from Table III we find $\epsilon_1=0.036$, $\epsilon_2=0.033$. Weighting these according to the luminosities of the stars yields the average value $z = e^2 \sin^2 i = 2\epsilon \sin^2 i = 0.055$ (cf. observed $z=0.032$). The computed ellipticity is largely independent of the value of L_1/L_2 . The observed and computed values could be made to agree by adopting the coefficients $u=0.35$, $y=0.3$ for limb and gravity darkening, respectively, or for the uniform case, $u=0$, $y=0.5$.

The absolute magnitudes were calculated from the equation

$$M(\text{bol}) = M_\odot(\text{bol}) - 5 \log \left(\frac{R}{R_\odot} \right) - 10 \log \left(\frac{T}{T_\odot} \right).$$

The spectral types given by Pearce are B5-B8. Petrie (2) concludes from microphotometer tracings that the secondary is probably later than the primary but that the evidence is slight. If the primary is taken as B5 with a temperature of 15,500 deg. on Kuiper's scale (14), then by making use of the surface brightness ratio $J_b/J_f=1.7$, and assuming that the radiation is of black-body quality, we find 12,000 deg. and B8 for the secondary. Using these temperatures and Kuiper's values of $M_\odot(\text{bol}) = +4.62$, $T_\odot = 5713$ deg., gives

$$M_1(\text{bol}) = -2.7, \quad M_2(\text{bol}) = -0.9$$

in satisfactory agreement with the empirical mass-luminosity relation.

The parallax of the system has been calculated from the combined absolute magnitude $M(\text{bol})$ and the apparent bolometric magnitude $m(\text{bol})$ corresponding to the mean light between eclipses. To obtain $m(\text{bol})$ both comparison stars are considered. The mean of 23 comparisons gave $C_2 - C_1 = 0.685$ mag. (m.s.e. of one comparison = 0.010), while for the mean light between eclipses we have $V - C_1 = 0.40$ mag. The IPv magnitudes of C_1 and C_2 are 6.15 and 6.51, giving two values for V the mean of which is 6.39 mag. Here the photoelectric magnitude differences have been applied directly to the IPv magnitudes because the spectral type of the variable (B5-B8) is intermediate between the comparison stars (B3 and B9). If the conversion to the IPv System ($\lambda_{\text{eff}} = 5430 \text{ \AA}$) is carried out, assuming black-body radiation and Kuiper's temperatures, the same result is obtained. Applying a weighted bolometric correction gives $m(\text{bol}) = 4.91$. From $M_1(\text{bol}) = -2.7$, $M_2(\text{bol}) = -0.9$ we find the combined value $M(\text{bol}) = -2.9$, and the parallax $0''.0027$ follows.

I am indebted to Dr A. R. Hogg for valuable discussion during the course of this work, to Dr Gerald E. Kron and Dr Olin J. Eggen for many helpful suggestions, and to Dr J. A. Pearce who has kindly supplied me with the results of his recent spectrographic observations.

Commonwealth Observatory,
Mount Stromlo,
Canberra:
1951 August 21.

* Here ϵ is the ellipticity and e the eccentricity of a meridian section of the star. To the first order in ϵ we have $e^2 = 2\epsilon$.

References

- (1) J. A. Pearce, *Publ. Dom. Astrophys. Obs.*, **6**, 70, 1932.
- (2) R. M. Petrie, *Publ. Dom. Astrophys. Obs.*, **8**, 319, 1950.
- (3) A. R. Hogg and P. W. A. Bowe, *M.N.*, **110**, 373, 1950.
- (4) F. H. Seares, *Ap. J.*, **98**, 302, 1943.
- (5) W. J. Luyten, *Ap. J.*, **84**, 85, 1936.
- (6) Z. Kopal, *Ap. J.*, **99**, 239, 1944.
- (7) J. E. Merrill, *Contrib. Princeton Univ. Obs.*, No. 23, 1950.
- (8) H. N. Russell, *Ap. J.*, **108**, 388, 1948.
- (9) T. G. Cowling, *M.N.*, **101**, 367, 1942.
- (10) Jan Mergentaler, *Contrib. Wroclaw Obs.*, No. 4, 1950.
- (11) Z. Kopal, *Harvard Obs. Monograph*, No. 6, 1946.
- (12) H. N. Russell, *Ap. J.*, **35**, 340; **36**, 54, 239, 385, 1912.
- (13) H. N. Russell, *Ap. J.*, **102**, 4, 1945.
- (14) G. P. Kuiper, *Ap. J.*, **88**, 429, 1938.

ERRATA

M.N., **110**, No. 6:

M. Ryle, F. G. Smith and B. Elsmore, *A preliminary survey of the radio stars in the Northern Hemisphere.*

P. 514, Table I, line 9, *for*

	Number	R.A.					Declination			
		h	m	s	m	s	°	'	°	'
	03·03	03	58	± 1	3					
<i>read</i>	03·03	03	58	± 1	30					
line 17, <i>for</i>	07·01	07	19	± 3			51	51	± 1	
<i>read</i>	07·01	07	19	± 3			51			
line 31, <i>for</i>	12·01	12	28	25	± 1	10	12	± 0	20	
<i>read</i>	12·01	12	28	25	± 0	10	12	55	± 0	20

P. 521, line 22, *for* (areas 1572 and 1604), *read* (years 1572 and 1604).

M.N., **110**, No. 6:

E. J. Öpik, *Transport of heat and matter by convection in stars.*

P. 559, heading, *for* (Received 1950 December 1), *read* (Received 1950 September 28).

In footnote, *for* 1950 September 28, *read* 1949 December 1.

P. 568, equation immediately preceding (33), *for* $n = n_a$, *read* $\bar{n} = n_a$.

P. 570, equation (43), *for* $(\omega \cos \phi)_2$, *read* $(\omega \cos \phi)^2$.

M.N., **111**, No. 1:

Mary Almond, *The summer daytime meteor streams of 1949 and 1950.*
 III. *Computation of orbits.*

P. 44, reference (5), *for* *Die Meteore*, *read* *Meteorströme*.

THE SO-CALLED PERIASTRON EFFECT IN ECLIPSING BINARIES*

D. J. K. O'Connell, S.J.

(Received 1951 November 28)

Summary

Many eclipsing binaries differ in brightness at the maxima before and after principal minimum. This is generally termed the "periastron effect". It is shown that the phenomenon is in general definitely not a periastron effect. From a study of 87 eclipsing binaries it is found that the difference in magnitude, Δm (positive when the maximum after principal minimum is the brighter), is a function of wave-length. For binaries of β Lyrae type, (1) Δm for light of about 4300 Å. (Δm_b) is positive; (2) Δm_b increases with increasing ellipticity of the stars and with increasing difference between the sizes and densities of the components; (3) the smaller and denser the smaller star is, the larger is Δm_b , the supergiant stars being taken separately.

A careful search has failed to find any binaries of β Lyrae type that contradict these conclusions.

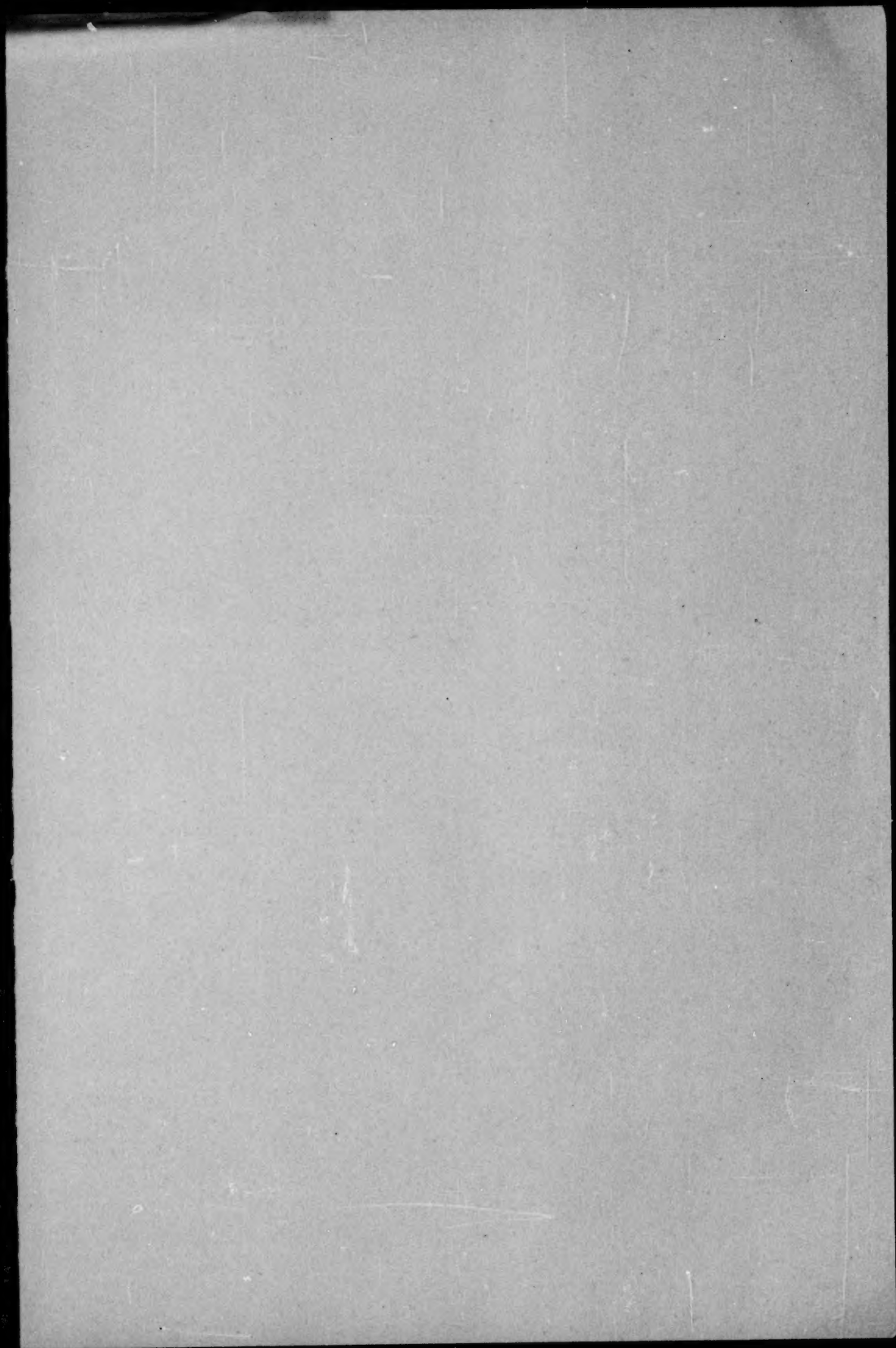
A very close correlation is found in binaries of β Lyrae type between Δm_b and $(\Delta m_b - \Delta m_y)$, where Δm_y is the value of Δm in yellow light. When there is a significant difference between the maxima, the maximum before principal minimum is the redder. The difference in colour increases with Δm_b .

For binaries of W Ursae Majoris type special difficulties arise owing to the equality, or near equality, of the minima. Nevertheless it seems that, so far as present information goes, they fit fairly well into the general scheme sketched above for binaries of β Lyrae type.

Thus the following facts require an explanation. For many eclipsing binaries the total light of the system, in blue light, is greater at maximum after principal minimum, i.e. at quadrature, when the star with greater surface brightness is approaching us and the fainter star receding, than it is half a period of revolution later, when the latter star is approaching us and the former receding. This difference increases with increasing ellipticity of the stars and with increasing difference between the sizes and densities of the components. There is, furthermore, the difference in colour between the maxima referred to above.

Various explanations of the phenomenon are examined. The conclusions reached in this paper fit in well with Struve's theory of a whirlpool, or ring, of gas surrounding close binary stars.

*The full text of this paper appears in *Riverview College Observatory Publications*, No. 10 (Vol. 2, No. 6), 1951.



CONTENTS

	PAGE
Meeting of 1951 November 9:	
Fellows elected	523
Junior Member elected	523
Presents announced... ..	523
Meeting of 1951 December 14:	
Fellows elected	523
Junior Member elected	525
Presents announced... ..	525
David S. Evans, Surface photometry of southern elliptical nebulae	526
P. B. Fellgett, An exploration of infra-red stellar magnitudes using the photo-conductivity of lead sulphide	537
F. Schmeidler, Proper-motion distribution and mean parallaxes of the stars of the <i>General Catalogue</i> in different galactic latitudes and longitudes	560
R. Hanbury Brown and C. Hazard, A radio survey of the Cygnus region.	
I. The localized source Cygnus (1)	576
Mary Almond, J. G. Davies and A. C. B. Lovell, The velocity distribution of sporadic meteors. I	585
Peter Naur, Computation of special perturbations by an electronic calculator	609
R. d'E. Atkinson and D. H. Sadler, On the use of mean sidereal time	619
D. H. Sadler, Amendment of the lunar ephemeris	624
Orren C. Mohler, Eclipse observations of the structure of the chromosphere	630
C. S. Gum, Photoelectric observations of BD -3° 1413 (HD 44701), a new eclipsing binary	634
Errata	641
Summary of paper in <i>Riverview College Observatory Publications</i> :	
D. J. K. O'Connell, S.J., The so-called periastron effect in eclipsing binaries	642